

DYNAMIC EQUIVALENTS FOR POWER SYSTEM STUDIES

By

R. P. ADGAONKAR

TH
EE/1979/D
Ad 39d



DEPARTMENT OF ELECTRICAL ENGINEERING
INDIAN INSTITUTE OF TECHNOLOGY KANPUR
JULY, 1979

DYNAMIC EQUIVALENTS FOR POWER SYSTEM STUDIES

A Thesis Submitted
in Partial Fulfilment of the Requirements
for the Degree of
DOCTOR OF PHILOSOPHY

By
R. P. ADGAONKAR

to the

DEPARTMENT OF ELECTRICAL ENGINEERING
INDIAN INSTITUTE OF TECHNOLOGY KANPUR
JULY, 1979

To

Rekha and Hrishikesh

EE-1979-D-ADG-DYN

L. I. T. KANPHER

CENTRAL LIBRARY

Acc. No. **A** 62185

• 7 MAY 1980

CERTIFICATE

It is certified that this work, "Dynamic Equivalents for Power System Studies" by R.P. Adgaonkar has been carried out under my supervision and that this work has not been submitted elsewhere for a degree.

Dr. M.A. Pai
Professor
Department of electrical Engineering
Indian Institute of Technology
Kanpur, India

ACKNOWLEDGEMENTS

It is with a deep sense of gratitude that I acknowledge the invaluable guidance received from Dr. M.A. Pai, who initiated me into the field of dynamic equivalents and has been a source of constant encouragement during this investigation.

I am thankful to Dr. K.R. Padiyar, Dr. S.S.Prabhu and Dr. L.P. Singh for some useful discussions in connection with this work. Also my thanks are due to all my fellow research scholars / K.Gomathi, Vijay Vittal, N.Arumugam, Y.P.Singh and C. Radhakrishna for their cooperation.

I am greatly indebted to the authorities of the College of Engineering, Goa for sponsoring me for Ph.D. degree under Quality Improvement Programme.

Lastly I thank M/s K.N. Tewari and Nihal Ahmad for their skilful typing.

R.P. Adgaonkar

TABLE OF CONTENTS

	Page
LIST OF FIGURES	vii
LIST OF TABLES	x
LIST OF PRINCIPAL SYMBOLS	xi
SYNOPSIS	xiv
 CHAPTER 1 INTRODUCTION	
1.1 Stability Studies	1
1.2 Statement of the Problem	1
1.3 The State of Art	4
1.4 Scope and Outline of the Thesis	21
 CHAPTER 2 IDENTIFICATION OF COHERENCY	
2.1 Introduction	27
2.2 Assumptions	29
2.3 Mathematical model of Power System	32
2.4 Analytical Solution	36
2.5 Identification of Coherent Generators	39
2.6 Direct Method of Coherency Analysis	40
2.7 Formation of Coherent Groups	42
2.8 Computation of Eigenvalues, Eigenvectors and Reciprocal Basis Vectors	43
2.9 Numerical Example	45
2.10 Changes in the Fault Location	55
2.11 Similarity Transformation Matrix	56

2.12	Numerical Examples	58
2.13	Discussion	63
2.14	Conclusion	66
CHAPTER 3	DECOMPOSITION OF POWER SYSTEMS AND CONSTRUCTION OF COHERENCY BASED EQUIVALENTS	
3.1	Introduction	68
3.2	Electromechanical Distance	69
3.3	Decomposition of Power System	70
3.4	Selection of the Boundaries	71
3.5	Numerical Examples	72
3.6	Construction of Coherency Based Equivalent	82
3.7	A Case Study	87
3.8	Conclusion	94
CHAPTER 4	DYNAMIC SIMPLIFICATION USING SINGULAR PERTURBATION THEORY (DYNAMIC STABILITY STUDIES)	
4.1	Introduction	95
4.2	Power System Model	96
4.3	Singular Perturbation Theory	102
4.4	Model Simplification Using Singular Perturbation Theory	104
4.5	Numerical Examples	110
4.6	Discussion	116
4.7	Conclusion	123

CHAPTER 5	DYNAMIC SIMPLIFICATION USING SINGULAR PERTURBATION THEORY (TRANSIENT STABILITY STUDIES)	
5.1	Introduction	124
5.2	System Model	124
5.3	Dynamic Simplification of the System Model	125
5.4	Single Machine Infinite Bus Example	128
5.5	Discussion and Conclusion	141
CHAPTER 6	CONCLUSION	
6.1	Summary and Conclusion	145
6.2	Scope for Further Research	149
REFERENCES		151
APPENDIX A		158
APPENDIX B		161
APPENDIX C		169
APPENDIX D		176
CURRICULUM VITAE		180

LIST OF FIGURES

Fig.No.		Page
1.1	Trajectories in a region of attraction around the post-fault operating point	12
2.1(a)	Approximate variation of accelerating power of a generator in faulted system	31
(b)	Equivalent reproduction of accelerating power in the unfaulted system	31
2.2	Single line diagram of 13 machine system	46
2.3	Base case swing curves of generators 9,11,12 and 13	51
2.4	Swing curves (closed form solution) of generators 9, 11, 12 and 13	52
2.5	Base case swing curves of generators 6 and 7	53
2.6	Swing curves (closed form solution) of generators 6 and 7	54
3.1	Decomposition of 13 machine system and formation of coherent groups	74
3.2	Single line diagram of 31 machine system	76
3.3	Decomposition of 31 machine system and formation of coherent groups	78
3.4	Base case swing curves of the generators in coherent group 1 (31 machine system)	83
3.5	Swing curves (closed form solution) of the generators in coherent group 1 (31 machine system)	84
3.6(a)	Coherent group no.1 in the full scale system	89
3.6(b)	Equivalent representation of coherent group no.1	90

Fig. No.		Page
3.7(a)	Coherent group no.2 in the full scale system	91
(b)	Equivalent representation	91
3.8	Responses of generator 1 in (i) full scale system and (ii) equivalent	92
3.9	Responses of $\Delta\delta_{43}$ in (i) full scale system and (ii) equivalent.	93
4.1	Transformation of machine current to network reference frame D-Q	99
4.2	Single machine infinite bus system	111
4.3	Responses of state variable $\Delta\delta$ (single machine infinite bus system)	113
4.4	Responses of state variable $\Delta E'_q$ (single machine infinite bus system)	114
4.5	Three machine system	115
4.6	Responses of state variable $\Delta\omega_1$ (three machine system)	117
4.7	Responses of state variable $\Delta\delta_2$ (three machine system)	118
4.8	Responses of state variable Y_{e4} of machine 1 (three machine system)	119
5.1	Single machine infinite bus system with a double circuit transmission line	129
5.2	Three winding model of a synchronous machine	130
5.3	Simplified model of an exciter-voltage regulator system	132
5.4	Simplified model of a turbine-governor system	132
5.5	Responses of state variable δ (single machine infinite bus system)	142

Fig. No.

Page

5.6	Responses of state variable ω (single machine infinite bus system)	143
5.7	Responses of state variable E_{fd} (single machine infinite bus system)	144
C.1	Multiport representation of a synchronous machine	170
C.2	Linear model of an exciter-voltage regulator System	175
C.3	Simplified linear model of a turbine-governor ^r system	175

LIST OF TABLES

Table No.		Page
2.1	[A'] matrix	48
2.2	[B] matrix	49
2.3	Coherency Indices	50
2.4	Coherency Indices	60
2.5	Coherency Indices	62
2.6	Computation times for Coherency Analysis in UPSEB System	64
3.1	Electromechanical Distances	72
3.2	Grouping of Coherent Generators in Region III	73
3.3	Grouping of coherent generators in Region Region II	75
3.4	Electromechanical Distances	77
3.5	Formation of Coherent Groups in Region II	80
3.6	Formation of Coherent Groups in Region III	81
4.1	Eigenvalues	121
4.2	Computation times	122

LIST OF TABLES

Table No.		Page
2.1	[A'] matrix	48
2.2	[B] matrix	49
2.3	Coherency Indices	50
2.4	Coherency Indices	60
2.5	Coherency Indices	62
2.6	Computation times for Coherency Analysis in UPSEB System	64
3.1	Electromechanical Distances	72
3.2	Grouping of Coherent Generators in Region III	73
3.3	Grouping of coherent generators in Region Region II	75
3.4	Electromechanical Distances	77
3.5	Formation of Coherent Groups in Region II	80
3.6	Formation of Coherent Groups in Region III	81
4.1	Eigenvalues	121
4.2	Computation times	122

LIST OF PRINCIPAL SYMBOLS

B_{ij}	imaginary part of the ij th element of reduced admittance matrix (p.u.)
D	damping coefficient (MJ/elec. rad./base MVA)
E	magnitude of internal voltage of a synchronous machine (p.u.)
$E.V.$	eigenvector
E''_N	voltage behind subtransient impedance (p.u.)
E''_D, E''_Q	D and Q axes components of E''_N (p.u.)
E''_d, E''_q	d and q axes components of E''_N (p.u.)
E'_d, E'_q	d and q axes components of the voltage behind transient reactance (p.u.)
E_{fd}	field voltage (p.u.)
G_{ij}	real part of the ij th element of reduced admittance matrix (p.u.)
H	inertia constant (secs.)
I_m	machine current (p.u.)
I_D, I_Q	D and Q axes components of machine current (p.u.)
I_d, I_q	d and q axes components of machine current (p.u.)
I_{kd}	d-axis damper winding current (p.u.)
I_{kq1}, I_{kq2}	q-axis damper currents (p.u.)
K_A, K_E, K_f	gains in exciter-voltage regulator system
K_g, K_h, K_1, K_2	gains in turbine-governor system
K'_g	(K_g/ω_o) augmented gain
M	$(2H/\omega_o)$ angular momentum (MJ-sec./Elec.rad./base MVA)

P_{ai}	accelerating power of generator at $t=0^+$ (p.u.)
P_e, P_g	electrical power output of synchronous machine (p.u.)
P_m	mechanical power input of synchronous machine (p.u.)
r_a	armature resistance (p.u.)
r_ℓ	transmission line resistance (p.u.)
t	time (secs.)
t_e	fault clearing time (secs.)
T'_{do}, T'_{qo}	d and q axes open circuit transient time constants (secs.)
T''_{do}, T''_{qo}	d and q axes open circuit subtransient time constants (secs.)
T_E	exciter time constant
T_R, T_{A1}, T_{A2}	time constants in voltage regulator system
T_d, T_g, T_c, T_h	time constants in turbine-governor system
T_e, T_m	electromechanical torque and mechanical torque input of synchronous machine (p.u.)
T_{mo}	mechanical input torque due to setting action of value (p.u.)
V_t	machine terminal voltage (p.u.)
V_D, V_Q	D and Q axes components of V_t (p.u.)
V_{ref}	reference voltage
x_{al}	armature leakage reactance (p.u.)
x_d, x_q	d and q axes synchronous reactances (p.u.)
x'_d, x'_q	d and q axes transient reactances (p.u.)
x''_d, x''_q	d and q axes subtransient reactances (p.u.)
x_{fl}	leakage reactance of field winding (p.u.)

$x_{kd\ell}$	leakage reactance of d axis damper winding (p.u.)
$x_{kq\ell 1}, x_{kq\ell 2}$	leakage reactances of q axis damper windings (p.u.)
x_{ℓ}	transmission line reactance (p.u.)
δ	rotor angle of synchronous machine with respect to a synchronously rotating reference frame (rad.)
δ_{ij}	$(\delta_i - \delta_j)$ relative rotor angle (rad.)
δ^0	rotor angle at an operating point (rad.)
ω	angular speed (rad./sec.)
ω_0	synchronous speed (rad./sec.)
ω_r	reference speed (rad./sec.)
ψ_d, ψ_q	d and q axes components of stator windings flux linkages (p.u.)
ψ_{fd}	field flux linkages (p.u.)
ψ_{kd}	flux linkages of d-axis damper windings (p.u.)
ψ_{kq1}, ψ_{kq2}	flux linkages of q-axis damper windings (p.u.)

The other symbols in the text are explained as and when they are introduced.

SYNOPSIS

R.P. ADGAONKAR

Ph.D.

Department of Electrical Engineering
Indian Institute of Technology, Kanpur

April 1979

DYNAMIC EQUIVALENTS FOR POWER SYSTEM STUDIES

Two major problems in the stability studies of present day large scale power systems are (i) dimensionality of the model and (ii) numerical stiffness of the system equations. The problem of dimensionality arises because of the large size of the interconnected power system and the recent trend to represent the dynamics of a generating unit (synchronous machine and the associated controls) in greater detail. In addition to the dimensionality, the full scale dynamic model of a large power system is associated with the problem of stiffness in the numerical integration because it accounts for both slow and fast phenomena in the system. Hence the digital simulation of large systems become expensive in terms of computer time. Since the digital simulation for different loading levels, network configurations and disturbances is a routine feature in the power system planning and operation, the use of full scale models is uneconomical and undesirable. Therefore, simplified and reduced order models of power systems, which, apart from alleviating the difficulties mentioned above, describe the response of the system within engineering accuracy, are constructed. The problem of

dynamic equivalence is concerned with deriving such reduced order models. This thesis addresses itself to some aspects of this problem for transient (nonlinear model) and dynamic stability (linear model) studies.

The concept of study system and external system (Undrill 1971), which is generally used in the development of an equivalent for transient stability studies, is familiar to power engineers. Thus the reduced model of a power system for transient stability studies consists of the full scale representation of the study system and an equivalent of the external system. Such a reduced order model (which we will refer as the equivalent of system) is used to obtain the response of the study system for local disturbances as it is affected by the external system. Among the equivalents for transient stability studies, the principle of coherency based dynamic equivalence is likely to be widely used in power industry because of its simplicity, accuracy and the fact that physical correspondence with the components of a power system is retained in the equivalent. The basic steps in the development of a coherency based dynamic equivalent are (i) identification of the groups of coherent generators valid for a set of fault locations in a given study system and (ii) dynamic aggregation of each coherent group into an equivalent generating unit.

Identification of coherent generators constitutes a key step in the construction of a coherency based dynamic

equivalent. Since the knowledge of coherent groups valid for a set of fault locations in the given study system is a basic requirement for constructing the equivalent, the problem is to identify the groups for multiple fault locations in the study system. The method for grouping the generators should be simple and efficient in terms of computer time. The reliability of results is of prime importance because there should not be any need to verify the results from the base case swing curves. Formation of coherent groups on the basis of base case transient stability studies results in prohibitively large computer times. Many of the existing methods of coherency analysis (Lee, Spadling, Voropai and others) do not reflect the maximum angular excursion between the generators during the transient period and hence are empirical. The method of linear simulation proposed by Podmore uses simplified swing curves and has been proved to be reliable by extensive testing. However, the method requires storage and comparison of swing curves. Furthermore the linear simulation has to be repeated for every change in the fault location. Therefore, there is a need for a direct criterion for coherency analysis which is suitable for multiple fault locations and does not resort to storage and comparison of swing curves.

Over the past few years, although the equivalising techniques have been perfected, the basis for determining the levels of complexity in modelling the generators (before an equivalent is developed) has remained largely heuristic. For

example, it has been a common practice to represent the generators away from the fault location with lesser detail than those in the vicinity of it, thereby ignoring completely the electromechanical effects during the transient period. In the literature, the admittance and reflection distance measures (Lee and Schweppe) are proposed for the above purpose. While the admittance distance is a static measure, the reflection distance partially reflects the electromechanical effects during the transient period. Therefore there is a need for an improved criterion which demarcates a power system into different regions for the purpose of modelling the generators.

The existing techniques for simplifying the linear dynamic models of power systems for dynamic stability studies are mainly based on modal analysis (Kuppurajulu, Altalib, Van Ness and others) i.e. retaining the dominant modes and eliminating insignificantly excited modes. This, however, involves the computation of eigenvectors and reciprocal basis vectors, which becomes unwieldy if the size of the system matrix is large. Therefore, the time required to compute the reduced model may prove to be prohibitive unless the equivalent is used for multiple stability studies. The state variable grouping technique (Kuppurajulu) does not require these computations but the method requires a priori knowledge of the behaviour of the state variables. Thus there exists a scope for developing simpler techniques with

a rigorous mathematical basis for simplifying the linear models of power systems for dynamic stability studies.

This thesis presents solution to some of the above mentioned problems. The scope of thesis is broadly divided into two parts.

- (i) Identification of coherent generators and decomposition of power systems using a new approach, and construction of coherency based dynamic equivalents.
- (ii) Application of the singular perturbation theory to obtain simplified models and simulate the power system for stability studies.

A chapterwise summary of the work done in this thesis is given below.

The first chapter includes introduction to the problem, a brief review of the existing methods and the scope of the thesis.

The second chapter deals with a new method for identifying the coherent generators in power systems. The method is analytical and uses the concept of coherency index for grouping the coherent generators. The linearised swing equations of the system are cast into the usual state space form after selecting the generator nearest to the fault location as reference generator. Effect of fault is taken into account in terms of an input vector for the linearized system as done by Podmore. A closed form solution of the system equations is obtained in terms of the decoupled modes.

The extent to which each mode is excited is determined by the fault condition under consideration. A new concept of coherency index, which is a measure of the maximum angular excursion between two machines during the transient period, is introduced. The coherency index exploits the nature of the closed form solution in terms of the eigenvectors, reciprocal basis vectors and the state of the system at the time of fault clearing. Therefore the coherency index between two machines serves as a logical criterion to determine the coherency between the machines. When it is required to determine the groups for different fault location in the study system, the eigenvectors and reciprocal basis vectors corresponding to a new reference generator are not recomputed. Instead they are derived from the existing ones by using a similarity transformation. The use of similarity transformation eliminates the repetitive computations for different fault locations. In a similar manner the method can be easily adapted for the change in the geographical configuration of the study system itself. Two power system examples are presented to validate the theory in practical systems.

In the third chapter, the problems of decomposition of power systems and construction of coherency based dynamic equivalents are taken up. The decomposition of a power system into different regions is primarily aimed at determining the relative degree of complexity in modelling the generators before an equivalent is developed. A new concept of

electromechanical distance, which is used as the basis for decomposition of a power system, is presented. The concept is similar to coherency index except that it is measured between a generator in the external system and the reference generator in the study system. The decomposition of the power system is linked with coherency analysis and the possibility of grouping the generators in each region separately is established. The equivalising methods for combining the terminal buses of coherent generators and the aggregation of coherent units are described. A case study of a typical power system in India illustrating the principle of coherency based equivalents is presented.

The rest of the thesis is devoted to the application of singular perturbation theory to the problems of dynamic simplification and simulation in power system stability studies. The primary motivation for using the singular perturbation technique is that, in this technique, the slow and the fast subsystems are solved separately and in two different time scales. The technique first reduces the model by neglecting the fast phenomena in the system. It then improves the approximation by reintroducing their effects as 'boundary layer correction' calculated in different time scale. Further improvements in the solution are possible by evaluating the subsequent terms in the asymptotic expansion. These features of the singular perturbation theory make it very suitable for application in large scale systems. The technique has been extensively applied in optimal control and linear

regulator problems by Kokotovic and others. It has also been used in other branches of engineering. However, so far, the technique has not been used in the stability studies of large scale power systems for model simplification and subsequent simulation.

The fourth chapter describes the application of singular perturbation theory to power system dynamic stability studies. First a state space model of a multimachine power system for dynamic stability studies using the detailed representation of the dynamics of the generating units is obtained. These system equations are transformed into the singular perturbation form by properly identifying the perturbation parameter ' ϵ ' in small rotating masses, small time constants and large gains etc. The use of ' ϵ ' in practical systems is symbolic and represents the presence of fast as well as slow subsystems. The presence of these subsystems in a given model is identified by a criterion, which examines the eigenvalues of the system matrix. The degenerate system i.e. setting $\epsilon = 0$ in the system equations gives the simplified model of the original system. In the simplified model, the identity of the corresponding state variables of the original system is retained. The response of the degenerate system is further improved by adding the terms corresponding to ' ϵ ' in the asymptotic expansion to obtain a first order solution. A single machine infinite bus and a three machine example is presented to illustrate the theory. It is also established that the first order solution

is a good approximation to the response of the original system and can be obtained with far less computer time as compared to simulating the original system.

Chapter five deals with the singular perturbation approach to the transient stability studies in power systems. The technique uses the method of asymptotic expansion as applied to nonlinear differential equations (initial value problem). The relevant theory is described and illustrated with the help of a numerical example. The difficulties encountered with nonlinear models of power systems are clearly brought out and explained.

A summary of the contributions in the thesis and the scope for further research in this field are given in the concluding chapter.

CHAPTER 1

INTRODUCTION

1.1 STABILITY STUDIES

Stability considerations have been recognised as an essential part of power system planning and operation for a long time. In the planning stage, routine stability calculations are made to ensure the stability of the system with proposed transmission and generator configurations. The stability studies are also necessary for coordination of system protection and design of control systems. In the 'on line' operation of power systems, quick stability calculations at regular intervals enable the operator in an energy control center to take corrective actions so as to ensure security of the system against likely contingencies. A power system engineer is primarily concerned with two types of stability studies namely (i) transient stability and (ii) dynamic stability. While the former is associated with large and aperiodic disturbances and uses nonlinear mathematical model, the latter is concerned with small signal analysis around an operating point. The disturbances considered for dynamic stability studies are continuous and small in magnitudes so that the linearised mathematical model is adequate.

1.2 STATEMENT OF THE PROBLEM

The mathematical model of a power system for stability

representing the dynamics of the generating units (synchronous machines and their controls) and a set of algebraic equations describing the interconnections through the transmission network. The major problems encountered in the dynamic simulation are (i) dimensionality of the model and (ii) 'stiffness' of the system equations. The problem of dimensionality arises due to the large size of a power system and is further aggravated by increased interconnections and the recent trend to represent the dynamics of the generating units in greater detail. It is highly uneconomical and undesirable to simulate a large sized model on a digital computer for different loading conditions, system configurations and disturbances. The other problem of numerical 'stiffness' of system equations arises because the system matrix has eigenvalues with very small as well as very large magnitudes. This necessitates use of prohibitively small time step size in numerical integration and hence the dynamic simulation becomes expensive in terms of the computer time. In order to reduce the computations and storage requirements without sacrifice in engineering accuracy, one resorts to simplified and reduced order models. The problem of dynamic equivalence is concerned with deriving such reduced order models. Some of the important aspects of the problem are (i) time of computation required for constructing the equivalent, (ii) an appropriate compromise between reduction in size and loss of accuracy and (iii) physical correspondence of the reduced system with the components of the original

system. The last aspect makes it possible to use the conventional stability programs, which have been perfected over the years, in simulating the reduced system without any modification.

This thesis addresses itself to this problem of dynamic equivalence and simulation of power systems for transient and dynamic stability studies through reduced order models. The first part of the thesis is concerned with coherency based dynamic equivalents for transient stability studies. The following problems from this area are investigated.

- (i) Identification of coherent generators in large scale power systems based on eigenvectors and reciprocal basis vectors of the linearized system.
- (ii) Decomposition of power systems into regions using techniques developed for (i) to determine the relative degree of complexity in modelling the generators.
- (iii) Construction of the dynamic equivalent.

The second half of the thesis deals with the application of singular perturbation theory to the problem of dynamic equivalence and simulation of power systems for transient and dynamic stability studies. The problems investigated are the following.

- (i) Modelling of power systems in the singular perturbation form for dynamic and transient stability studies.

- (ii) Development of the reduced order model and the subsequent improvement in the response using singular perturbation theory.

We now briefly review the pertinent literature in these areas before outlining the objectives and scope of the thesis.

1.3 THE STATE OF ART

1.3.1 Dynamic Equivalents for Transient Stability Studies:

In the development of dynamic equivalents for transient stability studies, a power system is generally divided into two parts namely (i) the study system and (ii) the external system. The study system is that part of the system in which the system behaviour is of direct interest and where a set of disturbances are considered. The part excluding the study system is the external system, which is equivalised. Thus the reduced model of a power system for transient stability studies consists of the full scale representation of the study system and an equivalent of the external system. Such a model (which we will refer to as the equivalent of the system) gives the response of the study system for the disturbances in the study system. If the external system has been properly equivalised, this response should agree within engineering accuracy with that of the original full scale system.

The existing techniques for constructing the equivalents for transient stability studies are broadly classified into three groups.

- (ii) Equivalents based on modal analysis [4-6].
- (iii) Equivalents based on coherency [7-14].

In (i), the generation and loads in the external system are equivalised based on the concept of distribution factors. However the resulting reduced order model may not preserve the dynamic characteristics of the original system to sufficient accuracy because the generators are equivalised irrespective of their different dynamic responses. The method of allocating the inertias to the equivalent generators [3] is heuristic. Therefore these equivalents give very approximate results. In a recent paper [72], new distribution factors are defined based on the concept of moment. Here the dynamic effects of inertias, generation and loads in the external system are transferred to the boundary buses using the laws of mechanics. For this purpose, the machine inertias, loads and generation at the respective buses are considered as forces and the transfer impedance between the two buses is considered as the distance.

In the modal equivalent method [4], the external system, where the disturbance propagated is assumed to be small, is modelled by linearised differential equations and the study system by the usual nonlinear differential equations. The external system matrix is reduced by retaining only the dominant modes. A mode is neglected [5] if (i) it decays fast as compared to other modes or (ii) it is insignificantly excited. Modal equivalents need computation of eigenvectors and reciprocal basis vectors, which becomes unwieldy if the

size of system matrix is large. A recent comprehensive testing of the modal equivalent method [6] indicates the suitability of the technique only when a number of faults in the study system are analysed using the same equivalent. The reduction of external system matrix needs a better understanding of mode selection process and any error in the judgement results in degradation of the performance of the modal equivalent. Furthermore, the reduced model does not retain the physical correspondence with the components of a power system.

In the coherency based equivalents [7-14], a group of generators having similar dynamic responses for a fault in the study system is replaced by an equivalent generator. References [7-9] describe algorithms for obtaining a reduced set of transient stability equations based on the concept of coherency. However, the reduced equations derived in these references do not reflect physical significance in terms of the normal power system components. A significant contribution in the area of coherency based dynamic equivalent was made by the research group of Systems Control Inc. [10-13]. Their approach of constructing the equivalent is practical and is likely to be widely used in power industry. The basic steps consist of the following.

- (i) Definition of the study system.
- (ii) Identification of groups of coherent generators in the external system which are valid for a set of disturbances in the study system.

- (iii) Reduction of coherent generator buses.
- (iv) Reduction of load buses.
- (v) Dynamic aggregation of coherent generating units.

The algorithms of identifying the groups of coherent generators reported in [12] are covered in Section 1.3.2. In the reduction of coherent generator buses, the terminal buses of the generators in a coherent group are replaced by an equivalent bus rather than combining the internal buses of the generators [7,8]. Such an approach decouples the problem of network reduction from that of dynamic aggregation of the generating units. The method used for reduction of load buses is selected based on linear or nonlinear representation of loads. A coherent group of generators is represented by an equivalent terminal bus and a generating unit connected to it. The procedure of determining the parameters of the equivalent generating unit from the parameters of the individual units in a coherent group is termed as dynamic aggregation of the generating units [12,13]. The components of generating units in a group such as synchronous machines, excitation-voltage regulator systems, turbine-governor systems etc. are aggregated separately. The technique for determining the parameters of an equivalent component is to numerically adjust the parameters so as to obtain minimal error between the frequency response of the transfer function of the equivalent component and the sum of frequency responses of the individual transfer

functions. The error to be minimised is the difference of squares in the two frequency responses at specified discrete frequencies.

The approach of Systems Control Inc. [12] has the following features.

(i) The development of equivalent is systematic and general, accommodating different types of synchronous machines, their control equipments and the nonlinear characteristics of loads.

(ii) The equivalent is composed of normal power system components and, therefore, is compatible with the existing transient stability programs.

(iii) The different tests on large scale power systems [12] demonstrate the capability of the equivalent to handle the transient stability simulation of large systems within a reasonable time.

Other references on the equivalents for transient stability studies are given in [14-21].

1.3.2 Coherency Analysis:

Identification of coherent generators in the external system valid for a disturbance/a set of disturbances in the study system is a key step in the development of coherency based dynamic equivalents. In the earlier stages of its development, the base case transient stability swing curves were compared to classify the coherent generators. However,

the numerical integration of nonlinear equations is time consuming and hence undesirable for the purpose of coherency analysis. Hence a need arose for more efficient and simple algorithms for coherency analysis and many researchers have contributed to this area.

(a) Pattern Recognition Method: Lee and Schweppe [22], based on extensive analog simulations, presented three features which are central to the phenomenon of coherency. The features are as follows:

$$r_1 = \frac{\frac{\text{Max}(a_i) - \text{Min}(a_i)}{i}}{\text{Max}(a_i)} \quad (1.1)$$

where a_i is the acceleration of generator 'i' at $t=0^+$.

$$r_2 = \frac{\text{Min}_{i \in C} \left[\text{Min}_{i \in C, j \neq i} (y_{ij}) \right]}{\text{Max}_{i \in C} \left[\text{Max}_{k \in \phi} (y_{ik}) \right]} \quad (1.2)$$

where C = set of machines considered for coherency,

ϕ = set of inner circle (study system) generators,

y_{ij} = transfer admittance between the generators 'i' and 'j'.

$$r_3 = \frac{\frac{\text{Max}(M_i) - \text{Min}(M_i)}{i}}{\text{Max}(M_i)} \quad (1.3)$$

The coefficient r_1 compares the degree of difference between the accelerations at $t=0^+$ of the machines considered for coherency. r_2 measures the electrical coupling between

the machines considered for coherency relative to the machines in the study system. The feature r_3 defines the similarity of inertias. A measure of the degree of coherency is defined by the coherency factor as

$$y = \max_t \left[\max_{i,j} \left[\frac{\Delta \delta_i(t) - \Delta \delta_j(t)}{\max(\Delta \delta_i, \Delta \delta_j)} \right] \right] ; \quad 0 \leq t \leq 1 \text{ sec.} \quad (1.4)$$

The coherency factor defines the allowable deviation in the relative rotor angle among coherent machines as a percentage of the maximum deviation in the transient period.

The coherency criteria for a 10% coherency factor 'y' is defined as

$$r_1 \leq 30\% , \quad r_2 \geq 3 \quad \text{and} \quad r_3 \leq 90\% \quad (1.5)$$

As it is clear from the definitions, the features r_1 , r_2 and r_3 are defined by the system parameters and the acceleration power at $t=0^+$. These features do not reflect the maximum deviation between the machines during the transient period. Therefore the method is empirical and lacks the required consistency in results [12].

(b) Technique using Singular Point: Spadling et al.[23] presented a technique for identifying coherent generators by making use of the singular point concept. In this technique, the rotor angles of the generators are compared at both the initial stable operating point and the nearest post-fault unstable equilibrium point corresponding to the

expected mode of instability for a given fault. Fig. 1.1 shows the region of attraction around the origin, which is the post-fault stable operating point. The pre-fault stable operating point (initial conditions) is denoted by $\underline{\delta}^0$ and the nearest unstable equilibrium (singular) point is denoted by $\underline{\delta}^S$. The authors claim that if the fault is cleared at t_2 , i.e. critical clearing time, the resulting trajectory is maximal and approaches the nearest unstable equilibrium point. However this fact is not observed in the base case transient stability studies because the singular point under consideration is unstable. Two generators 'i' and 'j' are classified as coherent if

$$|\delta_{ij}^0 - \delta_{ij}^S| \leq \epsilon \quad (1.6)$$

where ϵ is the tolerance.

The computational effort required by this method is very small i.e. the solution of a set of $(n-1)$ nonlinear algebraic equations for a n machine system to obtain the required singular point $\underline{\delta}^S$. For this purpose, the mode of instability for a given fault has to be assumed apriori. This, in general, is a very difficult problem and depends on type, location of fault and system loading conditions. The criterion (1.6) verifies the features of coherency only at two points of the trajectory. Generators which are geographically remote may satisfy the criterion (1.6). Therefore the criterion is to be backed up by the concept of admittance distance [22].

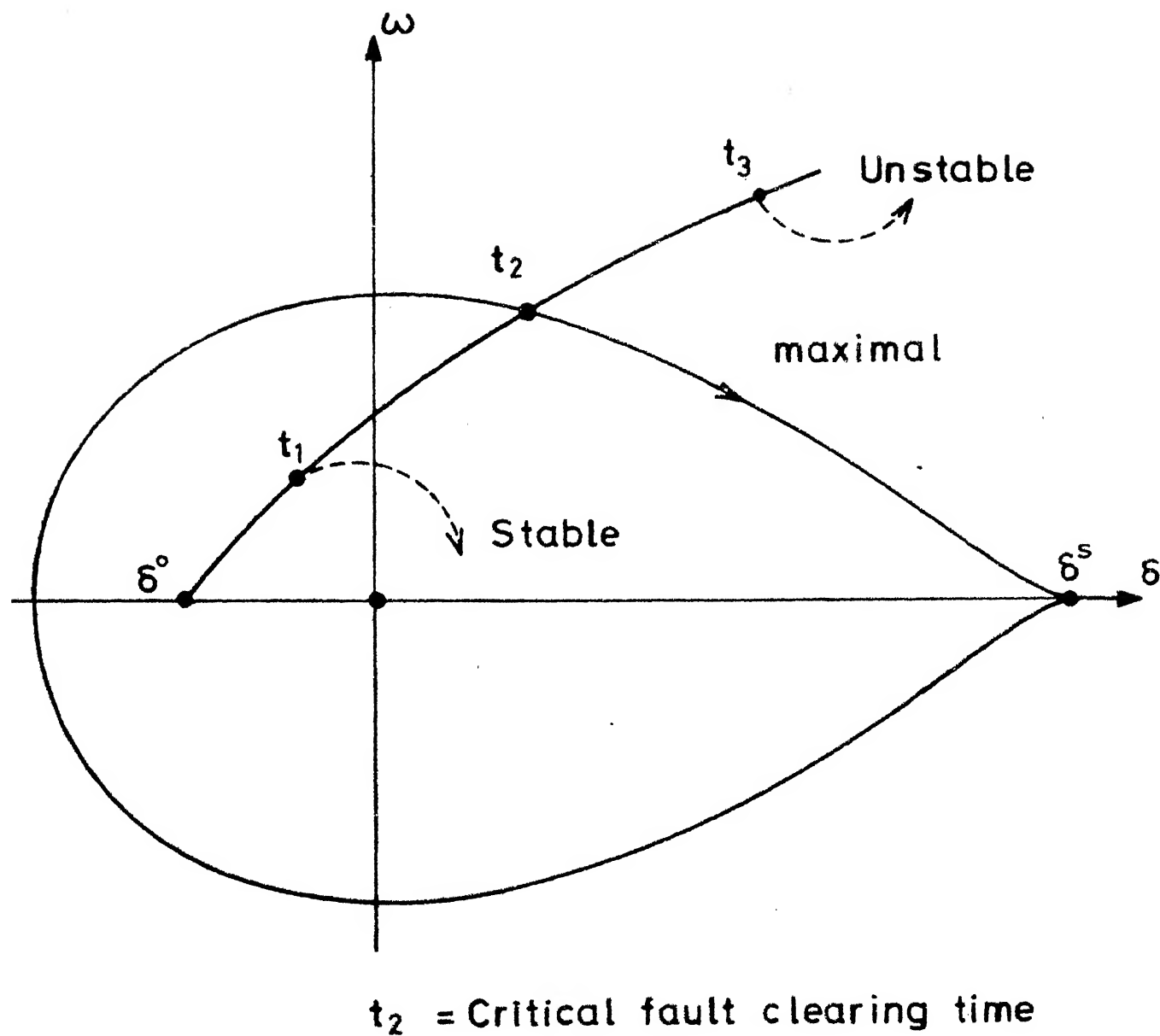


Fig.1-1 Trajectories in a region of attraction around the post-fault stable operating point

(c) Linear Simulation Method: The method of linear simulation [24], proposed by Podmore, essentially determines the groups of coherent generators by comparing the swing curves obtained from the simplified linear model of the system. An important aspect of this method is the manner in which a fault condition is reflected. The response of a faulted system is approximated by the response of the unfaulted system when each generator is subjected to a step input. The magnitude of the step input to a generator is equal to the accelerating power of the generator at $t=0^+$ and duration of the input is equal to the clearing time of fault.

Considering the classical models for the generators, the linearised swing equations for mechanical motion of the i th synchronous generator in a ' n ' machine system is given by

$$M_i \frac{d(\Delta\omega_i)}{dt} = \Delta P_{mi} - \Delta P_{gi} - D_i \Delta\omega_i \quad (1.7)$$

$$\frac{d(\Delta\delta_i)}{dt} = \Delta\omega_i \quad i=1,2,\dots,n \quad (1.8)$$

the d.c. load flow equations are

$$\begin{bmatrix} \Delta \underline{P}_g \\ \Delta \underline{P}_l \end{bmatrix} = \begin{bmatrix} H_{gg} & H_{gl} \\ H_{lg} & H_{ll} \end{bmatrix} \begin{bmatrix} \Delta \underline{\delta} \\ \Delta \underline{\theta} \end{bmatrix} \quad (1.9)$$

where \underline{P}_g and $\underline{\delta}$ = the powers and rotor angles at generator internal buses,

\underline{P}_l and $\underline{\theta}$ = the powers and voltages angles at load buses.

The elements of the Jacobian H are derived from the appropriate partial derivatives or, if the flat voltage profile is assumed,

it may be derived directly from the [B] matrix of the fast decoupled load flow [25]. The different types of disturbances are reflected in ΔP_{mi} , ΔP_{li} or ΔP_{gi} depending upon the electrical fault, loss of load or loss of generation. The swing curves are obtained by integrating the equations (1.7) and (1.8) by trapezoidal rule [26] and solving the network equations (1.9) at the end of each integration step. The groups of coherent generators are determined by processing the swing curves in a clustering algorithm [12].

The modelling of disturbances proposed in this method is valid for typical fault clearing times and the swing curves obtained from the linear model are shown to preserve the coherency property in the system. Therefore, the method is simple and efficient. The extensive testing of the method on different practical power systems [12] has proved the reliability of the results. However, the simulation has to be repeated for every change in the fault location and the method needs storage and comparison of swing curves.

(d) Other Methods: The use of Laplace transform and Fourier transform have also been attempted in [12, 30]. However these approaches have not been found computationally attractive as compared to linear simulation. Schlueter et al. [27] derived an expression for r.m.s. coherency measure [11] using the linearised model [24]. Their method uses probabilistic model of power system disturbances and the concept of modes in deriving the expression for r.m.s. coherency measure.

Pai and Narayana [14] viewed the coherency between the generators from the energy concept. In their approach, two generators 'i' and 'j' are classified as coherent if the potential energy component associated with this pair is zero during the transient period. Mathematically the criterion is expressed as

$$P.E._{ij}(t) = E_i E_j B_{ij} \int_0^{\sigma_{ij}} [\sin(\sigma_{ij} + \delta_{ij}^0) - \sin \delta_{ij}^0] d\sigma_{ij} < \epsilon \quad (1.10)$$

where $\sigma_{ij} = \delta_{ij} - \delta_{ij}^0$

Voropai [28] derives certain coherency coefficients from the following equation for a pair of machines.

$$\frac{d^2 \delta_{ij}}{dt^2} = P_{ij} - D_{ij} \sin \delta_{ij} - A_{ij} \quad (1.11)$$

where P_{ij} , D_{ij} and A_{ij} are assumed as constant. The concept of equal area criterion is used to derive these coefficients. An examination of the above equation shows that the interconnections of the machines 'i' and 'j' with the rest of the system are completely ignored. Therefore, such decoupled equations are not valid in multimachine systems. The ' α ' and ' β ' coefficients for coherency analysis derived by Varwandkar [29] are also constrained by a similar drawback.

The above survey of coherency analysis indicates that there are many methods of coherency analysis in the literature. However, many of them lack the mathematical basis, consistency

of results or they are not tested for large scale systems. The most promising technique, however, is that of linear simulation [12, 24]. The approximations involved in this method have been validated on large scale power systems. The method is simple and efficient. However, it requires the computation and comparison of swing curves and the process has to be repeated as the fault is moved in the study system. The same is true if the geographical configuration of the study system is changed. The method presented in this thesis overcomes some of these drawbacks. Our approach using the linearised model, develops coherency indices derived from the eigenvectors and reciprocal basis vectors for determining the groups of coherent generators. The method is shown to be useful when different fault locations are considered or the study system gets changed. Its demonstration for a large realistic systems establishes its utility for practical applications.

1.3.3 Simplified Models for Dynamic Stability Studies:

The techniques for simplifying the linear models of power systems used in dynamic stability studies are mainly based on modal methods [31-38]. In the modal methods, the dominant modes are retained in the reduced model and the insignificantly excited modes are neglected. Kuppurajulu and Elangovan[39] derived three different reduced models for initial, intermediate and final responses using the eigenvalue grouping technique. Davison's method [31] has been applied to simplify the linear dynamic models of power systems by Altalib and

Krause [41]. They have used a decentralised approach in the sense that, first the reduced order model of each subsystem such as exciter-voltage regulator system, turbine governor system etc. is reduced separately and these individual reduced order models are combined to obtain the reduced model of the system. Radhakrishna et al.[42] proposed the decomposition of full scale system model into different subsystems based on the criterion for weakly coupled systems given in [43]. Each of these subsystems is reduced individually and the reduced subsystems are combined to obtain the equivalent of the original system. These decomposition techniques, however, need to be tested for large power systems to establish their practical utility.

In the topological method presented by Van Ness [44], the block diagram and the interconnections that are to exist in the reduced order model are apriori specified. Such a specification of the topology determines the nonzero elements of $[A]$ matrix. As in the modal methods, the eigenvalues of the reduced system are chosen from the eigenvalues of the original system. Some elements of eigenvectors are also chosen but there must be some relaxation of eigenvectors in order that the required topology can be realised. Then the values of nonzero elements of $[A]$ matrix, which give the required eigenvalues and eigenvectors, are computed. The method is not simple to use in practice because in some cases the solution may not exist and it is difficult to determine the parameters

that will give the desired eigenvalues and eigenvectors. In the subsequent paper [45] the author used the optimisation techniques to determine the parameters of the specified reduced model. The difference between the specified and the actual eigenvectors is minimised subject to the constraints that the reduced matrix has the specified eigenvalues.

The methods for simplifying linear models of power systems, which do not resort to the eigenvectors and reciprocal basis vectors, are the classical method [44] and state variable grouping technique [39]. In the classical method, the dynamic elements such as time constants, rotating masses etc., whose effect on the system response is considered to be negligible, are deleted. The classical method is simple but gives the least accurate representation of the original system. In the state variable grouping technique, the state variables \underline{X} of the original system

$$\dot{\underline{X}} = [\underline{A}] \underline{X} + [\underline{B}] \underline{u} \quad ; \quad \underline{X}(0) = \underline{X}^0 \quad (1.12)$$

are grouped as

$$\begin{bmatrix} \dot{\underline{X}}_1 \\ \dot{\underline{X}}_2 \end{bmatrix} = \begin{bmatrix} \underline{A}_{11} & \underline{A}_{12} \\ \underline{A}_{21} & \underline{A}_{22} \end{bmatrix} \begin{bmatrix} \underline{X}_1 \\ \underline{X}_2 \end{bmatrix} + \begin{bmatrix} \underline{B}_1 \\ \underline{B}_2 \end{bmatrix} \underline{u} \quad (1.13)$$

The groups \underline{X}_1 and \underline{X}_2 are associated with large and small time constants in the system respectively. The state variables \underline{X}_1 (which vary slowly as compared to \underline{X}_2) are assumed to be constant during the initial period. Then the transient

response in the initial period is represented by the simplified model

$$\begin{aligned}\underline{\dot{X}}_1 &= \underline{X}_1^0 \\ \underline{\dot{X}}_2 &= [A_{22}]\underline{X}_2 + [A_{21}]\underline{X}_1^0 + [B_2]\underline{u}\end{aligned}\quad (1.14)$$

During the final stages of the transient response, the fast ~~transients~~ would have decayed and $\underline{\dot{X}}_2 = \underline{0}$. Hence the system model for the final stages of the transient response is given by

$$\underline{\dot{X}}_1 = [A^*]\underline{X}_1 + [B^*]\underline{u}\quad (1.15)$$

where $[A^*] = [A_{11} - A_{12} A_{22}^{-1} A_{21}]$ and $[B^*] = [B_1 - A_{12} A_{22}^{-1} B_2]$

The method is simple and intuitively correct. But the grouping of state variables is not backed up by mathematical criterion and one has to have apriori knowledge of the behaviour of the state variables. The boundary separating the periods of initial and final responses is not clearly defined. Later we will show that the models (1.15) and (1.14) can be derived from the singular perturbation approach.

An inspection of the preceding methods for the simplification of linear models of power systems brings out the following points:

(i) Modal techniques, though mathematically sound, need a clear understanding of mode selection process and computation of eigenvectors and reciprocal basis vectors.

(ii) State variable grouping technique is efficient but needs the apriori knowledge of the behaviour of the state variables. Therefore the validity of results largely depends upon the human judgement.

The above review underlines the need for a distinct and simple approach to the model simplification and simulation problem in dynamic stability studies. In the approach presented in this thesis, the response of the full scale model is considered as a perturbation of the response of the reduced system. Singular perturbation theory is well known in the mathematical literature. In the next section, we briefly review the important aspects and the applications of the singular perturbation theory pertinent to the power system problems.

1.3.4 On the Singular Perturbation Technique to Power System Problem:

Two important features of the singular perturbation technique which make it suitable for large scale power systems are the following:

(i) Firstly the technique reduces the size of the given model by neglecting the fast phenomena in the system. It then reintroduces the effect of the fast phenomena as a correction term known as the boundary layer correction.

(ii) The fast and slow subsystems are solved separately and in different time scales, thereby alleviating the stiffness problem associated with the original system of equations.

An excellent review of the singular perturbations and order reduction in control theory is given in Ref. [46]. The paper also gives a thorough list of references on the theory and applications of singular perturbation technique. A few important references which are useful for the application of the technique in power system studies, are given in [46-60]. Although the technique has been extensively used for model simplification in control theory and other branches of engineering, so far it has not been used in the studies of large scale power systems. A recent paper by Chow et al. [57] deals with the singular perturbation analysis of systems with sustained high frequency oscillations. In this paper the theory is illustrated by a three machine power system example, where the high frequency oscillations arise between two coherent machines. In the technique for model simplification of power systems presented in this thesis, we have basically used the solution of the initial value problem in terms of asymptotic expansions given by O'Malley [50].

1.4 SCOPE AND OUTLINE OF THE THESIS

With the preceding background of the work done in the area of dynamic equivalents and model simplification for power system stability studies, we now present the main objectives of the thesis and a chapterwise summary.

The main objectives of the thesis are as follows:

(i) Development of an effective criterion for coherency recognition which does not resort to simulation and comparison

of swing curves and is suitable for determining the coherent groups valid for a set of fault locations in the study system.

(ii) Decomposition of the power system by means of a criterion into different regions for determining the relative degree of details in modelling of the generators. This criterion is consistent with the criterion for coherency analysis.

(iii) Development of a technique based on the singular perturbation theory for the model simplification and simulation in transient and dynamic stability studies.

A chapterwise summary of the thesis is given below.

Chapter 2 is concerned with the problem of identification of coherent generators. The problem is introduced by enumerating the desirable features of a method for coherency analysis. The assumptions of linearity, classical models for generators and a typical modelling of electrical disturbances [24] are made in the formulation of the mathematical model for coherency analysis. Selecting a generator near the fault location as reference, the linearised swing equations are cast into the usual state space form as

$$\dot{\underline{X}} = [\underline{A}] \underline{X} + [\underline{B}] \underline{u} \quad (1.17)$$

The forcing function \underline{u} , which is the vector of accelerating powers of the generators at $t=0^+$, reflects the fault under consideration. The vector \underline{X} and the matrices $[\underline{A}]$ and $[\underline{B}]$ are defined separately for the cases of uniform and non-uniform damping in the system. Assuming that the matrix $[\underline{A}]$ has all

distinct eigenvalues, the closed form solution of (1.17) is obtained in terms of the decoupled modes. A new concept of coherency index, which is a bound on the maximum deviation in the rotor angle between two machines during the transient period, is introduced. The expression for coherency index is derived from the closed form solution of (1.17). The coherency index ' h_{ij} ' is used as a criterion for identifying the coherency between the generators ' i ' and ' j '. A systematic procedure for grouping the coherent generators is presented. In order to determine the coherent groups for a different fault location in the same study system or in a different study system, a change of the reference generator may be necessary. In such cases, the eigenvectors and the reciprocal basis vectors corresponding to a new reference generator are not recomputed. Instead they are derived from the existing ones by using a similarity transformation matrix. The similarity transformation matrix can be easily obtained by inspecting the state variables with respect to the new reference generator. This feature of the method eliminates repetitive computations of eigenvectors and reciprocal basis vectors, when different fault locations are considered. The technique of grouping the generators and the use of similarity transformation is validated on typical power system examples.

The third chapter deals with the decomposition of the power system and linking of the concept with the grouping of coherent generators. The concept of electromechanical

distance which is also a bound on the maximum deviation of a generator with respect to the reference generator in the study system, is used as a criterion for decomposing the external system into three or more regions. The study system, by definition, constitutes the innermost region. There are two motivations behind the decomposition of the external system.

(i) It helps in determining the relative degree of detail in modelling of the generators.

(ii) The concept of electromechanical distance is used to delineate the boundaries between the regions in such a manner that a generator in one region is not coherent with a generator in another region. This simplifies the procedure for formation of coherent groups.

The theory of such a unified approach for decomposition and coherency analysis is presented and validated on a power system example. Chapter 3 also contains a case study for a typical power system illustrating the principle of coherency based dynamic equivalents.

Chapter 4 addresses itself to the problem of model simplification and simulation of the power system for dynamic stability studies using singular perturbation technique. Firstly the singular perturbation theory as applied to the initial value problem [50] is explained. The important features of the technique are brought out and the motivation behind the application of the technique to the problem of dynamic stability studies is stated. A systematic procedure

for formulating a state space model of a multimachine system in the form

$$\dot{\underline{y}} = [\underline{A}] \underline{y} + [\underline{B}] \underline{u} ; \quad \underline{y}(0) = \underline{y}^0 \quad (1.18)$$

is presented. The system model is transformed into the singular perturbation form as

$$\begin{bmatrix} \dot{\underline{x}} \\ \epsilon \dot{\underline{z}} \end{bmatrix} = \begin{bmatrix} \underline{A}_{11} & \underline{A}_{12} \\ \underline{A}_{21} & \underline{A}_{22} \end{bmatrix} \begin{bmatrix} \underline{x} \\ \underline{z} \end{bmatrix} + \begin{bmatrix} \underline{B}_1 \\ \underline{B}_2 \end{bmatrix} \underline{u} \quad (1.19)$$

with $\underline{x}(0) = \underline{x}^0$ and $\underline{z}(0) = \underline{z}^0$, by properly identifying the perturbation parameter ' ϵ ' in the system equations. A logical criterion for grouping the state variables \underline{y}^T as $[\underline{x}^T, \underline{z}^T]$, representing respectively the slow and fast variables, is presented. The technique first reduces the model (1.19) by neglecting the fast phenomena and then accounts for the effect of the fast phenomena by the addition of a 'boundary layer correction'. The decomposition of (1.18) into the fast and slow subsystems helps in understanding the structural properties of the system and gives computational advantages as compared to the integration of (1.18). The computational benefits are derived mainly due to larger time step size permissible in the numerical integration of the slow and fast subsystems. A single machine-infinite bus and a three machine example are presented to illustrate the application of the theory to dynamic stability studies of power systems.

The singular perturbation theory can, in general, be extended to nonlinear system models. In Chapter 5, an attempt is made to solve the transient stability problem using singular perturbation technique. The basic requirement in the singular perturbation theory is to separate the variables \underline{y}^T in the model as $[\underline{x}^T, \underline{z}^T]$ as the slow and fast state variables and \underline{z} should be expressed as a function of \underline{x} and \underline{u} . This imposes restrictions on the selection of \underline{z} variables in a nonlinear model of power system. Furthermore, the computation of the improved response involves the solution of sets of differential equations having variable coefficients. A single machine-infinite bus power system example is solved illustrating the features of the technique.

The concluding and the sixth chapter highlights the major contributions of the thesis. Certain problems encountered during the course of this thesis are discussed and the suggestions for future work are then given.

CHAPTER 2

IDENTIFICATION OF COHERENCY

2.1 INTRODUCTION

A critical review of the existing methods for coherency analysis has been presented in Section 1.3.2 of the preceding chapter. Towards the end of the review a need for an improved criterion for identifying coherent generators has been brought out. In this chapter, an attempt is made to develop such a criterion and validate it on practical power systems. Before we describe the proposed technique, we define coherency between generators and coherency measures.

a) Maximum Angular Excursion Measure [11]: For all practical purposes, two generators, say 'i' and 'j', are defined as coherent if

$$|\Delta\delta_i(t) - \Delta\delta_j(t)| < \epsilon \text{ for } 0 \leq t \leq T \quad (2.1a)$$

where δ_i = rotor angle of generator 'i'

T = total transient period

ϵ = tolerance.

The value of ϵ is usually taken as 2.5° or 5° .

b) Root Mean Square Measure [11]: For all practical purposes, two generators 'i' and 'j' are defined as coherent if

$$\sqrt{\frac{1}{T} \int_0^T (\Delta\delta_i - \Delta\delta_j)^2 dt} < \mu \quad (2.1b)$$

where μ is the tolerance.

The maximum angular excursion measure accounts for the maximum deviation in the rotor angles between the machines during the transient period. The r.m.s. coherency measure reflects the change in the transfer of energy between the generators during the transient period. The former measure is generally preferred in the formation of groups [11] because it ensures that there is no large difference between the rotor angle of the equivalent generator in the reduced system and the corresponding angles of the individual generators belonging to the coherent group in the full scale system.

The desirable characteristics of the method for identifying coherent generators are that (i) the method must be simple to apply and efficient in terms of computer time, (ii) the results must be reliable, (iii) human judgement must be minimised and (iv) the method must be adaptable for multiple fault locations.

In the proposed method, a new concept of coherency index is introduced and used as a criterion for identifying the groups of coherent generators. The linearised swing equations of the system are cast into the usual state space form, with the forcing function reflecting the fault under consideration [24]. Then a closed form solution of the system equations is obtained in terms of the decoupled modes. A coherency index between two machines, which reflects a bound on the maximum angular excursion between the machines during the

transient period, is derived from the above closed form solution and used as a criterion for coherency analysis. A systematic procedure for grouping the generators is presented. The method does not require the storage and comparison of swing curves. The technique is easily adaptable for multiple fault locations i.e. for changes in the fault location in a study system or for changes in the geographical configuration of the study system itself. The proposed technique is validated on typical power system examples.

2.2 ASSUMPTIONS

The following assumptions, which are same as those in [24], are made in developing the mathematical model for coherency analysis.

(i) Groups of coherent generators can be determined by considering the linearised mathematical model of the power system. This is justified from the observation in the usual transient stability studies that the groups of coherent generators are independent of the size of disturbance. This assertion can be easily confirmed by considering a fault and observing that the coherent behaviour of the generators is not altered by changing the fault clearing time.

(ii) Groups of coherent generators are independent of the detailed modelling of a generating unit. Therefore a classical synchronous machine model is considered. This

assumption is based on the argument that though the control equipments have appreciable effect on the damping in the system, the natural frequencies, which predominantly determine the coherent behaviour of generators, do not alter appreciably [73].

(iii) The response of a faulted system is approximated by the response of the unfaulted system by increasing the mechanical input power of each generator by an amount P_{ai} (accelerating power at $t = 0^+$) for the time equal to fault clearing time only.

For typical fault clearing times and inertia constants, the accelerating power of each generator in the faulted period remains nearly constant. An approximate variation of the accelerating powers in the post-fault period can be reproduced by applying a step input to each generator as shown in Fig. 2.1. Other implicit assumption in the above modelling of an electrical fault is that the effect of changes in the network configuration of the study system and of the subsequent changes in the load flow on the coherent behaviour of the machines is ignored. Such a modelling of an electrical fault is valid for small fault clearing times and large systems.

In hypothesis (iii), accelerating power of each generator at $t=0^+$ is computed from the voltage profile at that instant. The required voltage profile in turn is

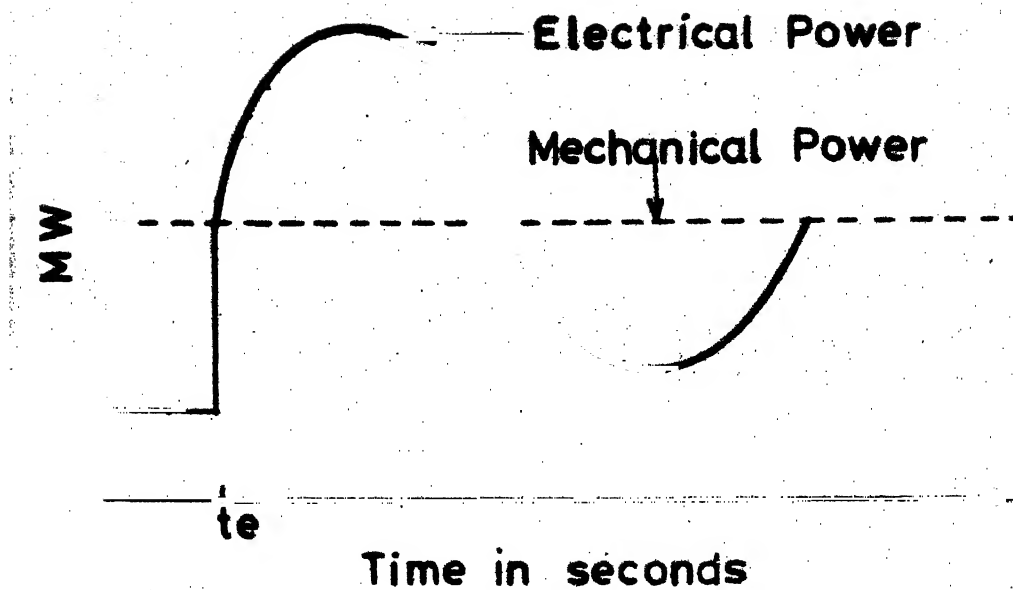


Fig.2-1a Approximate variation of accelerating power of a generator in faulted system

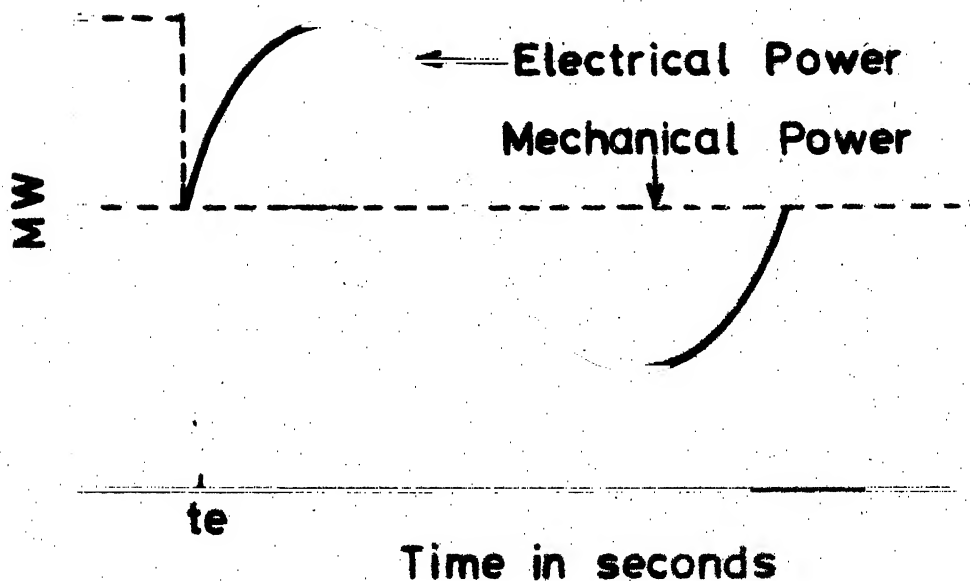


Fig. 2-1b Equivalent reproduction of accelerating power in the unfaulted system

computed either by a load flow solution at $t = 0^+$ or by a simpler noniterative procedure given below.

(i) The constant voltage behind reactance together with the reactance of each generator is converted into a Norton's equivalent. The magnitude of the current source is constant.

(ii) Treating the transient reactances now as shunt branches, the bus admittance matrix $[Y]$ is computed.

(iii) The network equations $\underline{I} = [Y]\underline{V}$ are then solved for voltages by simulating the fault and the new generator powers are computed [12].

2.3 MATHEMATICAL MODEL OF POWER SYSTEM

In a power system having 'n' number of generators, swing equation of the i th generator is given by

$$M_i \frac{d^2 \delta_i}{dt^2} + D_i \frac{d\delta_i}{dt} = P_{mi} - \sum_{j=1}^n (G_{ij} \cos \delta_{ij} + B_{ij} \sin \delta_{ij}) E_i E_j$$

$$i = 1, 2, \dots, n \quad (2.2)$$

Linearizing (2.2) around an operating point, we have

$$M_i \frac{d^2(\Delta\delta_i)}{dt^2} + D_i \frac{d(\Delta\delta_i)}{dt} = \Delta P_{mi} - \sum_{\substack{j=1 \\ j \neq i}}^n E_i E_j (-G_{ij} \sin \delta_{ij}^0 + B_{ij} \cos \delta_{ij}^0) \Delta\delta_{ij}$$

$$i = 1, 2, \dots, n \quad (2.3)$$

Under the hypotheses (i) - (iii) and considering the n th machine as reference generator, equation (2.3) is cast into the state space form in the usual manner for the faulted

and post-fault state of the system as follows.

$$\dot{\underline{X}} = [A] \underline{X} + [B] \underline{u} ; \quad 0 \leq t \leq t_e \quad \text{with} \quad \underline{X}(0) = \underline{0} \quad (2.4)$$

$$\dot{\underline{X}} = [A] \underline{X} ; \quad t \geq t_e \quad \text{with} \quad \underline{X}(t_e) = \underline{X}_e \quad (2.5)$$

where \underline{X}_e = state of the system at time ' t_e ' evaluated from (2.4)

$\underline{u} = [\Delta P_{m1}, \Delta P_{m2}, \dots, \Delta P_{mn}]^T$, n -dimensional vector of accelerating powers.

The vector \underline{X} and the matrices $[A]$ and $[B]$ are defined for the cases of uniform and non-uniform damping separately [71].

Uniform Damping: For $C = D_1/M_1 = D_2/M_2 = \dots = D_n/M_n$, \underline{X} , $[A]$ and $[B]$ are defined as

$$\underline{X} = [\Delta \delta_{1n}, \Delta \delta_{2n}, \dots, \Delta \delta_{n-1,n}, \Delta \omega_{1n}, \Delta \omega_{2n}, \dots, \Delta \omega_{n-1,n}]^T, \\ (2n-2) \text{ dimensional vector}$$

$$[A] = \begin{array}{c} \begin{array}{cc} & \begin{array}{c} n-1 \\ \hline \end{array} \\ \begin{array}{c} n-1 \\ \hline \end{array} \end{array} \left[\begin{array}{cc} [0] & [I] \\ \hline [A'] & -C[I] \end{array} \right]$$

$$[B] = \begin{array}{c} \begin{array}{c} n-1 \\ \hline \end{array} \end{array} \left[\begin{array}{cccccc} & & & & \begin{array}{c} n \\ \hline \end{array} \\ & & & & [0] \\ \hline & 1/M_1 & 0 & \dots & 0 & -1/M_n \\ 0 & 1/M_2 & \dots & 0 & -1/M_n \\ \vdots & \vdots & & \vdots & \vdots \\ 0 & 0 & \dots & 1/M_{n-1} & -1/M_n \end{array} \right]$$

The elements of $[A']$ are given by

$$a_{ii} = - \sum_{\substack{j=1 \\ j \neq i}}^n \frac{E_i E_j}{M_i} (-G_{ij} \sin \delta_{ij}^0 + B_{ij} \cos \delta_{ij}^0) \\ - \frac{E_n E_i}{M_n} (-G_{ni} \sin \delta_{ni}^0 + B_{ni} \cos \delta_{ni}^0) \\ a_{ij} = \frac{E_i E_j}{M_i} (-G_{ij} \sin \delta_{ij}^0 + B_{ij} \cos \delta_{ij}^0) - \frac{E_n E_j}{M_n} (-G_{nj} \sin \delta_{nj}^0 + B_{nj} \cos \delta_{nj}^0) \quad i \neq j$$

Non-uniform Damping: For $C_1 \neq C_2 \neq \dots \neq C_n$ (where $C_i = D_i/M_i$);

\underline{X} , $[A]$ and $[B]$ are defined as

$$\underline{X} = [\Delta \delta_{1n}, \Delta \delta_{2n}, \dots, \Delta \delta_{n-1,n} \mid \Delta \omega_1, \Delta \omega_2, \dots, \Delta \omega_n]^T, \\ (2n-1) \text{ dimensional vector}$$

$$[A] = \begin{array}{c} \begin{array}{c} n-1 \\ n-1 \end{array} \quad \begin{array}{c} n-1 \\ [0] \end{array} \quad \begin{array}{c} n \\ \begin{array}{c} 1 \ 0 \ \dots \ 0 \ -1 \\ 0 \ 1 \ \dots \ 0 \ -1 \\ \cdot \ \cdot \ \cdot \ \cdot \\ 0 \ 0 \ \dots \ 1 \ -1 \end{array} \end{array} \\ \hline \begin{array}{c} n \\ [A'] \end{array} \quad \begin{array}{c} \begin{array}{c} -C_1 \ 0 \ \dots \ 0 \\ 0 \ -C_2 \ \dots \ 0 \\ \cdot \ \cdot \ \cdot \ \cdot \\ 0 \ 0 \ \dots \ -C_n \end{array} \end{array} \end{array}$$

The elements of $[A']$ are given by

$$a_{ii} = - \sum_{\substack{j=1 \\ j \neq i}}^n \frac{E_i E_j}{M_i} (-G_{ij} \sin \delta_{ij}^0 + B_{ij} \cos \delta_{ij}^0)$$

$$a_{ij} = \frac{E_i E_j}{M_i} (-G_{ij} \sin \delta_{ij}^0 + B_{ij} \cos \delta_{ij}^0) \quad i \neq j$$

$$[B] = \begin{matrix} & & n \\ & & [0] \\ n-1 & \left[\begin{array}{cccc} \text{---} & \text{---} & \text{---} & \text{---} \\ 1/M_1 & 0 & \dots & 0 \\ 0 & 1/M_2 & \dots & 0 \\ \cdot & \cdot & & \cdot \\ 0 & 0 & \dots & 1/M_n \end{array} \right] \end{matrix}$$

The primary motivation for selecting different state variables in the above two cases is to avoid the occurrence of a zero eigenvalue. The selection of state variables is also consistent with the concept of minimal realization as explained in Ref. [71]. In the subsequent analysis, we consider the case of uniform damping only for the sake of simplicity. However, the analysis is valid even for non-uniform damping by taking appropriate [A] and [B] matrices.

The elements of [A'] depend upon the system parameters and the pre-fault operating point. The expressions for the elements of [A] and [B] are general. However, if as in Ref. [24], the linearisation is done around the no-load operating point i.e. the flat voltage profile, then the elements of [A'] can be directly derived from Stott's [B'] matrix [25] and the inertia constants.

In equations (2.4) and (2.5), the elements of [A], [B] and the state vector X depend upon the choice of the

reference generator, whereas the vector \underline{u} , which reflects the fault under consideration, does not depend on it. For the sake of convenience and in order to establish a consistent relationship between \underline{X} , $[A]$ and $[B]$ with \underline{u} , we will always select a generator close to the fault location as the reference generator. Such a choice of reference generator gives the state variables as the relative rotor angles and velocities with respect to a generator, which is sensitive to the fault. The selection of reference generator near a fault location also forms the basis of the decomposition of a power system described in the next chapter.

2.4 ANALYTICAL SOLUTION

If the eigenvalues of matrix $[A]$ are distinct (which is generally the case with practical systems) the corresponding eigenvectors are linearly independent and the modes of oscillations are decoupled from each other. Let the matrix $[A]$ have 'm' pairs of complex and $(2n-2m-2)$ real eigenvalues. The response of the system in the faulted state i.e. the solution of equation (2.4) is given as (Refer Appendix A for details)

$$\underline{X}_f(t) = [P] \underline{z}_p(t) \quad (2.6)$$

where \underline{X}_f = state of the system in the faulted period

2m columns (2n-2m-2) columns

$$[P] = [p_1', p_1'', p_2', p_2'', \dots, p_m', p_m'' \mid p_{2m+1}, p_{2m+2}, \dots, p_{2n-2}]$$

(2n-2)x(2n-2) matrix

$$\underline{z}_p(t) = \begin{bmatrix} 1 - e^{\alpha_1 t} \cos \beta_1 t \\ \alpha_1 t e^{\alpha_1 t} \sin \beta_1 t \\ \vdots \\ 1 - e^{\alpha_m t} \cos \beta_m t \\ \alpha_m t e^{\alpha_m t} \sin \beta_m t \\ \vdots \\ -1 + e^{\alpha_{2m+1} t} \\ \vdots \\ -1 + e^{\alpha_{2n-2} t} \end{bmatrix} \quad \begin{matrix} 2m \\ (2n-2)\text{dimensional} \\ \text{vector} \\ 2n-2m-2 \end{matrix}$$

For $i = 1, 2, \dots, m$, p_i' and p_i'' are defined as

$$p_i' = \frac{\beta_i^2}{\alpha_i^2 + \beta_i^2} \left[\left(-\frac{\alpha_i}{\beta_i^2} k_i' + \frac{k_i''}{\beta_i} \right) \underline{x}_i' - \left(\frac{k_i'}{\beta_i} + \frac{\alpha_i}{\beta_i^2} k_i'' \right) \underline{x}_i'' \right]$$

$$p_i'' = \frac{\beta_i^2}{\alpha_i^2 + \beta_i^2} \left[\left(\frac{k_i'}{\beta_i} + \frac{\alpha_i}{\beta_i^2} k_i'' \right) \underline{x}_i' + \left(-k_i' \frac{\alpha_i}{\beta_i^2} + \frac{k_i''}{\beta_i} \right) \underline{x}_i'' \right]$$

For $i = 2m+1, 2m+2, \dots, 2n-2$

$$p_i = (k_i' / \alpha_i) \underline{x}_i'$$

$$k_i' = \langle \underline{y}_i', \hat{\underline{u}} \rangle, \quad k_i'' = \langle \underline{y}_i'', \hat{\underline{u}} \rangle, \quad \hat{\underline{u}} = [B] \underline{u}$$

$$\lambda_i = \alpha_i + j\beta_i = \text{eigenvalue of matrix } [A]$$

$$\underline{x}_i = \underline{x}_i' + j\underline{x}_i'' = \text{eigenvector of matrix } [A] \text{ corresponding to } \lambda_i$$

$$2\underline{y}_i = \underline{y}_i' + j\underline{y}_i'' = \text{reciprocal basis vector to } \underline{x}_i.$$

The eigenvectors and reciprocal basis vectors are normalised and satisfy the relationships [70] between them as given below.

$$\begin{aligned} \langle \underline{X}'_i, \underline{Y}'_i \rangle &= 1, & \langle \underline{X}''_i, \underline{Y}''_i \rangle &= 1 \\ \langle \underline{X}'_i, \underline{Y}''_i \rangle &= 0 & \langle \underline{X}''_i, \underline{Y}'_i \rangle &= 0 \end{aligned} \quad (2.7)$$

Similarly the response of the system in the post-fault period i.e. the solution of equation (2.5) is given as (Refer Appendix A for details).

$$\underline{X}_{pf}(t) = [S] \underline{z}_s(t) \quad (2.8)$$

where

\underline{X}_{pf} = state of the system in the post-fault period

$$[S] = \begin{array}{c} \begin{array}{cc} \text{2m columns} & \text{(2n-2m-2) columns} \end{array} \\ \begin{bmatrix} \underline{s}_1', \underline{s}_1'', \underline{s}_2', \underline{s}_2'', \dots, \underline{s}_m', \underline{s}_m'' & | & \underline{s}_{2m+1}, \underline{s}_{2m+2}, \dots, \underline{s}_{2n-2} \end{bmatrix} \\ \text{(2n-2) x (2n-2) matrix.} \end{array}$$

$$\underline{z}_s(t) = \begin{bmatrix} e^{\alpha_1 t} \cos \beta_1 t \\ e^{\alpha_1 t} \sin \beta_1 t \\ \vdots \\ e^{\alpha_m t} \cos \beta_m t \\ e^{\alpha_m t} \sin \beta_m t \\ \vdots \\ e^{\alpha_{2m+1} t} \\ e^{\alpha_{2m+2} t} \\ \vdots \\ e^{\alpha_{2n-2} t} \end{bmatrix} \quad \begin{array}{l} \text{2m} \\ \text{(2n-2)-dimensional vector} \\ \text{(2n-2m-2)} \end{array}$$

For the modes corresponding to complex eigenvalues, $i = 1, 2, \dots, m$

$$\underline{s}_i' = (\underline{\ell}_i' \underline{X}_i' + \underline{\ell}_i'' \underline{X}_i'') ; \quad \underline{s}_i'' = (\underline{\ell}_i'' \underline{X}_i' - \underline{\ell}_i' \underline{X}_i'')$$

For the modes corresponding to the real eigenvalues,

$$i = 2m+1, \dots, 2n-2, \quad \underline{s}_i = (\underline{\ell}_i' \underline{X}_i')$$

The scalars $\underline{\ell}_i'$ and $\underline{\ell}_i''$ are defined as

$$\underline{\ell}_i' = < \underline{Y}_i', \underline{X}_e > \quad ; \quad \underline{\ell}_i'' = < \underline{Y}_i'', \underline{X}_e > \quad (2.9)$$

The first $2m$ columns of $[P]$ and $[S]$ correspond to the complex modes and the remaining $(2n-2m-2)$ columns correspond to the nonoscillatory modes respectively. The scalars $\underline{\ell}_i'$ and $\underline{\ell}_i''$ in (2.6) and $\underline{\ell}_i'$ and $\underline{\ell}_i''$ in (2.9) depend upon the fault under consideration.

2.5 IDENTIFICATION OF COHERENT GENERATORS

From the above theory we now summarise the possible ways of identifying coherent generators including the conventional methods of coherency analysis.

(i) Base Case Swing Curves: In this case, the swing curves are obtained by numerically integrating the base case swing equation (2.2). The network changes due to the initiation and clearance of a fault are considered. These swing curves are compared and the groups are determined by using the criterion (2.1a).

(ii) Linear Simulation: In this method, the linearised swing equations (2.3) are numerically integrated over the

transient period by using the trapezoidal rule and a fault is reflected as given in hypothesis (iii). The resulting swing curves are compared.

(iii) Use of Closed Form Solution: The swing curves for a given fault are computed by substituting for different values of 't' in (2.6) and (2.8) and compared.

In the next section we present a direct method for coherency analysis which does not resort to comparison of the swing curves. All the above methods of coherency analysis are critically compared in Section 2.13.

2.6 DIRECT METHOD OF COHERENCY ANALYSIS

For the typical small fault clearing times obtainable in power systems, the differences in the rotor angles at $t=0^+$ and $t=t_e$ are very small. Hence it is sufficient to examine only the response (2.8) in the post-fault for ascertaining the coherency among the generators. To classify the generators 'i' and 'j' as coherent, the maximum angular deviation between the state variables $\Delta\delta_{in}$ and $\Delta\delta_{jn}$ should be examined. From equation (2.8), we have

$$\Delta\delta_{in} = \langle \underline{r}_i, \underline{z}_s(t) \rangle ; \quad \Delta\delta_{jn} = \langle \underline{r}_j, \underline{z}_s(t) \rangle \quad (2.10)$$

where \underline{r}_j and \underline{r}_i are the row vectors of matrix [S] corresponding to the state variables $\Delta\delta_{jn}$ and $\Delta\delta_{in}$ respectively. The expression for $\Delta\delta_{ij}$ is then written from (2.10) as

$$\Delta\delta_{ij} = \langle (\underline{r}_i - \underline{r}_j), \underline{z}_s(t) \rangle \quad (2.11)$$

Now consider the theoretical coherency between the generators 'i' and 'j' i.e. $\Delta\delta_{ij}(t) = 0$. The condition for theoretical coherency is satisfied if $\|\underline{r}_i - \underline{r}_j\| = 0$, where $\|\cdot\|$ represents the Euclidean norm. Since perfect coherency is rarely achieved, a practical coherency criterion, where certain tolerance is admissible, is needed. This criterion should have theoretical basis and physical justification. The following discussion provides the justification.

Suppose that the eigenvalues of $[A]$ are all complex with zero real parts, then $\|\underline{r}_i\|$ and $\|\underline{r}_j\|$ represent the bounds on the maximum amplitude of state variables $\Delta\delta_{in}$ and $\Delta\delta_{jn}$ respectively. This point is explained as follows.

(i) The length of vector $\underline{z}_s(t)$ is constant at any instant of time. Therefore, in a $2m$ -dimensional space, the vector $\underline{z}_s(t)$ is rotating and always constitutes the radius of a hypersphere.

(ii) $\Delta\delta_{in}$ and $\Delta\delta_{jn}$ will have the possible maximum amplitudes when $\underline{z}_s(t)$ is collinear with \underline{r}_i and \underline{r}_j respectively. Since the length of vector $\underline{z}_s(t)$ is constant, $\|\underline{r}_i\|$ and $\|\underline{r}_j\|$ are the bounds on the amplitudes of state variables $\Delta\delta_{in}$ and $\Delta\delta_{jn}$ respectively.

The above bounds are also valid if the matrix $[A]$ has eigenvalues with negative real parts. With the classical representation for generators, usually the eigenvalues of $[A]$ have small or zero real parts. This method of argument leads

2.6.2 Coherency Index ' h_{ij} ' :

Generators 'i' and 'j' are classified as practically coherent if

$$h_{ij} = \frac{\| \underline{r}_i - \underline{r}_j \|}{\text{Max } \| \underline{r}_k \|_{k=1,2,\dots,n-1}} < \epsilon \quad (2.12)$$

where h_{ij} is the coherency index between the generators 'i' and 'j' and ' ϵ ' is the tolerance. In physical terms, the numerator represents how far the respective components \underline{r}_i and \underline{r}_j differ from each other and thus gives a qualitative measure of deviation between $\Delta\delta_{in}$ and $\Delta\delta_{jn}$. The denominator represents the normalising factor.

a) Selection of ϵ : In processing the swing curves for coherency, usually the tolerance of $\pm 2.5^\circ$ or $\pm 5^\circ$ is taken irrespective of the maximum angular excursion in the system. Since the coherency index is defined as a normalised measure, the value of ϵ will depend upon the normalising factor $\text{Max } \| \underline{r}_k \|$, $k = 1, 2, \dots, n-1$. As a rule of thumb, the value of ϵ is approximately selected by the following relationship

$$\epsilon \approx \frac{\text{Allowable tolerance in degrees}}{\text{Max } \| \underline{r}_k \|_{k=1,2,\dots,n-1} \text{ in degrees}}$$

2.7 FORMATION OF COHERENT GROUPS

The procedure for forming the groups of coherent generators uses a transitive process [12] i.e. if generator 'a' is coherent with generator 'b' and generator 'a' is

is coherent with generator 'c', then the generators 'b' and 'c' are also coherent. In the grouping process, a comparison generator is defined for each coherent group and all other eligible generators are always compared against this generator in order to determine whether they should be included in the same group or not.

To start with all generators in the external system are marked as eligible and any generator (usually the farthest from the fault location), say 'i', is selected as the comparison generator of the group one. The coherency indices h_{ij} 's for all j 's belonging to the set of eligible generators are computed. The first group of coherent generators is determined by applying the criterion for coherency (2.12). Then the generators included in the first group are deleted and the rest of the generators in the external system are marked eligible for forming the second group. The second group of coherent generators is formed in a similar manner. In this way all possible groups of coherent generators in the external system are determined.

2.8 COMPUTATION OF EIGENVALUES, EIGENVECTORS AND RECIPROCAL BASIS VECTORS

In this section, we outline a method for computing the eigenvalues, eigenvectors and reciprocal basis vectors of $[A]$ from those of the submatrix $[A']$, which is of dimension $(n-1, n-1)$ (uniform damping).

Suppose λ is an eigenvalue of $[A]$ with the associated eigenvector $(\underline{x}_1^T, \underline{x}_2^T)$, where \underline{x}_1 and \underline{x}_2 are $(n-1)$ -dimensional vectors. Then we have

$$\left[\begin{array}{c|c} [0] & [I] \\ \hline [A'] & -C[I] \end{array} \right] \begin{bmatrix} \underline{x}_1 \\ \underline{x}_2 \end{bmatrix} = \lambda \begin{bmatrix} \underline{x}_1 \\ \underline{x}_2 \end{bmatrix} \quad (2.13)$$

This gives

$$\underline{x}_2 = \lambda \underline{x}_1$$

$$[A'] \underline{x}_1 = \lambda(\lambda + C) \underline{x}_1 \quad (2.14)$$

Hence, it follows that if λ' is an eigenvalue of $[A']$, then there are two corresponding eigenvalues of $[A]$ such that

$$\lambda(\lambda + C) = \lambda'$$

$$\text{or} \quad \lambda = \frac{-C \pm \sqrt{C^2 + 4\lambda'}}{2} \quad (2.15)$$

The following possibilities exist:

λ'	λ
positive real	positive real and negative real
negative real	a complex conjugate pair or two negative real eigenvalues
complex pair	two complex pairs

Our experience with $[A']$ matrices for different systems shows that all the eigenvalues of $[A']$ are usually negative real. Moreover, since $(C^2 + 4\lambda')$ is generally less than zero

because of small damping, we will always have complex eigenvalues of $[A]$. Then the eigenvalues, eigenvectors and reciprocal basis vectors of $[A]$ can be easily derived from those of $[A']$ by using equations (2.15) and (2.14). The reciprocal basis vectors of $[A']$ are derived from the corresponding eigenvectors of $[A']^T$. This facilitates the computation of coherency indices h_{ij} 's directly from the eigenvalues, eigenvectors and reciprocal basis vectors of $[A']$ itself.

The above technique is, however, not applicable if nonuniform damping in the system is considered.

2.9 NUMERICAL EXAMPLE

Before considering the problem of identifying the coherent generators for multiple fault locations, we now illustrate the above theory with the help of a typical power system in India. The power system belongs to the Uttar Pradesh State Electricity Board and consists of 71 buses, 94 transmission lines and 13 generators. A single line diagram of the system is shown in Fig. 2.2 and the complete system data is given in Appendix B. The study system, which constitutes the western part of the system and the external system are defined as follows (Fig. 2.2).

Study system = generators 1-5

External system = generators 6-13.

A three phase fault on bus 8 cleared in 0.1 sec. is considered. The generator 4 which is close to the fault location is taken as the reference generator.

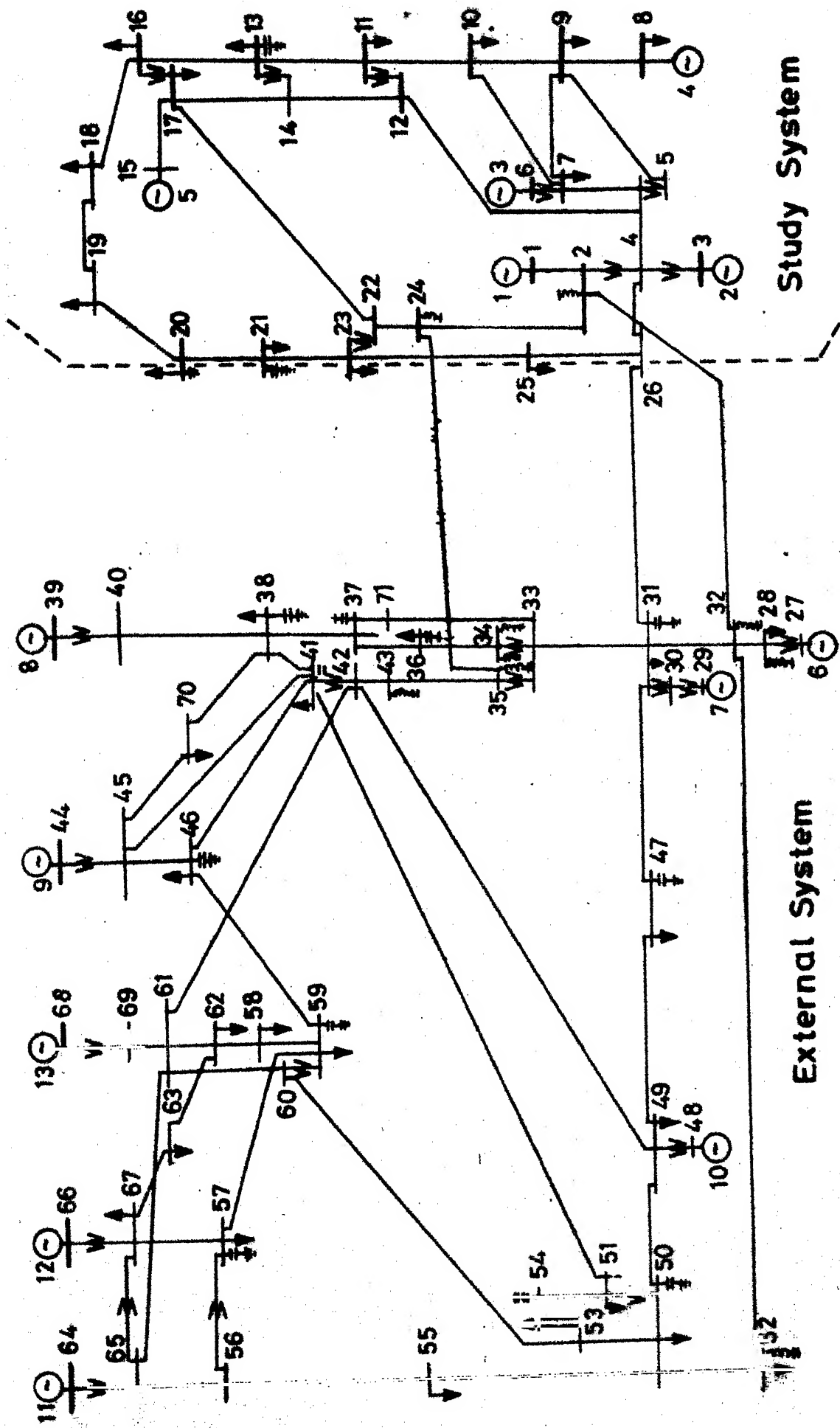


Fig. 2-2 Single line diagram of 13 machine system

The matrices $[A']$ and $[B]$ for the above system are given in Tables 2.1 and 2.2 respectively. The eigenvalues of $[A']$, which are all real and negative, are given below.

-200.253, -38.031 -116.525 -63.877 -140.665 -78.662
 -90.955 -117.436 -105.392 -110.187 -114.532 -109.394

For the sake of brevity, the eigenvectors and the reciprocal basis vectors of $[A']$ are not given here. The vector \underline{u} which reflects the fault under consideration is given by

$$\underline{u}^T = [1.2883, 1.0813, 0.2153, 1.4850, 0.4586, 0.5103, 0.6874, \\ 0.0794, 0.3455, 0.9142, 0.5072, 0.1544, 0.1575]$$

The coherency indices are computed by using the procedure in Section 2.8. These coherency indices are given in Table 2.3 and the table is written in accordance with the procedure for formation of coherent groups as explained in Section 2.7.

The coherent groups with a tolerance $\epsilon = 0.35$ corresponding to 5° in the base case studies are given below.

Group 1 : generators 9, 11, 12 and 13

Group 2 : generators 6 and 7

These results are verified by plotting the swing curves from both (i) the base case simulation and (ii) the closed form solution given in equations (2.6) and (2.8). These swing curves for the generators in the above two groups are given in Figs. 2.3 to 2.6. The base case swing curves indicate that the results obtained from the direct method are satisfactory.

Table 2.1 : [i'] Matrix

-98.918	3.656	-4.184	2.355	7.174	4.440	0.320	1.404	4.511	2.012	0.601	0.569
27.583	-137.510	0.351	4.380	4.923	4.781	0.248	1.074	3.845	1.526	0.456	0.433
5.544	8.865	-112.110	1.158	0.965	0.846	0.025	0.164	0.555	0.247	0.073	0.071
17.070	3.700	-3.355	-115.307	4.184	4.793	0.397	1.780	4.601	2.235	0.670	0.662
34.931	0.910	-4.477	2.774	-174.100	22.381	1.015	5.006	22.052	9.097	2.698	2.429
23.370	2.053	-4.354	4.175	25.536	-178.609	1.844	6.547	30.261	9.248	2.765	2.570
-5.511	-20.169	-6.900	-1.122	3.125	5.681	-90.018	14.876	15.636	9.723	2.966	2.812
-10.614	-23.538	-7.284	-2.532	0.695	1.407	2.387	-55.631	10.764	10.345	3.215	2.874
-0.595	-16.742	-6.513	-0.551	8.805	11.396	1.927	9.120	-100.976	15.476	4.625	4.117
-10.654	-23.614	-7.293	-2.721	1.471	1.315	1.070	7.562	13.365	-68.581	12.764	7.428
-10.776	-23.693	-7.302	-2.753	1.368	1.200	1.051	7.644	12.820	41.706	-96.347	7.216
-8.435	-22.304	-7.138	-2.233	2.640	2.435	1.434	10.026	16.923	35.584	10.571	-107.802

Table 2.2 : [B] Matrix

[0]

12x13

0.077	0.0	0.0	0.0	0.0	0.0	0.0	0.0	0.0	0.0	0.0	0.0	-0.150
0.0	0.111	0.0	0.0	0.0	0.0	0.0	0.0	0.0	0.0	0.0	0.0	-0.150
0.0	0.0	0.520	0.0	0.0	0.0	0.0	0.0	0.0	0.0	0.0	0.0	-0.150
0.0	0.0	0.0	0.386	0.0	0.0	0.0	0.0	0.0	0.0	0.0	0.0	-0.150
0.0	0.0	0.0	0.0	0.392	0.0	0.0	0.0	0.0	0.0	0.0	0.0	-0.150
0.0	0.0	0.0	0.0	0.0	0.370	0.0	0.0	0.0	0.0	0.0	0.0	-0.150
0.0	0.0	0.0	0.0	0.0	0.0	0.966	0.0	0.0	0.0	0.0	0.0	-0.150
0.0	0.0	0.0	0.0	0.0	0.0	0.0	0.184	0.0	0.0	0.0	0.0	-0.150
0.0	0.0	0.0	0.0	0.0	0.0	0.0	0.0	0.128	0.0	0.0	0.0	-0.150
0.0	0.0	0.0	0.0	0.0	0.0	0.0	0.0	0.0	0.140	0.0	0.0	-0.150
0.0	0.0	0.0	0.0	0.0	0.0	0.0	0.0	0.0	0.0	0.459	0.0	-0.150
0.0	0.0	0.0	0.0	0.0	0.0	0.0	0.0	0.0	0.0	0.0	0.678	-0.150

157.075

Table 2.3 : Coherency Indices

Comparison Generator of Group	12	10	8	7
Generators in External System				
6	0.8261	0.7119	0.7831	0.2616*
7	0.7879	0.6554	0.7552	0.0*
8	0.5157	0.6897	0.0	-
9	0.1643*	-	-	-
10	0.6507	0.0	-	-
11	0.1382*	-	-	-
12	0.0*	-	-	-
13	0.3379*	-	-	-

$$\text{Max } \|\underline{r}_k\|, k = 1, \dots, n-1 = 0.2425$$

$$\epsilon = 0.35$$

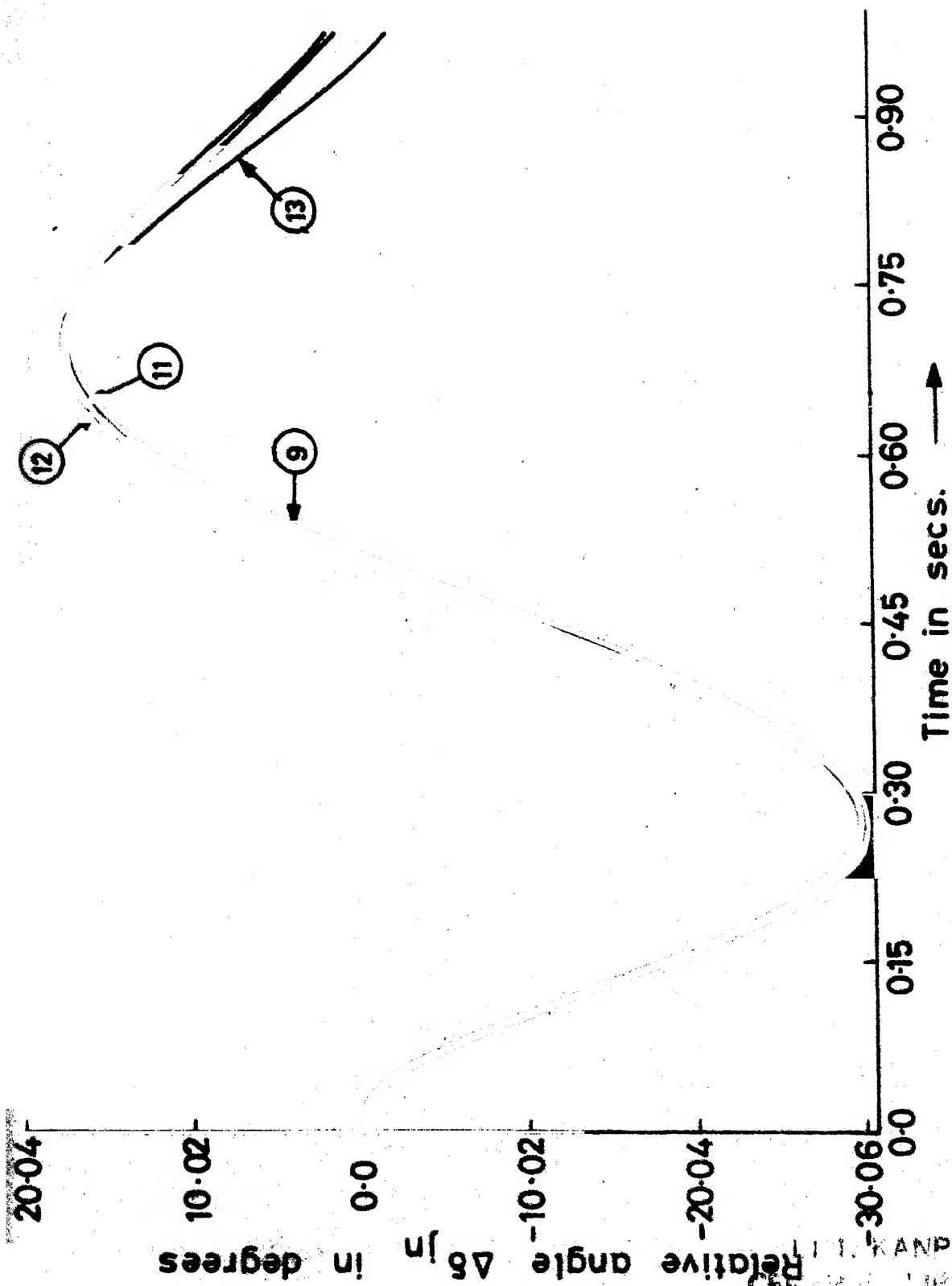


Fig. 2.3 Base case swing curves of generators 9, 11, 12 and 13

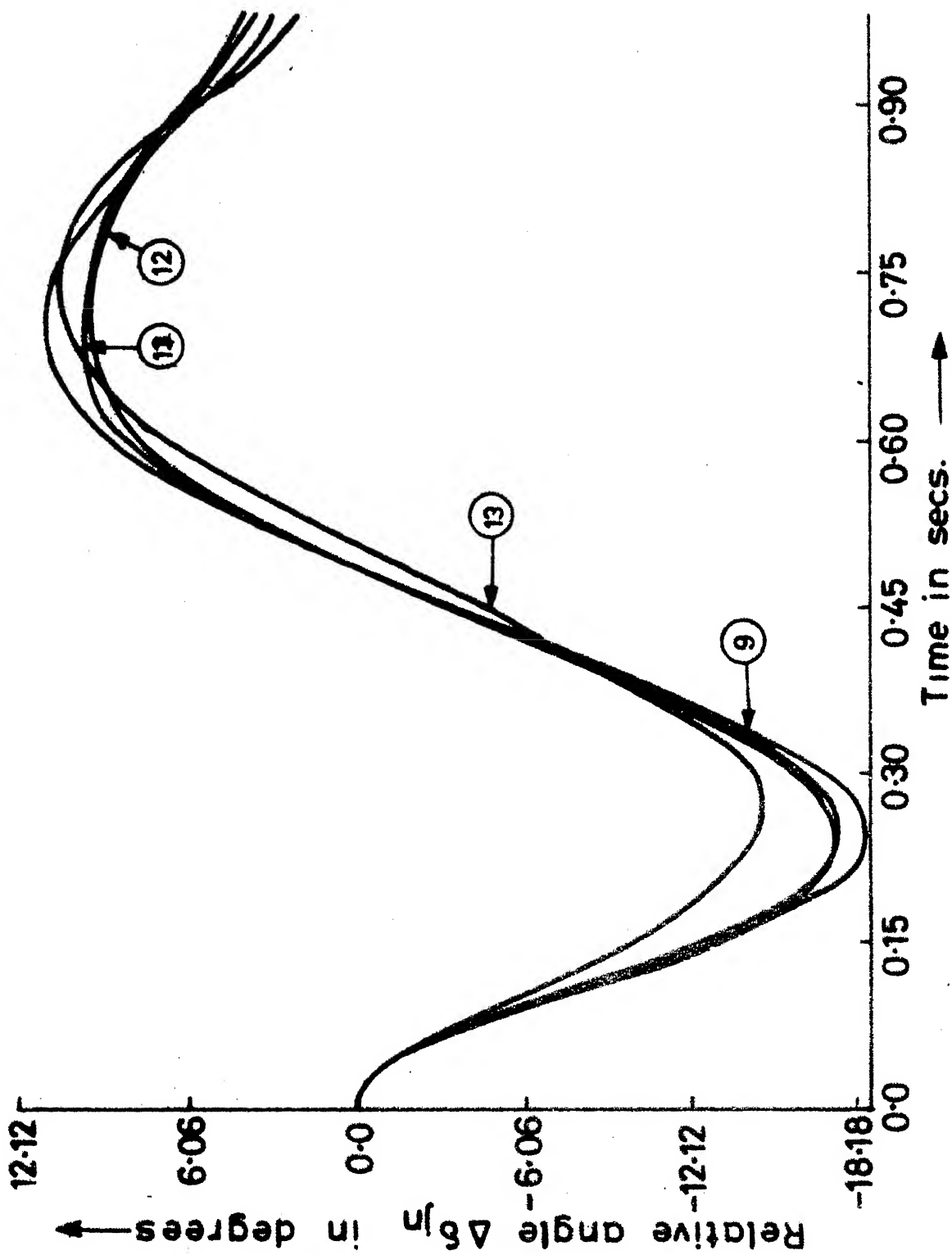


Fig. 2.4 Swing curves (closed form solution) of generators 9, 11, 12 and 13

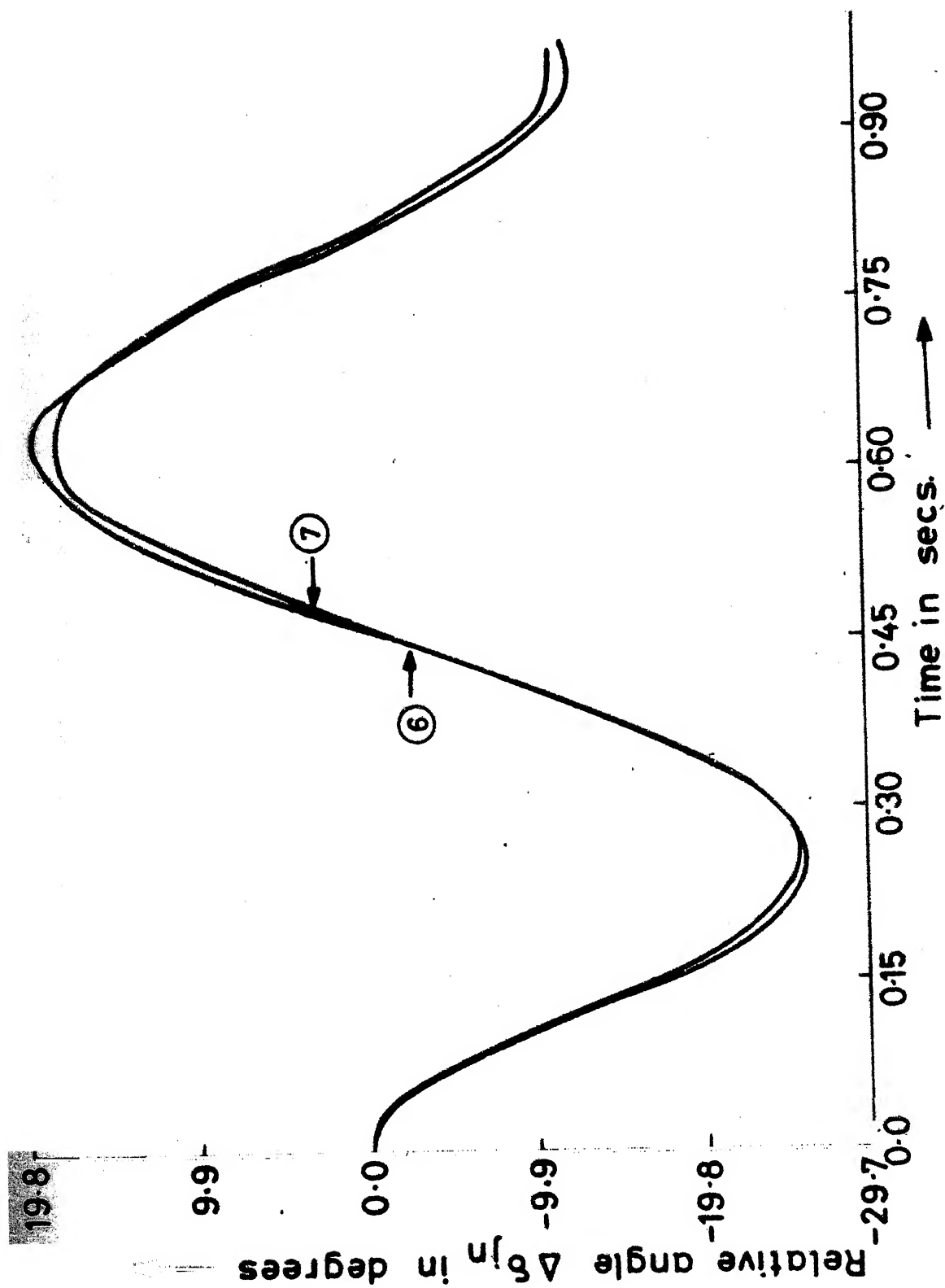


Fig. 2.5 Base case swing curves of generators 6 and 7

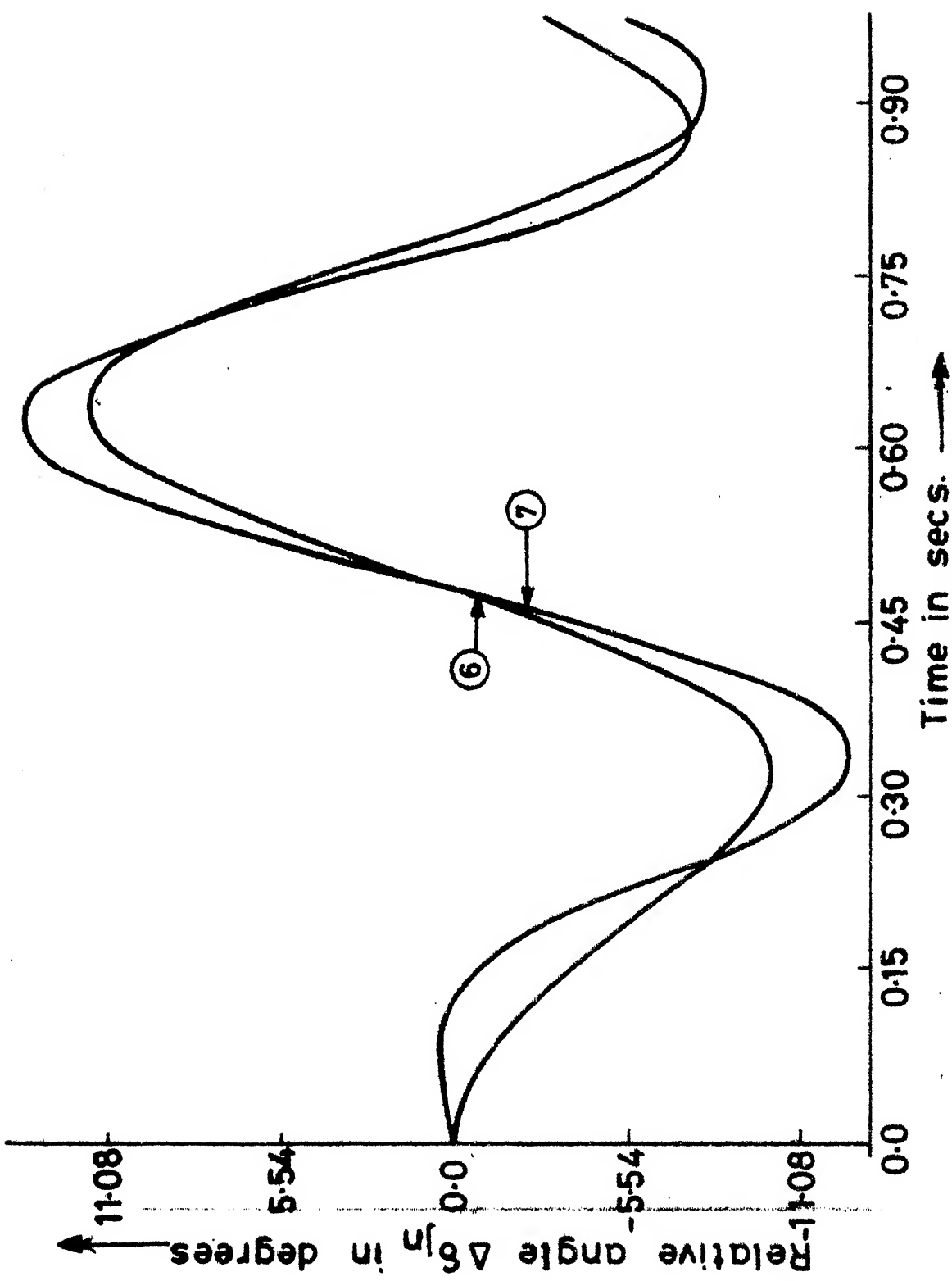


Fig. 2.6 Swing curves (closed form solution) of generators 6 and 7

2.10 CHANGES IN THE FAULT LOCATION

The problem of identifying coherent groups for different fault locations is an important problem in coherency analysis for the following reasons.

(i) Consider a case where the concept of study system is not used and an equivalent is reconstructed for every individual fault location. In such case, whenever the fault location is changed, new groups of coherent generators are to be determined (discussion on Ref. [24]).

(ii) When the concept of study system and external system is used, we need a group of coherent generators valid for a set of fault locations in the study system for constructing the equivalent. In such a case, the groups of coherent generators for individual fault locations in the study system are determined and then a set of coherent groups valid for all the fault locations is selected.

(iii) Suppose the geographical configuration of the study system is altered and it is required to construct an equivalent for the new study system, then the step (ii) has to be repeated for new study system.

Whenever a fault location is shifted, the following changes are incorporated in equations (2.6) and (2.8).

(i) Accelerating power of each generator at $t=0^+$ is recomputed resulting in a different forcing function u .

(ii) Since a generator close to the fault is selected as the reference generator, a change of the fault location

may necessitate the change in the reference generator. The recomputation of new $[A]$ matrix, its eigenvectors and reciprocal basis vectors is avoided by the use of similarity transformation described in the next section. The eigenvectors and reciprocal basis vectors can be easily derived from the existing ones and a transformation matrix.

(iii) These changes are correspondingly reflected in new values of k_i' and k_i'' in (2.6). The new values of λ_i' and λ_i'' are then computed from \underline{X}_e as given in (2.9).

2.11 SIMILARITY TRANSFORMATION MATRIX

Suppose we have already grouped the generators for a given fault with the reference generator, say 'q'. Now it is required to group the generators for a different fault location and the corresponding reference generator is 'p'. Let the two state vectors be denoted by \underline{X}_q and \underline{X}_p and the two system matrices by $[A_q]$ and $[A_p]$ respectively. For a given pre-fault loading condition, the two matrices are related through a similarity transformation matrix. The transformation matrix is given by

$$\underline{X}_q = [T] \underline{X}_p \quad (2.16)$$

where

$$\underline{X}_q = \begin{bmatrix} \Delta \delta_q \\ \Delta \omega_q \end{bmatrix} \quad \underline{X}_p = \begin{bmatrix} \Delta \delta_p \\ \Delta \omega_p \end{bmatrix}$$

The components of \underline{X}_q and \underline{X}_p are defined in equation (2.4).

Then by inspection $[T]$ is obtained as

$$[T] = \begin{matrix} & \begin{matrix} n-1 & n-1 \end{matrix} \\ \begin{matrix} n-1 \\ n-1 \end{matrix} & \begin{bmatrix} [T'] & [O] \\ [O] & [T'] \end{bmatrix} \end{matrix}$$

For $p > q$, matrix $[T']$ is given by

$$\begin{matrix} \begin{bmatrix} \Delta \delta_{1q} \\ : \\ \Delta \delta_{q-1,q} \\ \hline \Delta \delta_{q+1,q} \\ : \\ \Delta \delta_{p-1,q} \\ \hline \Delta \delta_{pq} \\ \hline \Delta \delta_{p+1,q} \\ : \\ \Delta \delta_{nq} \end{bmatrix} & \begin{matrix} q-1 \\ \\ p-q-1 \\ \\ p-1^{th} \text{ row} \\ \\ n-p \end{matrix} & = & \begin{matrix} \begin{matrix} q^{th} \\ q-1 \text{ column} \end{matrix} & \begin{matrix} p-q-1 & n-p \end{matrix} \\ \begin{bmatrix} -1 & & & \\ [I] & : & [O] & [O] \\ & -1 & & \\ \hline & -1 & & \\ [O] & : & [I] & [O] \\ & -1 & & \\ \hline \underline{0} & -1 & \underline{0} & \underline{0} \\ \hline & -1 & & \\ [O] & : & [O] & [I] \\ & -1 & & \end{bmatrix} & \begin{bmatrix} \Delta \delta_{1p} \\ : \\ \Delta \delta_{q-1,p} \\ \hline \Delta \delta_{qp} \\ \hline \Delta \delta_{q+1,p} \\ : \\ \Delta \delta_{p-1,p} \\ \hline \Delta \delta_{p+1,p} \\ : \\ \Delta \delta_{np} \end{bmatrix} \end{matrix}$$

where $[I]$ is the identity matrix of appropriate dimension.

For $p < q$, matrix $[T']$ is obtained in a similar fashion. Then

$$\begin{aligned} [A_p] &= [T]^{-1} [A_q] [T] \\ [B_p] &= [T]^{-1} [B_q] \end{aligned} \quad (2.17)$$

The eigenvectors of matrix $[A_p]$ can be derived from the eigenvectors of $[A_q]$ by the relation

$$(E.V.)_p = [T]^{-1} (E.V.)_q \quad (2.18)$$

The matrix $[T]^{-1}$ need not be computed explicitly. Instead it is written as

$$[T]^{-1} = \left[\begin{array}{c|c} [T']^{-1} & [0] \\ \hline [0] & [T']^{-1} \end{array} \right]$$

where $[T']^{-1}$ is obtained by inspecting the state variables and is given by

$$\begin{array}{c} \begin{array}{c} \Delta\delta_{1p} \\ : \\ \Delta\delta_{q-1,p} \\ \hline \Delta\delta_{qp} \\ \hline \Delta\delta_{q+1,p} \\ : \\ \Delta\delta_{p-1,p} \\ \hline \Delta\delta_{p+1,p} \\ : \\ \Delta\delta_{np} \end{array} \\ \begin{array}{c} q-1 \\ \\ q^{th} \text{ row} \\ \\ p-q-1 \\ \\ n-p \end{array} \end{array} = \begin{array}{c} \begin{array}{cc} q-1 & p-q-1 \end{array} \begin{array}{c} p-1^{th} \\ \text{column} \end{array} \begin{array}{c} n-p \end{array} \\ \begin{array}{c} \begin{array}{c} [I] \quad [0] \\ \hline \underline{0} \quad \underline{0} \\ \hline [0] \quad [I] \\ \hline [0] \quad [0] \end{array} \end{array} \begin{array}{c} \begin{array}{c} -1 \\ : \\ -1 \\ \hline -1 \\ : \\ -1 \\ \hline -1 \\ : \\ -1 \end{array} \end{array} \begin{array}{c} \begin{array}{c} [0] \\ \hline \underline{0} \\ \hline [0] \\ \hline [I] \end{array} \end{array} \end{array}$$

$$\begin{array}{c} \begin{array}{c} \Delta\delta_{1q} \\ : \\ \Delta\delta_{q-1,q} \\ \hline \Delta\delta_{q+1,q} \\ \hline \Delta\delta_{p-1,q} \\ \hline \Delta\delta_{pq} \\ \hline \Delta\delta_{p+1,q} \\ : \\ \Delta\delta_{nq} \end{array} \end{array}$$

2.12 NUMERICAL EXAMPLES

We now demonstrate the use of similarity transformation in the grouping of coherent generators for different fault locations. Consider the power system in Section 2.9. The coherent groups corresponding to two typical fault locations are given below.

a) Fault on Bus 15 (Same Study System): The study system is the same as in Section 2.9. The groups of coherent generators for a three phase fault on bus 15 and cleared in 0.1 second are to be identified. We have $[A']$ matrix, its eigenvectors and reciprocal basis vectors with generator 4 as the reference generator. For the fault on bus 15, generator 5 is taken as the reference generator. The new eigenvectors and the reciprocal basis vectors are derived by using the technique of similarity transformation given in Sections 2.10 and 2.11. The vector \underline{u} of the accelerating powers of the generators at $t = 0^+$ is given by

$$\underline{u}^T = [1.222, 0.902, 0.086, 0.103, 0.920, 0.514, 0.713, \\ 0.082, 0.354, 0.960, 0.516, 0.157, 0.159]$$

The coherency indices are given in Table 2.4, The coherent groups for a tolerance 0.21 are as follows.

Group 1 : generators 9, 11, 12 and 13

Group 2 : generators 6 and 7

As indicated in Section 2.6.2 earlier, tolerance ϵ is small in this case because of the higher value of $\text{Max} \|\underline{r}_k\|$,
 $k = 1, 2, \dots, n-1$.

By moving the fault location in the study system, we have ascertained that the above groups are satisfactory for all fault locations in the study system.

Table 2.4 : Coherency Indices

Comparison Generator of Group	12	10	8	7
Generators in External System	6			
6	0.4025	0.3870	0.3749	0.1732*
7	0.3770	0.3613	0.3588	0.0*
8	0.3881	0.2586	0.0	-
9	0.1134*	-	-	-
10	0.3027	0.0	-	-
11	0.03811*	0.0	-	-
12	0.0*	-	-	-
13	0.1259*	-	-	-

$$\text{Max } \|\underline{x}_k\| \quad , \quad k = 1, 2, \dots, n-1 = 0.399$$

$$\epsilon = 0.21$$

b) Fault on Bus 68 (Different Study System): The new study system is taken as

Study system : generators 8, 9, 11, 12, 13

External system: generators 1-7 and 10.

A three phase fault on bus 68 cleared in 0.1 sec. is considered. The generator 13 is taken as the reference generator. New eigenvectors and the reciprocal basis vectors are computed using the similarity transformation given in Sections 2.10 and 2.11. The vector \underline{u} for the fault is given by

$$\underline{u}^T = [1.104, 0.779, 0.060, 0.028, 0.469, 0.521, 0.724, \\ 0.082, 0.375, 0.997, 0.648, 0.201, 0.445]$$

The coherency indices are given in Table 2.5 and the coherent groups corresponding to $\epsilon = 0.3$ are

Group 1 : generators 1 and 2

Group 2 : generators 6 and 7

c) Other Numerical Examples:

In order to demonstrate the applicability of the direct method of coherency analysis for large systems, we have tested the method on a power system given in Ref.[8] consisting of 31 generators, 133 buses and 258 transmission lines. The coherency indices and the groups for different fault locations are reported in Ref. [74]. The coherent groups agree with the base case swing curves. The coherent groups in this system corresponding to one fault location are

Table 2.5 : Coherency Indices

Comparison Generator of Group	1	3	4	5	6
Generators in External System					
1	0.0*	-	-	-	-
2	0.1805*	-	-	-	-
3	0.4227	0.0	-	-	-
4	0.7166	0.4284	0.0	-	-
5	0.5242	0.6185	0.8011	0.0	-
6	0.5526	0.6260	0.8089	0.7033	0.0*
7	0.5218	0.6014	0.7790	0.6693	0.2659*
10	0.3982	0.6040	0.7358	0.6089	0.6605

$$\text{Max } \|r_k\|, k = 1, 2, \dots, n-1 = 0.2747$$

$$\epsilon = 0.30$$

given in the next chapter, where a modified method for grouping of coherent generators is presented.

2.13 DISCUSSION

Some of the important aspects of the techniques for coherency analysis presented in this chapter are given below.

(i) The primary motivation for the analytical approach using the concept of modes was to eliminate the repetitive computation of swing curves, when the groups valid for a set of faults in the study system are determined. This objective has been achieved by the appropriate use of the similarity transformation (Sections 2.10 and 2.11). To illustrate this point, the computation times for different methods to identify the groups in UPSEB system corresponding to three different fault locations are summarized in Table 2.6. It is evident from the table that the computation time for the base case swing curves and linear simulation is proportional to the number of fault locations. But in the direct method and in the closed form solution method the additional computer time requirement for a subsequent fault location is about 29.5% and 39.6% respectively.

(ii) The linearised swing curves exhibit reduced amplitudes and increased frequency of oscillations as compared to the base case swing curves. This observation agrees with that in [24].

(iii) In the mathematical modelling of power system (Section 2.3), we have considered only electrical faults as the disturbances. It is possible to obtain a general

Table 2.6 : Computation Times for Coherency Analysis in
UPSEB System.

No. of fault locations considered	Base Case Swing Curves	Particulars	Proposed Techniques Swing Curves from Closed Form solution	The Direct Method	Linear Simula- tion
1	14.0	(a)	4.05	4.05	
		(b)	0.68	0.68	
		(c)	1.90	1.90	
		(d)	1.16	-	
		(e)	-	0.04	
		Total time	7.79	6.67	6.82 (includes 1.9 sec. for (c))

2	28.0	(f)	0.03	0.03	
		(c)	1.90	1.90	
		(d)	1.16	-	
		(e)	-	0.04	
		Total time (inclusive of the above)	10.88	8.64	13.64

3	42.0	(f)	0.03	0.03	
		(c)	1.90	1.90	
		(d)	1.16	-	
		(e)	-	0.04	
		Total time (inclusive of the above two)	13.97	10.61	20.46

Continued..

Notes:

- (i) All entries in the table are CPU times in seconds on Dec System 10.
- (ii) Swing curves in the base case and the linear simulation method are plotted for 1 sec. only with an interval of 0.01 and 0.05 sec. respectively.
- (iii) Computer time for comparison of swing curves/coherency indices which is usually very small, is not included.
- (iv) Computer programs for the base case transient stability and network reduction in step (a) do not use sparsity technique whereas the programs for computation of the accelerating powers in step (c) and the linear simulation method make use of sparsity technique.

Particulars

- (a) Network reduction and computation of $[A']$ matrix.
- (b) Computation of eigenvectors and reciprocal basis vectors of $[A']$.
- (c) Computation of accelerating powers of the generators at $t = 0^+$.
- (d) Computation of swing curves from the closed form solution.
- (e) Computation of coherency indices.
- (f) Computation of the new eigenvectors from the existing ones and a similarity transformation matrix.

mathematical model of the system, which also considers other types of disturbances such as loss of generation, tripping of a transmission line etc. In fact such a state space model is given in Ref.[27]. The theory presented in this chapter applies to such a generalised model as well.

(iv) In the grouping of coherent generators (Section 2.7), the selection of comparison generator of a coherent group is arbitrary and the process is transitive. Therefore, for a given fault, the groups of coherent generators need not be unique. However, the size of the equivalised external system will not be affected.

(v) The direct method gives a more physical insight into the dynamics of the system than the procedure involving processing of a large number of swing curves for coherency.

(vi) A possible criticism of the method may be computation of eigenvectors and reciprocal basis vectors for large scale systems. Although not explored in this thesis, the concept of dominant modes may alleviate this difficulty.

2.14 CONCLUSION

In this chapter we have presented two techniques for identifying coherency (i) by comparing the swing curves obtained from closed form solution and (ii) the direct method using coherency indices. The concept of similarity transformation has been used to eliminate the repetitive computations involved in determining coherency for different fault locations

in the study system. This fact makes the method attractive as compared to existing methods. Validity of the method has been tested on realistic power systems.

CHAPTER 3

DECOMPOSITION OF POWER SYSTEMS AND CONSTRUCTION OF COHERENCY BASED EQUIVALENTS

3.1 INTRODUCTION

Another problem, in addition to dynamic equivalence, facing power engineers is how accurate the model for a generating unit should be as one moves away from the fault location. This can be considered either as a step prior to dynamic equivalencing or a problem in itself. For a long time, it has been the common practice to represent the generators 'away' from the fault location with lesser detail than those in the 'vicinity' of it. Such a classification of generators is not precise and is based upon the experience with the system studies. A logical basis for determining the levels of complexity in modelling the generators is the electromechanical interaction between the machines during the transient period. The electromechanical interaction between two machines can be judged by (i) the maximum angular excursion or (ii) the synchronising power flow between the machines. In the literature, the admittance and reflection distance measures [22] have been proposed for the purpose of modelling the generators. While the admittance distance is purely a static measure, the reflection distance does not reflect the electromechanical interaction between the machines during the entire transient period.

In this chapter, we (i) present a new method for the decomposition of a power system for the purpose of modelling the generators, which incorporates the electromechanical interaction between the machines during the transient period, (ii) establish a link between the decomposition of power system and the direct method of coherency analysis presented in Section 2.6 for grouping of coherent generators and (iii) present a case study for a realistic power system to illustrate the principle of equivalencing. The relevant equivalising procedure is also described briefly.

3.2 ELECTROMECHANICAL DISTANCE (EMD)

We define EMD between a generator in the external system and the reference generator in the study system as a bound on the maximum angular excursion between the two during the transient period. In terms of the mathematical development of the previous chapter, the EMD between the generators 'i' and 'n' is defined from equation (2.10) as

$$d_{in} = \frac{\| \underline{r}_i \|}{\text{Max. } \| \underline{r}_k \|_{k=1,2,\dots,n-1}} \quad (3.1)$$

where generator 'i' belongs to the set of generators in the external system and 'n' is the reference generator in the study system. 'd_{in}' as defined in equation (3.1) gives a per unit bound on the maximum angular deviation between the generators 'i' and 'n'.

3.3 DECOMPOSITION OF POWER SYSTEM

Based on the concept of EMD, a power system is divided into different regions for a given fault location. The division is done with respect to a reference generator, which, as stated in Section 2.3.1, is selected close to the fault location. The study system, by definition, constitutes region I, which corresponds to inner circle defined in Ref. [22]. The proposed criteria for the demarcation of a power system into different regions is the following:

- Region I : Study system
- Region II : $b_1 < d_{in} \leq b_2$
- Region III : $b_2 < d_{in} \leq b_3$
- Region IV : $b_3 < d_{in} \leq 1$

where b_1 , b_2 and b_3 are the known constants, which define the boundaries between the regions.

Since the transient behaviour of the generators in a study system subjected to the local disturbances is to be investigated in detail, the level of complexity in representing the dynamics of generators in the study system should be the highest. The generators in region IV being far away (in the sense of EMD) from the reference generator can be represented by either classical models or the dynamics of the generators in this region may be altogether neglected. The degree of details in modelling the generators in regions II and III is suitably graded in between these two extremes.

3.4 SELECTION OF THE BOUNDARIES

After decomposition of power system into regions, coherency analysis follows. Since the generators belonging to different regions are modelled with different degrees of details and difficult to aggregate [12], a coherent group spread over two or more regions is undesirable. Therefore, while selecting the boundaries b_2 and b_3 , we have to ensure that a generator in one region will not be coherent with the generator in another region. This is done as follows.

Coherency between the generators 'i' and 'j' implies that

$$d_{in} \approx d_{jn} \quad (3.2)$$

i.e. the generators are equidistant (in the sense of EMD) from the reference generator. However, the reverse may not be true. Hence (3.2) forms a necessary condition for coherency because in the definition of EMD, the sign of the deviation is not considered. Thus if ' d_{in} ' and ' d_{jn} ' do not satisfy (3.2), it is guaranteed that the generators 'i' and 'j' will not be coherent. The adjustment of boundaries is done so that the generators satisfying (3.2) belong to one region only. First the generators in the external system are arranged in the order of increasing EMD's. When a boundary b_i is selected, we will verify that the two generators on opposite sides of the boundaries and

close (in the sense of EMD) to it are not coherent by computing the corresponding coherency index given in equation (2.12). The selection of values of b_i 's is, however, left to the system planner. Such a division of power system facilitates the grouping of coherent generators in each region separately. We now illustrate the above technique of decomposition of power system and the subsequent grouping of coherent generators with two numerical examples.

3.5 NUMERICAL EXAMPLES

3.5,1 Example 1:

Consider the power system and the fault location given in Section 2.9. Generator 4 is taken as the reference generator and the EMD's of the generators in the external system are given in Table 3.1.

Table 3.1 : Electromechanical Distances

Generators in the External System	d_{in}	Remarks
7	0.6873	
6	0.7052	Region II
10	0.7486	
-----		$h_{10,13} = 0.3700$
13	0.8838	$\epsilon = 0.35$
8	0.9411	
11	0.9605	Region III
12	0.9868	
9	1.0	

$$\text{Max} \|\underline{r}_k\| = 0.2425$$

The power system is divided into three different regions as shown in Fig.3.1 using the technique given in the previous section.

Region I : Study system, generators 1-5

Region II : generators 6,7 and 10

$$(0.65 < d_{in} \leq 0.75)$$

Region III: generators 8,9,11,12,13

$$(0.75 < d_{in} \leq 1)$$

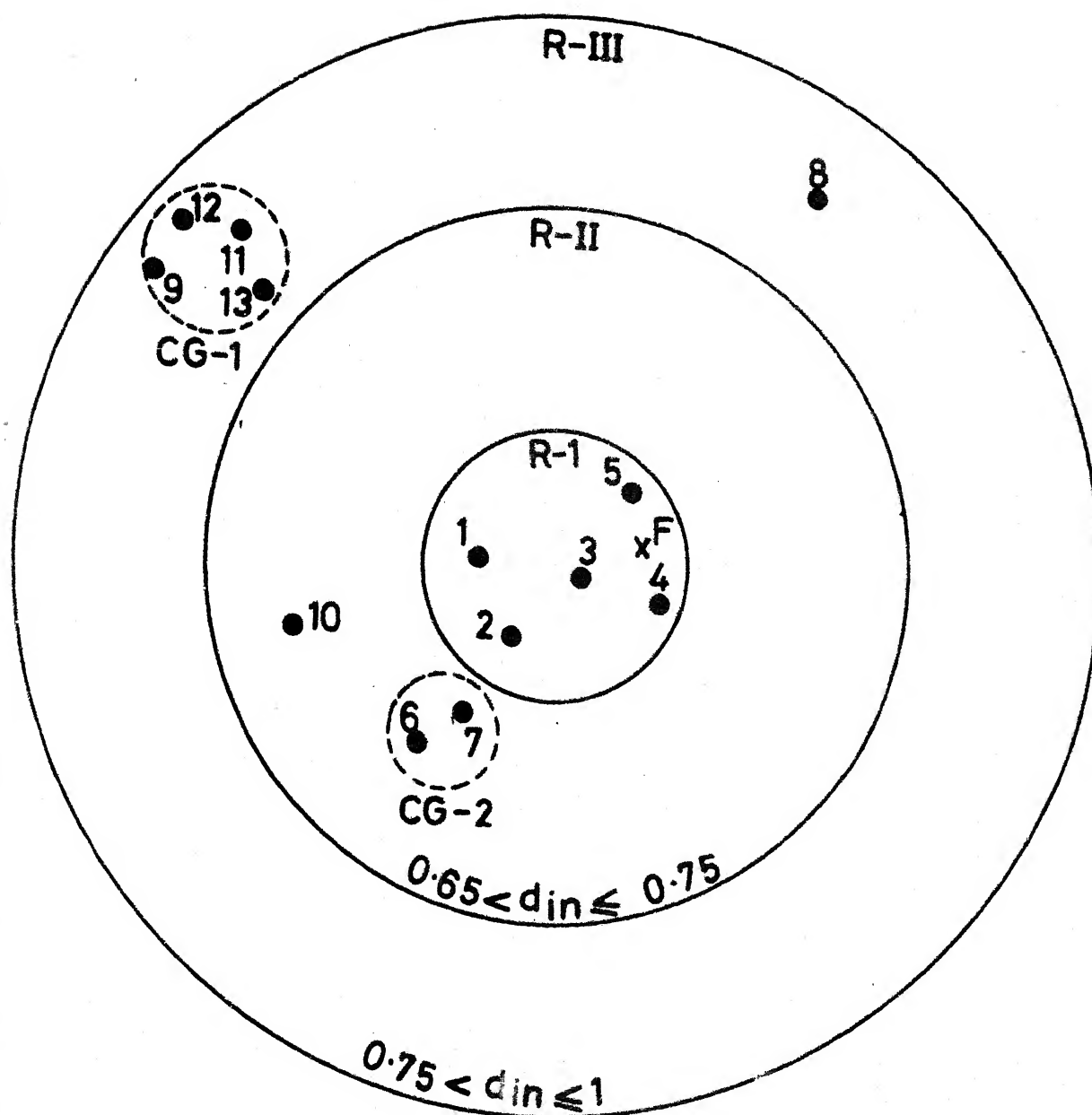
The coherent generators in each region are grouped separately using (2.13) as given in Tables 3.2 and 3.3. The coherent groups are as follows:

Region III : Coherent group 1 : generators 9,11,12,13

Region II : Coherent group 2 : generators 6 and 7

Table 3.2: Grouping of Coherent Generators in Region III.

Comparison generator of group	12	8	
Generators in Region III			
8	0.5157	0.0	
9	0.1643*	-	
11	0.1382*	-	$\epsilon = 0.35$
12	0.0*	-	$\text{Max} \ \underline{r}_k \ = 0.2425$
13	0.3379*	-	$k=1,2,\dots,n-1$



R = Region
 CG = Coherent group
 F = Fault location

Fig. 3-1 Decomposition of 13 machine system and formation of coherent groups

Table 3.3 : Grouping of Coherent Generators in Region II

Comparison generator of group	10	6	
Generators in Region II.			
6	0.7119	0.2616*	$\epsilon = 0.35$
7	0.6554	0.0*	$\text{Max } \underline{r}_k = 0.2425$
10	0.0	-	$k=1,2,\dots,n-1$

3.5.2 Example 2:

In this example, the decomposition and the subsequent coherency analysis of a power system consisting 31 generators, 132 buses and 258 transmission lines is presented. The single line diagram of the system is given in Fig. 3.2 and the system data is taken from Ref.[8], which for the sake of brevity is not reproduced here. The following case is considered.

Study system : generators 4, 5, 7, 18, 19 and 20

External system : rest of the generators

Fault : a three phase fault on the terminals
of generator 5 cleared in 0.1 sec.

Reference : generator 5.

Decomposition: The electromechanical distances for the above case are listed in Table 3.4. The proposed decomposition of the system is given below and is shown in Fig.3.3.

Region I : Study system, generators 4,5,7,18,19 and 20

Table 3.4 : Electromechanical Distances

Generators in External System	d_{in}	Remarks
28	0.1290	
21	0.1290	
8	0.1301	
10	0.1327	
22	0.1331	
31	0.1352	Region II
30	0.1469	
11	0.1499	
12	0.1542	
23	0.1840	
27	0.1973	
26	0.2060	
-----		$h_{26,29} = 0.2846$
29	0.2165	$\epsilon = 0.12$
6	0.2234	
9	0.2244	
25	0.2306	
1	0.2331	Region III
13	0.2405	
14	0.2454	
24	0.2703	
16	0.2880	
15	0.2977	
-----		$h_{15,3} = 0.6551$
3	0.5665	$\epsilon = 0.12$
17	0.6565	Region IV
2	1.0	

$$\text{Max} \|\underline{r}_k\| = 0.8583$$

$$k=1, 2, \dots, n-1$$

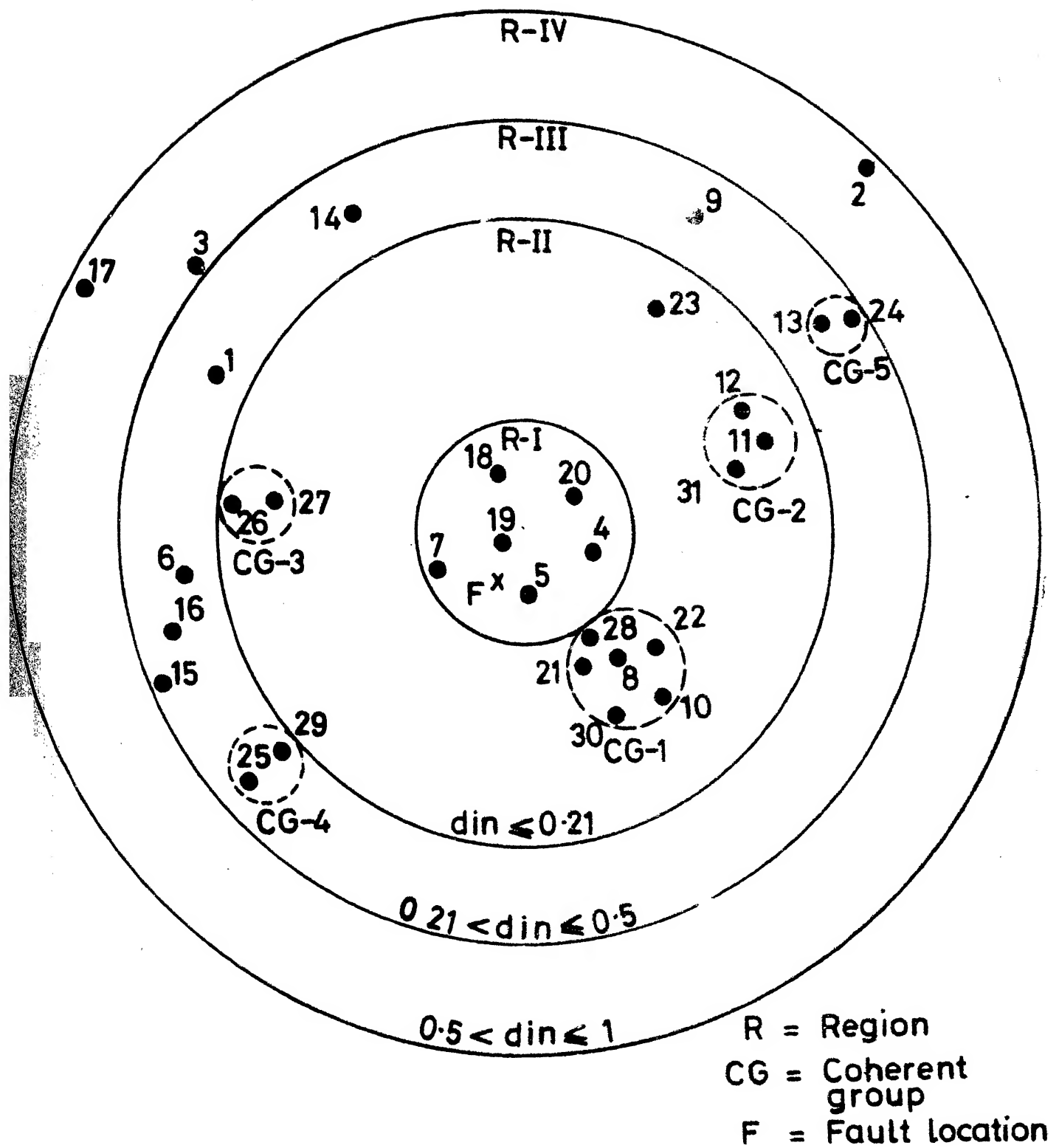


Fig. 3.3 Decomposition of 31 machine system and formation of coherent groups

Region II : generators 28, 21, 8, 10, 22, 31, 30, 11,
 $0.1 < d_{in} \leq 0.21$ 12, 23, 27 and 26

Region III : generators 29, 6, 9, 25, 1, 13, 14, 24, 16,
 $0.21 < d_{i1} \leq 0.3$ and 15

Region IV : generators 3, 17 and 2
 $0.5 < d_{in} \leq 1.0$

We have ensured that there is no coherent group spread over two regions by computing the coherency index for two generators close to each boundary as shown in Table 3.4.

Groups of Coherent Generators: The coherency indices for the generators in the regions II and III are given in Tables 3.5 and 3.6 respectively. The groups of coherent generators for the tolerance $\epsilon = 0.12$ corresponding to $\pm 5^\circ$ in base case studies are given below and shown in Fig. 3.3.

Region II group 1 : generators 30, 28, 22, 21, 10 and 8
 group 2 : generators 31, 12, and 11
 group 3 : generators 26 and 27

Region III group 4 : generators 29 and 25
 group 5 : generators 24 and 13

In region IV, there is no coherent group as is evident from the EMD's in that region. The above coherent groups are verified from both (i) the base case swing curves and (ii) the swing curves from the closed form solution. As an example,

Table 3.5 : Formation of Coherent Groups in Region II

Comparison generator of group	30	31	26	23
Generators in the region II				
8	0.0963*	-	-	-
10	0.0678*	-	-	-
11	0.1746	0.1014*	-	-
12	0.1864	0.1135*	-	-
21	0.0964*	-	-	-
22	0.0940*	-	-	-
23	0.2162	0.1894	0.2349	0.0
26	0.2249	0.1855	0.0*	-
27	0.1977	0.1739	0.0682*	-
28	0.1125*	-	-	-
30	0.0*	-	-	-
31	0.1516	0.0*	-	-

$$\text{Max } \|r_k\| = 0.8583$$

$$k = 1, 2, \dots, n-1$$

$$\epsilon = 0.12$$

Table 3.6 : Formation of Coherent Groups in Region III

Comparison generator of group	25	24	16	15	14	9	6	1
Generators in Region III								
1	0.3602	0.3048	0.4477	0.4691	0.2256	0.2747	0.3591	0.0
6	0.2413	0.4532	0.2380	0.2125	0.3192	0.8907	0.0	-
9	0.3453	0.3553	0.4370	0.4573	0.2436	0.0	-	-
13	0.4201	0.1058*	-	-	-	-	-	-
14	0.3169	0.3100	0.4190	0.4395	0.0	-	-	-
15	0.4297	0.5431	0.3406	0.0	-	-	-	-
16	0.6660	0.6790	0.0	-	-	-	-	-
24	0.4580	0.0*	-	-	-	-	-	-
25	0.0*	-	-	-	-	-	-	-
29	0.1200*	-	-	-	-	-	-	-

$$\text{Max.} \|\underline{r}_k\| = 0.8583$$

$$k = 1, 2, \dots, n-1$$

$$\epsilon = 0.12$$

the base case and the closed form solution swing curves for the generators in coherent group 1 are given in Figs. 3.4 and 3.5 respectively.

3.6 CONSTRUCTION OF COHERENCY BASED EQUIVALENT

After classifying the generators in the external system into different coherent groups, the next step is to replace each coherent group by an equivalent unit. In this section we describe briefly the equivalising procedure of Systems Control Inc. [12,13] which forms the basis for the case study presented in Section 3.7.

3.6.1 Reduction of Coherent Generator Buses:

In this method, the terminal buses of the generators in a coherent group are connected together instead of combining the internal buses of the generators as in [7,8]. Such an approach decouples the problem of network reduction from that of dynamic aggregation of the generating units. It also facilitates the equivalent to be compatible with the existing transient stability programs.

The network equations of the system are arranged in the following manner.

$$\begin{bmatrix} \underline{I}_a \\ \underline{I}_b \\ \underline{I}_c \end{bmatrix} = \begin{bmatrix} [Y_{aa}] & [Y_{ab}] & [0] \\ [Y_{ba}] & [Y_{bb}] & [Y_{bc}] \\ [0] & [Y_{ca}] & [Y_{cc}] \end{bmatrix} \begin{bmatrix} \underline{V}_a \\ \underline{V}_b \\ \underline{V}_c \end{bmatrix} \quad (3.3)$$

where 'c' represents 'q' number of terminal buses of the

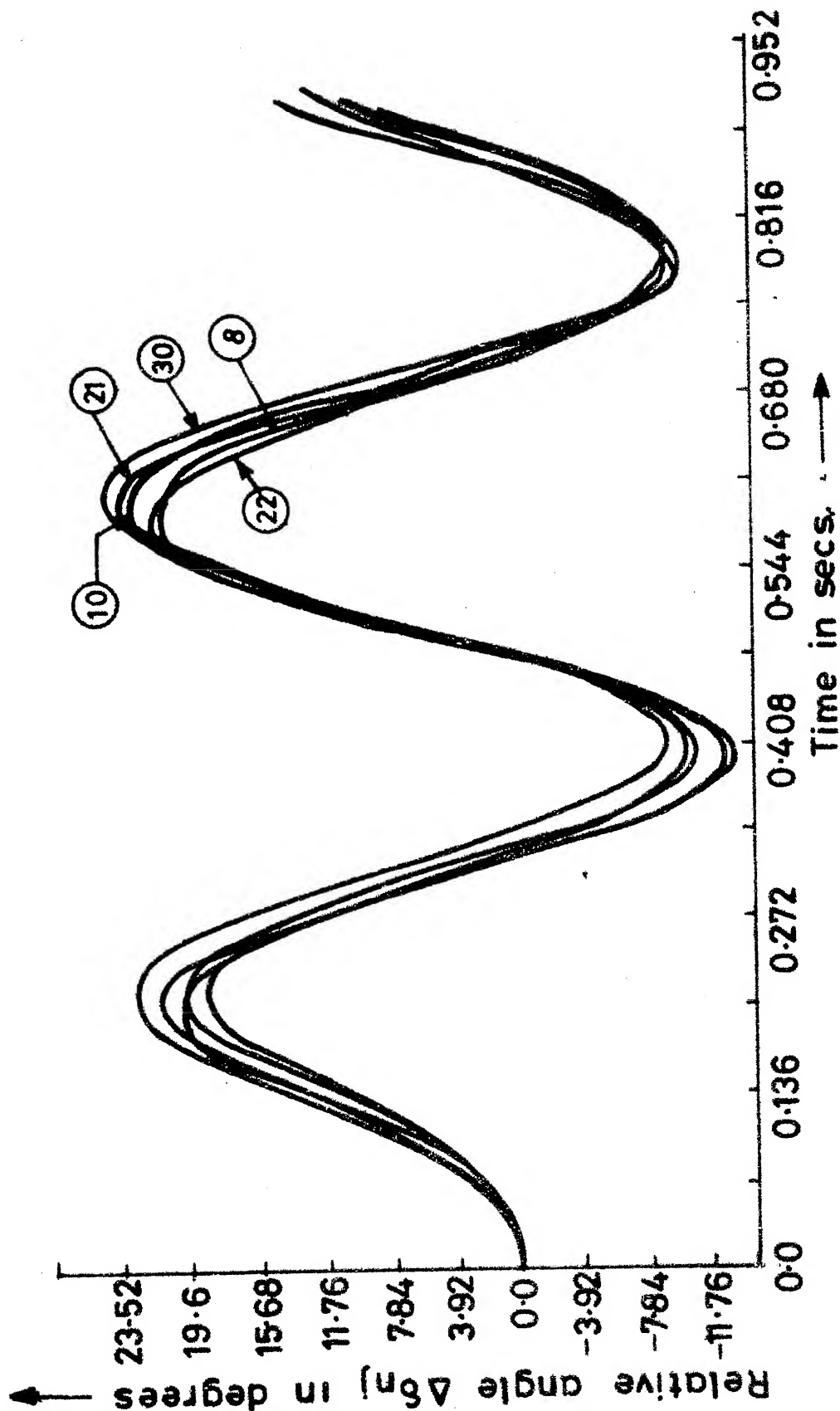


Fig. 3.4 Base case swing curves of the generators in coherent group 1 (31 machine system)

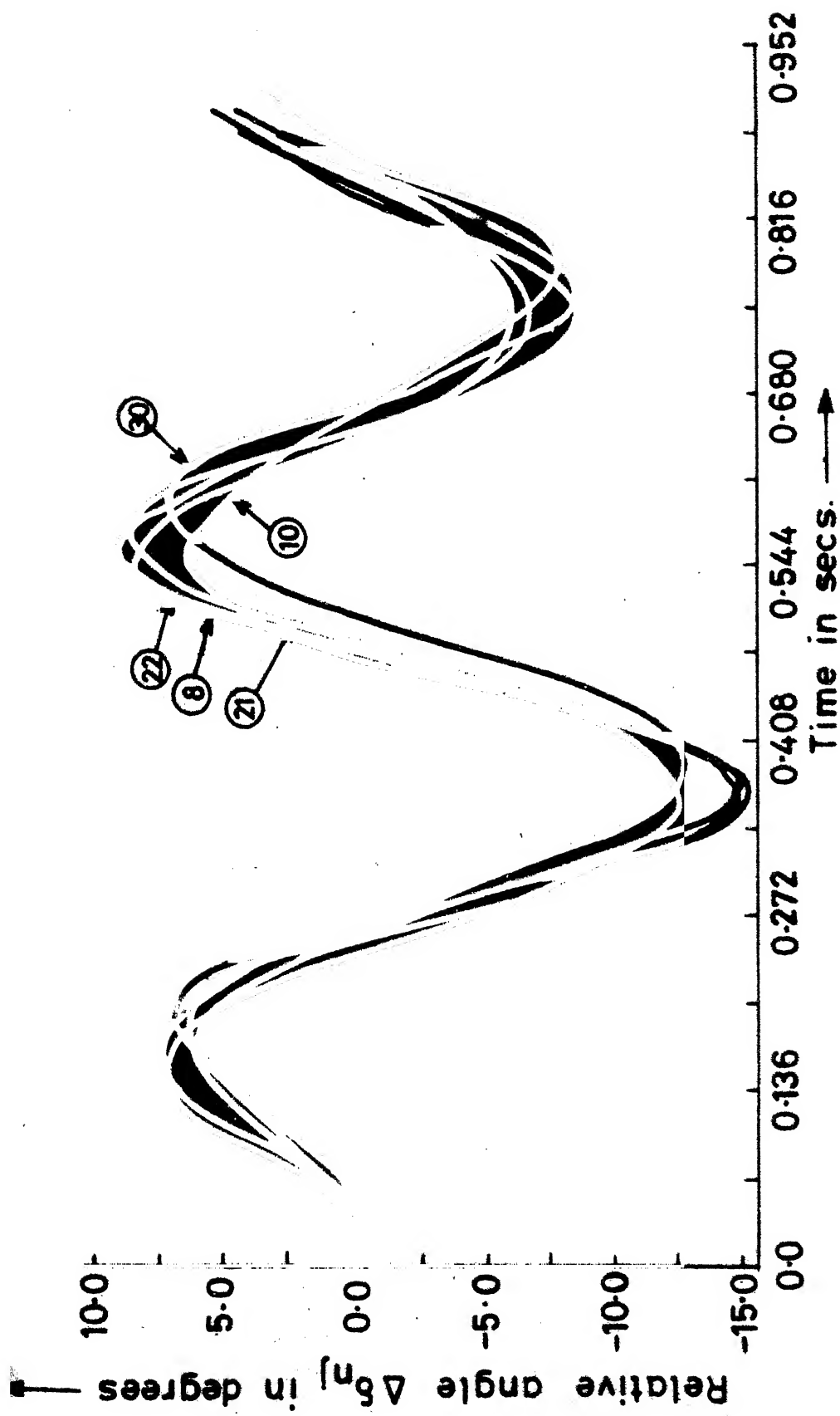


Fig. 3.5 Swing curves (closed form solution) of the generators
in coherent group 1 (31 machine system) 84

generators in a coherent group, 'b' includes the boundary buses of the group, which are 'k' in number, and the buses in rest of the network are included in 'a'. Since the replacement of the buses in 'c' is not going to affect the structure or the parameters in 'a', we will consider only the buses 'b' and 'c' in the reduction process. The network equations in (3.3) for groups 'b' and 'c' for the purpose of reduction are

$$\begin{bmatrix} I_1 \\ \vdots \\ I_k \\ \hline I_{k+1} \\ \vdots \\ I_{k+q} \end{bmatrix} = \begin{bmatrix} y_{11} & \cdots & y_{1k} & y_{1,k+1} & \cdots & y_{1,k+q} \\ \vdots & & \vdots & \vdots & & \vdots \\ y_{k1} & \cdots & y_{kk} & y_{k,k+1} & \cdots & y_{k,k+q} \\ \hline y_{k+1,1} & \cdots & y_{k+1,k} & y_{k+1,k+1} & \cdots & y_{k+1,k+q} \\ \vdots & & \vdots & \vdots & & \vdots \\ y_{k+q,1} & \cdots & y_{k+q,k} & y_{k+q,k+1} & \cdots & y_{k+q,k+q} \end{bmatrix} \begin{bmatrix} V_1 \\ \vdots \\ V_k \\ \hline V_{k+1} \\ \vdots \\ V_{k+q} \end{bmatrix} \quad (3.4)$$

Since the last 'q' buses in (3.4) are replaced by an equivalent bus 't', equation (3.4) becomes

$$\begin{bmatrix} I_1 \\ \vdots \\ I_k \\ \hline I_t \end{bmatrix} = \begin{bmatrix} y_{11} & \cdots & y_{1k} & y_{1t} \\ \vdots & & \vdots & \vdots \\ y_{k1} & \cdots & y_{kk} & y_{kt} \\ \hline y_{t1} & \cdots & y_{tk} & y_{tt} \end{bmatrix} \begin{bmatrix} V_1 \\ \vdots \\ V_k \\ \hline V_t \end{bmatrix} \quad (3.5)$$

The correspondence between (3.4) and (3.5) is established by the principle that (i) the total power of a coherent group should be preserved in the equivalent and (ii) the power

flows over the interconnecting lines should be preserved in the equivalent.

The expressions for the unknown quantities in (3.5) are then determined as [12]

$$\begin{aligned}
 y_{tb} &= \sum_{i=k+1}^{k+q} y_{ib} \frac{V_i^*}{V_t^*} \\
 y_{bt} &= \sum_{i=k+1}^{k+q} y_{ib} \frac{V_i}{V_t} \\
 y_{tt} &= \sum_{i=k+1}^{k+q} \sum_{j=k+1}^{k+q} y_{ij} \frac{V_i}{V_t} \frac{V_j^*}{V_t^*}
 \end{aligned} \tag{3.6}$$

where 'b' is a boundary bus between the group and the rest of the network. The elements in (3.6) are readily determined if V_t i.e. the voltage of the equivalent terminal bus is known. The choice of V_t is arbitrary and is usually taken as the average of the all terminal voltages in the group.

$$|V_t| = \sum_{i=k+1}^{k+q} \frac{|V_i|}{q}, \quad \theta_t = \sum_{i=k+1}^{k+q} \frac{\theta_i}{q} \tag{3.7}$$

In general, $y_{tb} \neq y_{bt}$, indicating the presence of a phase shifting transformer between a boundary bus 'b' and the terminal bus 't'.

3.6.2 Dynamic Aggregation of Coherent Units:

The process of determining the parameters and the equivalent generation from the corresponding parameters and the generations of the individual generating units

is termed as the dynamic aggregation of the generating units. Assuming the classical models for the generators, an equivalent generator representing a coherent group is defined by the following quantities and parameters.

$$\text{Generation : } P_{g(eq)} = P_{g,k+1} + P_{g,k+2} + \dots + P_{g,k+q}$$

$$Q_{g(eq)} = Q_{g,k+1} + Q_{g,k+2} + \dots + Q_{g,k+q}$$

$$\text{Load at the terminal bus: } P_{l(eq)} = P_{l,k+1} + P_{l,k+2} + \dots + P_{l,k+q}$$

$$Q_{l(eq)} = Q_{l,k+1} + Q_{l,k+2} + \dots + Q_{l,k+q}$$

$$\text{Inertia : } M_{eq} = M_{k+1} + M_{k+2} + \dots + M_{k+q}$$

$$\text{Damping Coefficient: } D_{eq} = D_{k+1} + D_{k+2} + \dots + D_{k+q}$$

$$\text{Generator Impedance : } 1/z'_{eq} = 1/z'_{k+1} + 1/z'_{k+2} + \dots + 1/z'_{k+q}$$

The procedure for replacing a coherent group by an equivalent generating unit and its modified interconnections as described in Sections 3.6.2 and 3.6.1 respectively is to be repeated for each coherent group. Since we have represented the loads by the constant impedances, the load buses are reduced by using the Gaussian elimination formula.

3.7 A CASE STUDY

In this section, we illustrate the principle of coherency based equivalent with the help of a case study for a typical power system. The power system considered

is described in detail in Section 2.9 and the study system and the external system are shown in Fig.2.2. The coherent groups valid for a set of fault locations in the study system as determined in Sections 2.9 and 2.12 are the following.

Group 1 : generators 9, 11, 12 and 13

Group 2 : generators 6 and 7

The procedure of equivalising for the coherent group 1 is shown in Fig. 3.6(a) and (b) and that for group 2 in Fig. 3.7 respectively. Thus, the equivalent of the system consists of 9 generators against 13 in the full scale system.

A three phase fault on bus 10 cleared in 0.1 sec by opening the line 10-7 is considered. The responses of generators 1 and 3 for this fault are given in Fig. 3.8 and Fig. 3.9 respectively for both (i) the full scale system and (ii) the equivalent system.

The responses of the generators in the equivalent of the system match closely with the responses in the full scale system. The computer time required for simulating the equivalent is about 65% of the time for the full scale simulation. This excludes the time for constructing the equivalent. A significant reduction in size and computer time is possible in large scale systems where the number of coherent groups is large. For example, as reported in Ref. [12], a power system having 337 generators is reduced to 166 generators and simulated in about 50% of the time

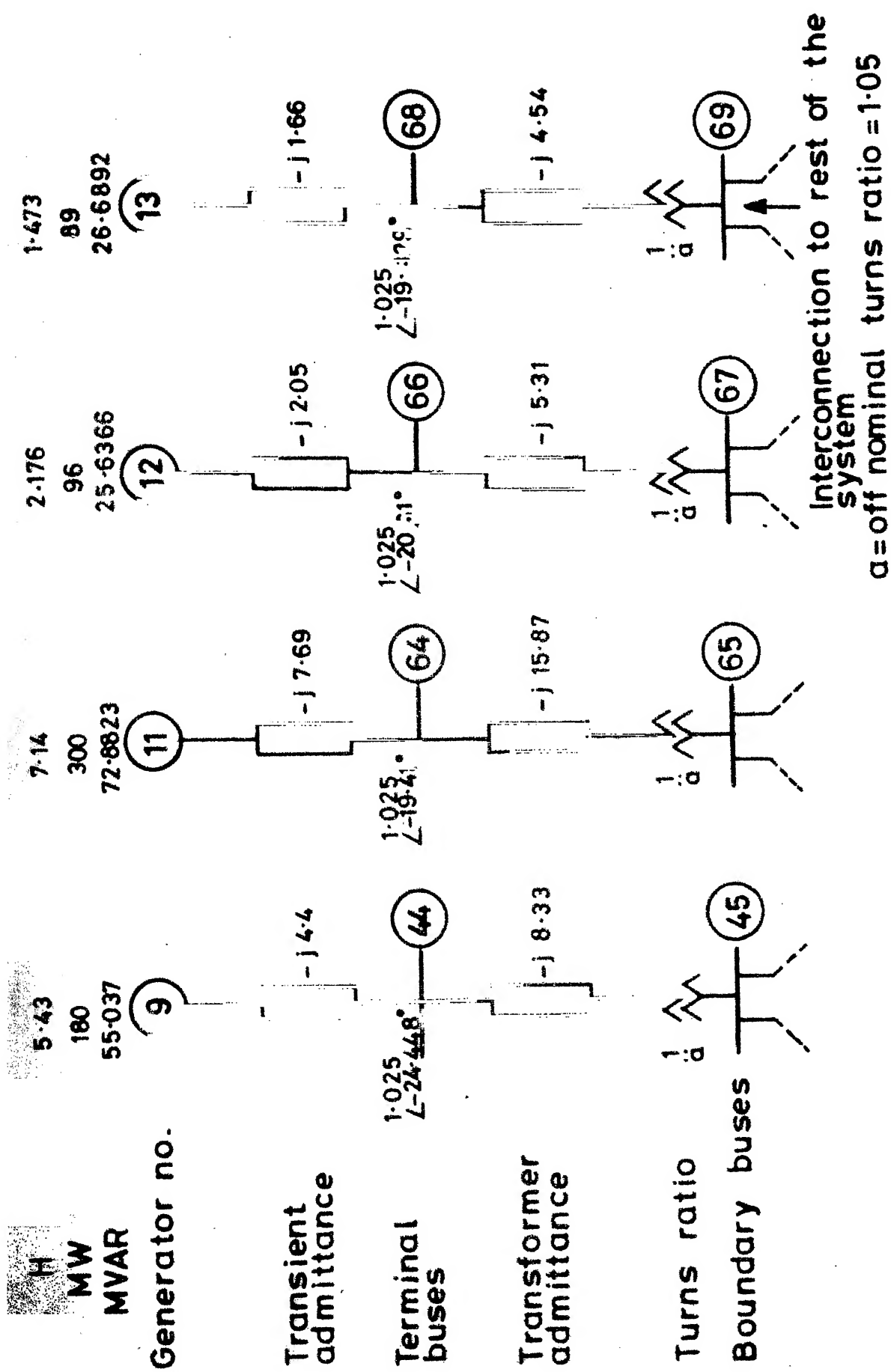


Fig. 3-6a Coherent group no.1 in the full scale system

H

MW

MVAR

16.219
665.0
180.2451

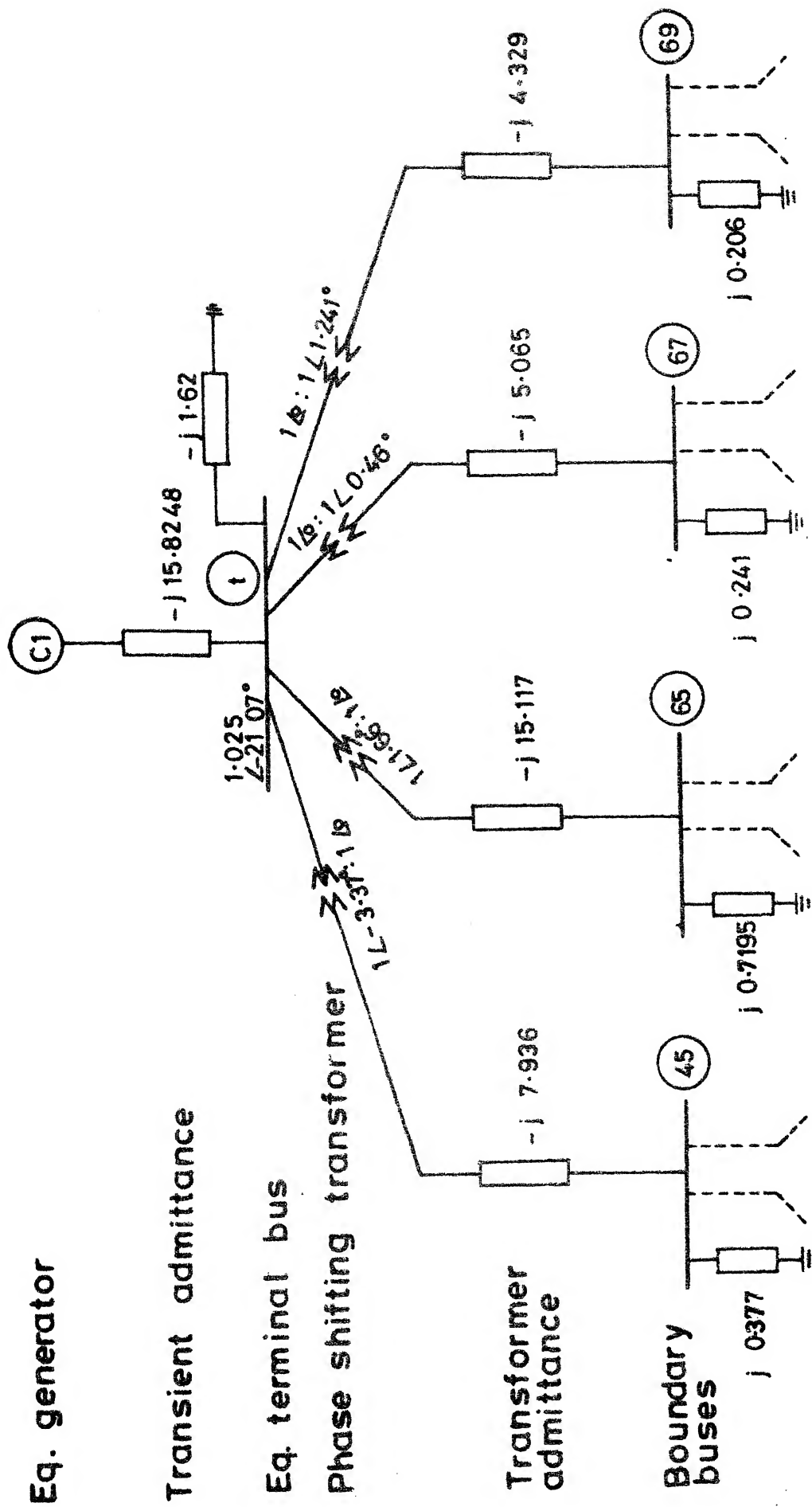


Fig. 3.6b Equivalent representation of coherent group no.1.

H	2.55	2.7	5.25
MW	304.0	261.0	565
MVAR	76.287	70.506	146.794

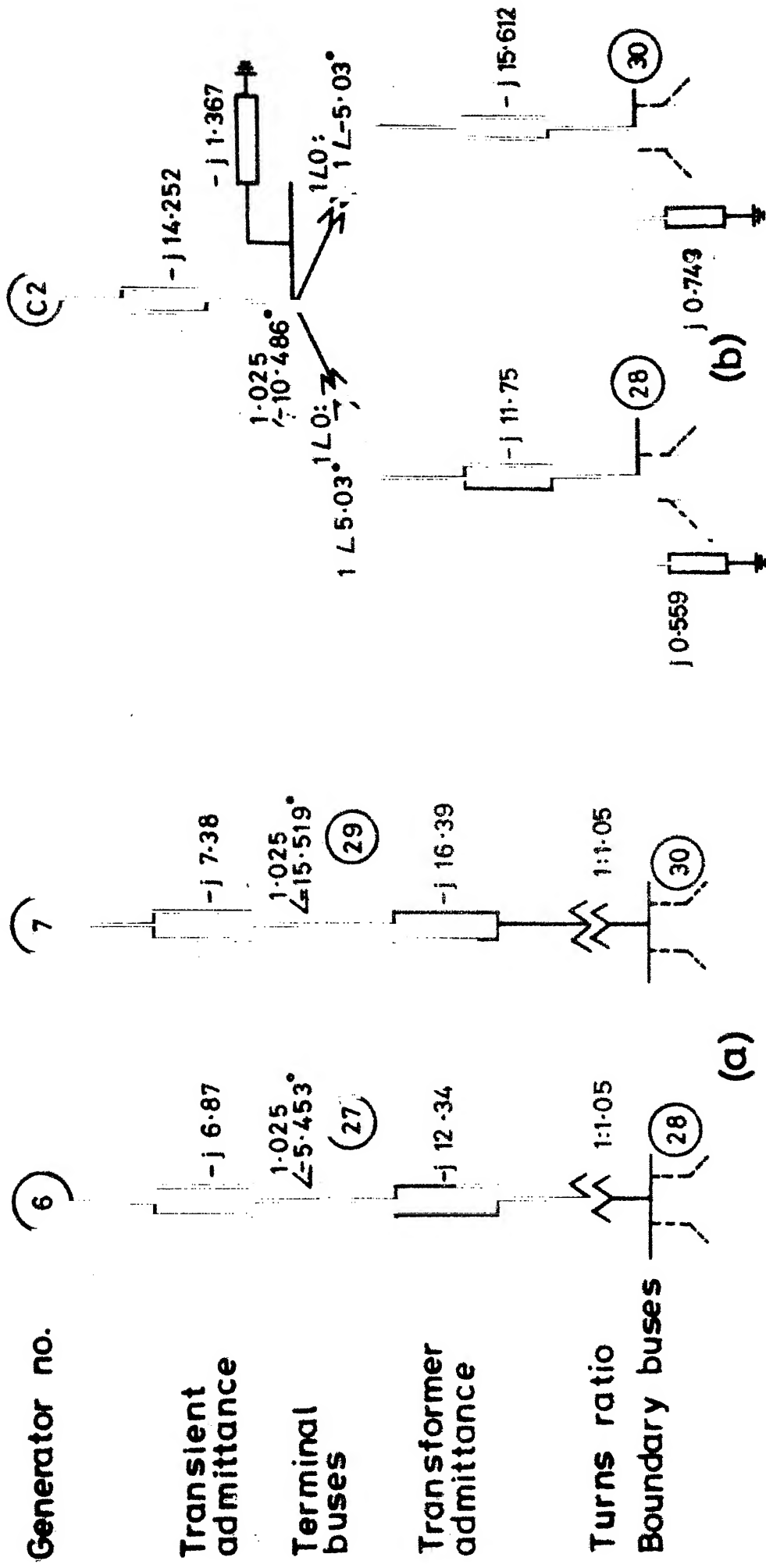


Fig. 3.7 (a) Coherent group no.2 in the full scale system
(b) Equivalent representation

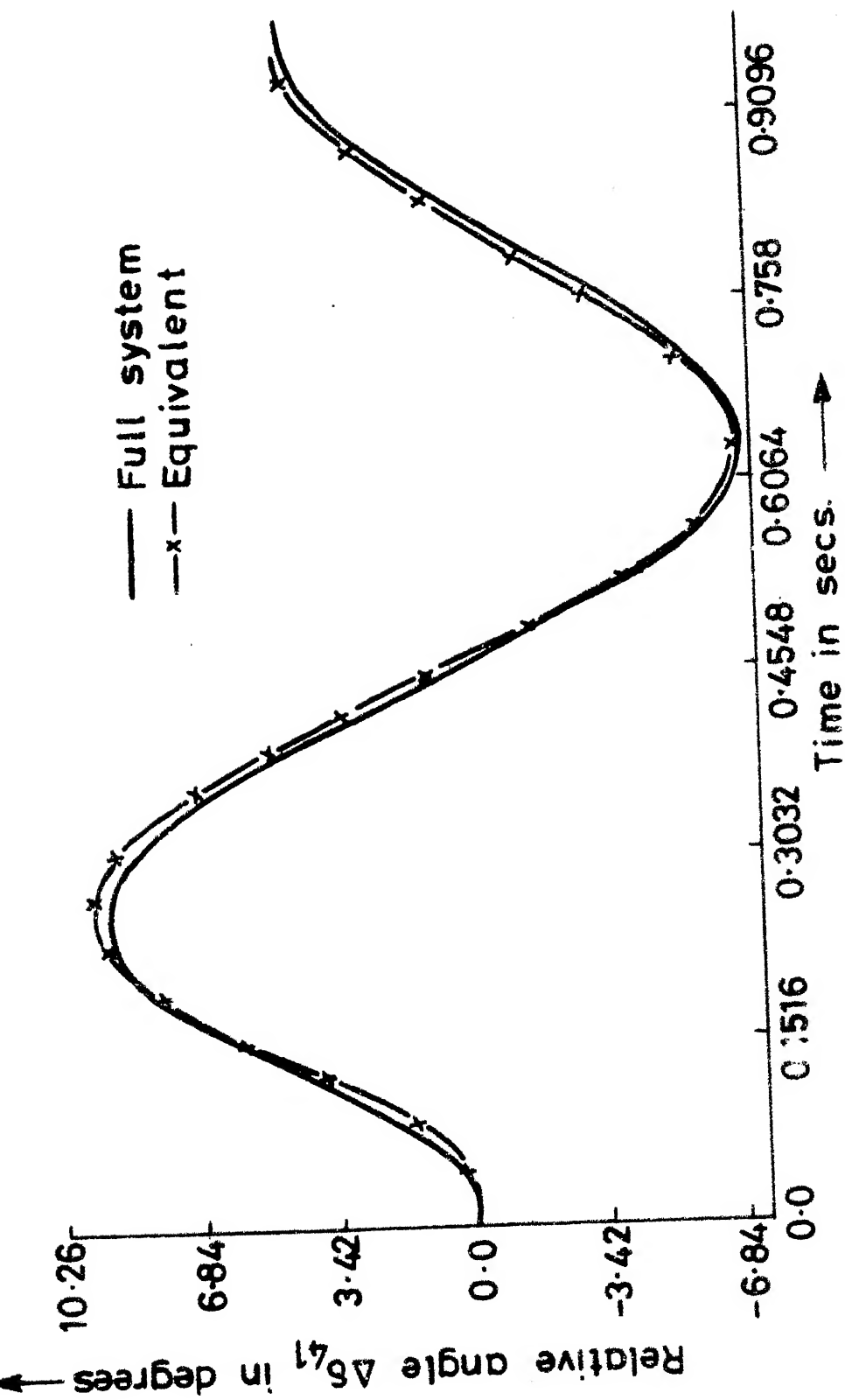


Fig. 3.8 Responses of generator 1 in (i) Full scale system and (ii) equivalent

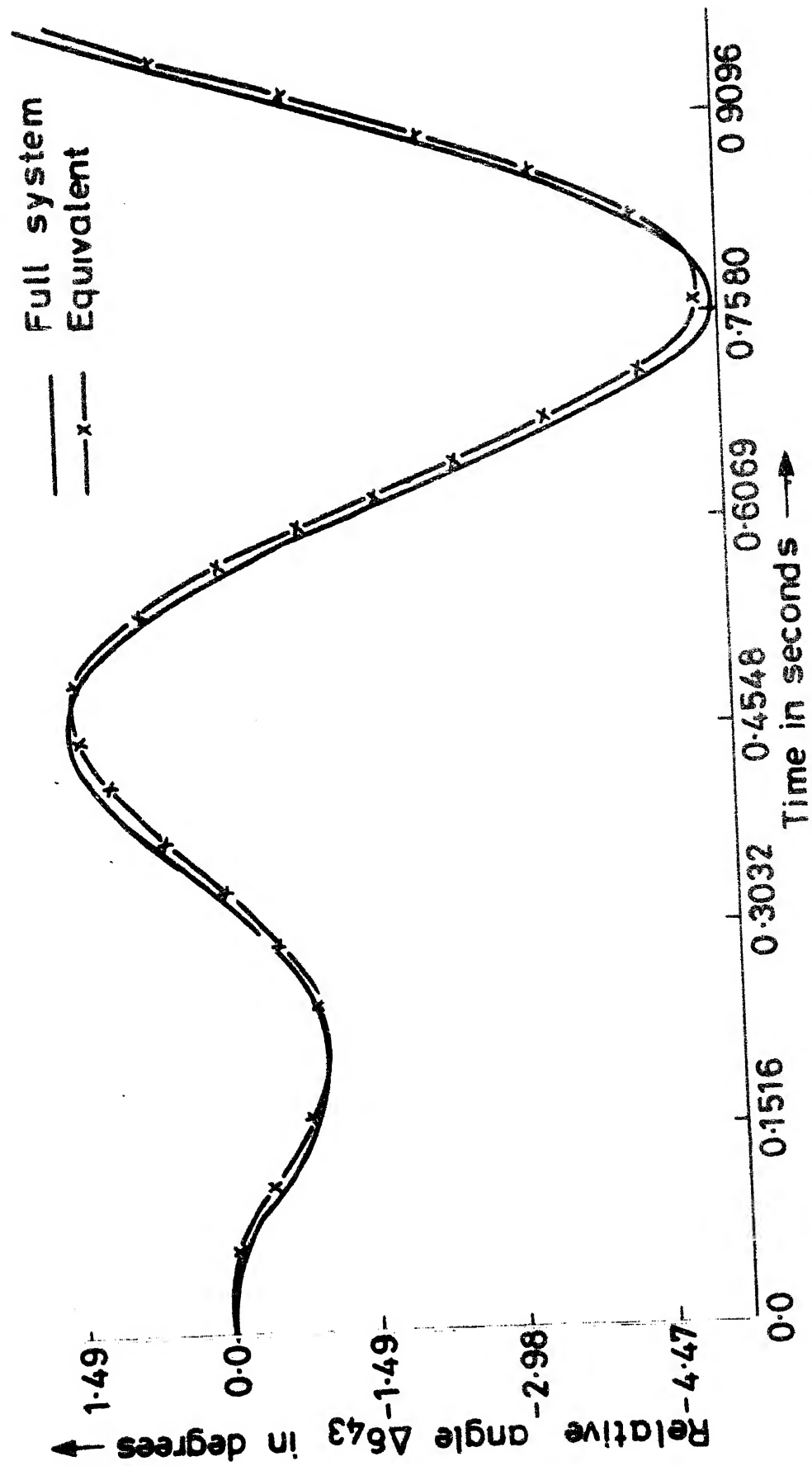


Fig. 3.9 Responses of $\Delta\delta_{43}$ in (i) Full system and (ii) Equivalent

required for full scale simulation. However, in the present case the advantage is realised by using the same equivalent for different fault locations in the study system.

3.8 CONCLUSION

In this chapter, we have presented a method for decomposition of a power system into different regions for modelling the generators. The criterion for decomposition incorporates the electromechanical effects between the machines during the transient period. The demarcation of a power system into different regions has also been used to simplify the procedure for grouping of coherent generators. The grouping technique and the construction of a coherency based equivalent have been demonstrated on a power system example.

CHAPTER 4

DYNAMIC SIMPLIFICATION USING SINGULAR PERTURBATION THEORY (DYNAMIC STABILITY STUDIES)

4.1 INTRODUCTION

A model of much interest to power engineers is of the form

$$\dot{\underline{y}} = [\underline{A}] \underline{y} + [\underline{B}] \underline{u} \quad \text{with} \quad \underline{y}(0) = \underline{y}^0 \quad (4.1)$$

This model is extensively used in the dynamic stability studies and in the design of control circuits. The recent trend to represent the dynamics of a generating unit in detail incorporates the effect of many small time constants. Ignoring completely the effect of these time constants in the simplified model gives rise to a less accurate representation of the given system. Therefore the technique for simplifying (4.1) should consider the effect of such time constants to improve the accuracy. A need for an effective technique for this purpose has been brought out in Section 1.3.3, in which the existing techniques for simplifying (4.1) have been discussed. In the proposed technique we make such an attempt by using singular perturbation theory.

This chapter is organised along the following lines.

Firstly a systematic algorithm to formulate the model (4.1) for a multimachine system using the detailed

representation of the generating units is presented. Then the model is written in the singular perturbation form (1.19) by treating the response of (4.1) as the perturbation of the response of the simplified system (reduced system). This needs the appropriate separation of the fast and slow state variables. The validity of the simplified system is ascertained by the condition given by Vidyasagar [60]. The subsequent improvement in the response is obtained by deriving the first order solution to (4.1) by using the method of asymptotic expansions. The technique results in solving a set of fast and slow subsystems separately and where the step size of integration could be larger than for the original system (4.1). The resulting computational saving makes this method attractive for model simplification. Single and three machine examples illustrate the technique.

4.2 POWER SYSTEM MODEL

A power system model for dynamic stability studies consists of a linearised set of differential equations (representing the dynamics of generating units) and a set of algebraic equations (describing their interconnections). These equations are cast in the state space form (4.1) by eliminating the non-state variables. We consider a synchronous machine, an exciter-voltage regulator system and a turbine-governor system as the components of a generating unit. A synchronous machine is represented by Riaz's hybrid

parameter model with equivalent rotor voltages as state variables [62,64]. The voltages $\Delta \hat{E}_d''$ and $\Delta \hat{E}_q''$ are chosen as state variables rather than $\Delta E_d''$ and $\Delta E_q''$ as defined in [62]. The rotor voltages $\Delta \hat{E}_d''$ and $\Delta \hat{E}_q''$ proportional to the flux linkages of the damper windings are associated with the time constants T_{q0}'' and T_{d0}'' . The rotor voltages $\Delta E_d''$ and $\Delta E_q''$ are then expressed as

$$\begin{aligned}\Delta E_q'' &= \Delta E_q' + \Delta \hat{E}_q'' \\ \Delta E_d'' &= \Delta E_d' + \Delta \hat{E}_d''\end{aligned}\tag{4.2}$$

The standard models for an exciter-voltage regulator system and a turbine-governor system as given in Ref. [65-68] are used. The details of modelling a generating unit are given in Appendix C. In the main text of the thesis, we will use only one symbolic state space equation for each component of a generating unit.

4.2.1 Generating Unit Model:

Consider a power system having 'n' number of generating units. The state space representation of ith generating unit with its own d-q axes as the reference frame is given by

$$\begin{bmatrix} \dot{y}_{mi} \\ \dot{y}_{ei} \\ \dot{y}_{ti} \end{bmatrix} = \begin{bmatrix} A_{mi} & C_{mei} & C_{mti} \\ C_{emi} & A_{ei} & 0 \\ C_{tmi} & 0 & A_{ti} \end{bmatrix} \begin{bmatrix} y_{mi} \\ y_{ei} \\ y_{ti} \end{bmatrix} + \begin{bmatrix} C_{mi} \\ C_{ei} \\ C_{ti} \end{bmatrix} \Delta I_{mi} + \begin{bmatrix} 0 & b_{mi} \\ b_{ei} & 0 \\ 0 & b_{ti} \end{bmatrix} u_{gi}$$

$i = 1, 2, \dots, n$

(4.3)

where \underline{y}_{mi} , \underline{y}_{ei} and \underline{y}_{ti} are the state vectors representing the dynamics of the i th synchronous machine, its exciter-voltage regulator system and the turbine-governor system respectively. These are defined as follows:

$$\underline{y}_{mi}^T = [\Delta E'_{qi}, \Delta \omega_i, \Delta \delta_i, \Delta E'_{di}, \Delta \hat{E}''_{qi}, \Delta \hat{E}''_{di}]$$

$$\underline{y}_{ei}^T = [\Delta E_{fdi}, y_{e2i}, y_{e3i}, y_{e4i}, y_{e5i}]$$

$$\underline{y}_{ti}^T = [y_{t1i}, y_{t2i}, y_{t3i}]$$

$\Delta \underline{I}_{mi}$ and \underline{u}_{gi} are defined as

$$\Delta \underline{I}_{mi}^T = [\Delta I_{di}, \Delta I_{qi}] \quad , \quad \underline{u}_{gi}^T = [\Delta V_{refi}, \Delta T_{moi}]$$

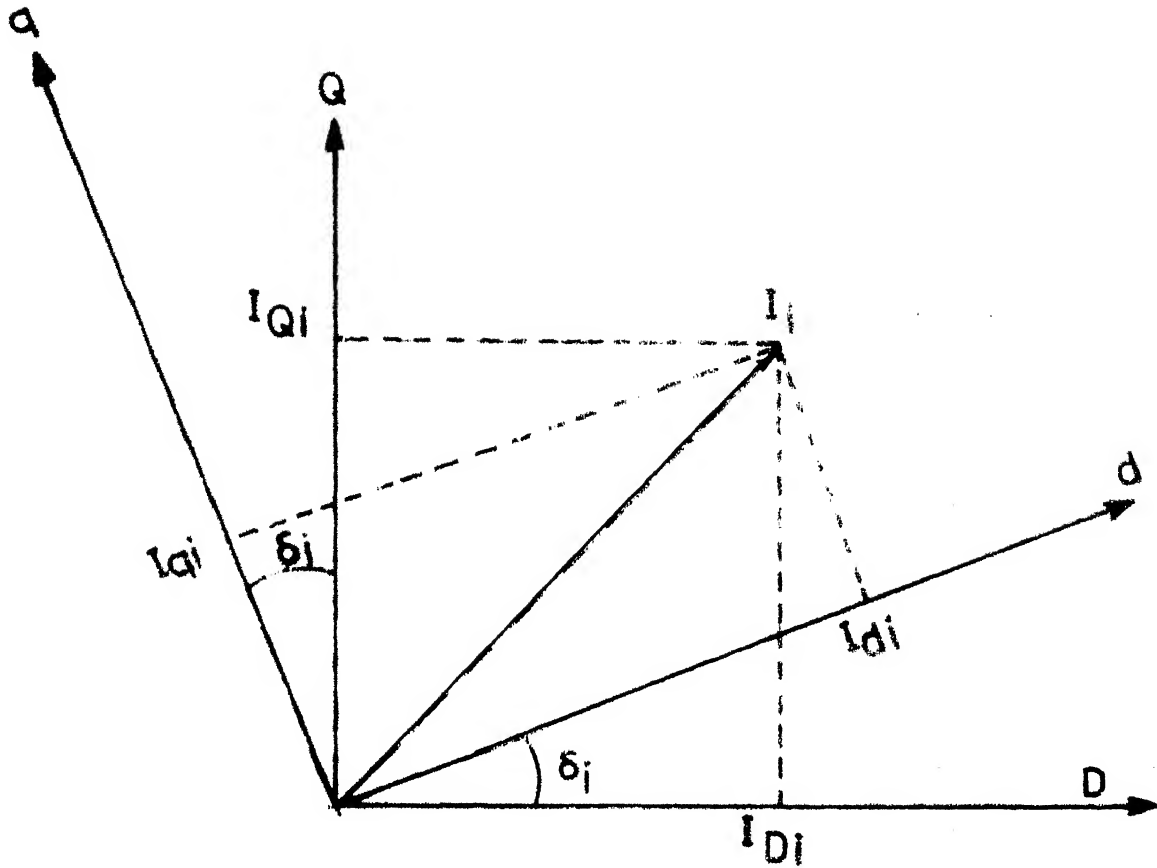
The details of equation (4.3) are given in Appendix C and the state variables \underline{y}_{ei} and \underline{y}_{ti} are identified on Figs. C.2 and C.3 of Appendix C respectively.

4.2.2 Transformation to the Network Reference Frame:

The following transformation is applied to refer the machine currents and voltages to a common network reference frame denoted by D-Q axes [64] (Fig.4.1)

$$\begin{bmatrix} I_{di} \\ I_{qi} \end{bmatrix} = \begin{bmatrix} \cos \delta_i & \sin \delta_i \\ -\sin \delta_i & \cos \delta_i \end{bmatrix} \begin{bmatrix} I_{Di} \\ I_{Qi} \end{bmatrix} \quad (4.4)$$

$i = 1, 2, \dots, n$



4.1 Transformation of machine current to network reference frame D-Q

On linearisation, equation (4.4) becomes

$$\Delta \underline{I}_{mi} = [S_i] \Delta \underline{I}_{Ni} + \underline{J}_i \Delta \delta_i \quad i=1,2,\dots,n \quad (4.5)$$

where

$$\Delta \underline{I}_{Ni}^T = [\Delta I_{Di}, \Delta I_{Qi}]$$

$$[S_i] = \begin{bmatrix} \cos \delta_i^0 & \sin \delta_i^0 \\ -\sin \delta_i^0 & \cos \delta_i^0 \end{bmatrix}; \quad \underline{J}_i = \begin{bmatrix} I_{qi}^0 \\ -I_{di}^0 \end{bmatrix}$$

4.2.3 Network Equations:

The transmission network equations describing the interconnections of the generating units are given by

$$\begin{bmatrix} \Delta I_{D1} \\ \Delta I_{Q1} \\ \vdots \\ \Delta I_{Dn} \\ \Delta I_{Qn} \end{bmatrix} = \begin{bmatrix} G_{11} & -B_{11} & \dots & G_{1n} & -B_{1n} \\ B_{11} & G_{11} & \dots & B_{1n} & G_{1n} \\ \vdots & \vdots & & \vdots & \vdots \\ G_{n1} & -B_{n1} & \dots & G_{nn} & -B_{nn} \\ B_{n1} & G_{n1} & \dots & B_{nn} & G_{nn} \end{bmatrix} \begin{bmatrix} \Delta E''_{D1} \\ \Delta E''_{Q1} \\ \vdots \\ \Delta E''_{Dn} \\ \Delta E''_{Qn} \end{bmatrix} \quad (4.6)$$

where $\Delta E''_{Di}$ and $\Delta E''_{Qi}$ are defined as

$$\Delta E''_{Di} = \Delta E'_{Di} + \Delta \hat{E}''_{Di} \quad (4.7)$$

$$\Delta E''_{Qi} = \Delta E'_{Qi} + \Delta \hat{E}''_{Qi}$$

The inverse transformation for voltages and currents is given by

$$\Delta \underline{E}_{Ni} = [S_i]^T \Delta \underline{E}_{mi} + \underline{L}_i \Delta \delta_i \quad i=1,2,\dots,n \quad (4.8)$$

where

$$\Delta \underline{E}_{Ni}'' = [\Delta E_{Di}'', \Delta E_{Qi}'']^T, \quad \Delta \underline{E}_{mi}'' = [\Delta E_{di}'', \Delta E_{qi}'']^T$$

$$\underline{L}_i = [-E_{Qi}^0, E_{Di}^0]^T$$

4.2.4 System Matrix:

The system matrix is formed by arranging the equations (4.3) for 'n' number of generating units and eliminating the non-state variables $\Delta \underline{I}_m^T = [\Delta I_{m1}^T, \dots, \Delta I_{mn}^T]$ by using equations (4.5), (4.6) and (4.8). The resulting system equation is given as

$$\dot{\underline{y}} = [A] \underline{y} + [B] \underline{u}, \quad \text{with } \underline{y}(0) = \underline{y}^0 \quad (4.9)$$

where

$$\underline{y}^T = [y_{g1}^T, y_{g2}^T, \dots, y_{gn}^T], \quad y_{gi}^T = [y_{mi}^T, y_{ei}^T, y_{ti}^T]$$

$$\underline{u}^T = [u_{g1}^T, u_{g2}^T, \dots, u_{gn}^T]$$

The rotor angles in (4.9) can be expressed with respect to a rotating d-q axes frame of a reference machine, thereby reducing the order of the system by one in accordance with the procedure given in Ref.[61,64].

Without loss of generality, let the dimensions of \underline{y} and \underline{u} be denoted by 'm' and 'r' respectively. Now we are concerned with the dynamic simplification and simulation of (4.9) using the singular perturbation technique. Before this

problem is taken up, we briefly review the singular perturbation theory as applied to the initial value problem in a linear time invariant system.

4.3 SINGULAR PERTURBATION THEORY

Suppose the system (4.9) is written in the singular perturbation form as

$$\begin{bmatrix} \dot{\underline{x}} \\ \epsilon \dot{\underline{z}} \end{bmatrix} = \begin{bmatrix} A_{11} & A_{12} \\ A_{21} & A_{22} \end{bmatrix} \begin{bmatrix} \underline{x} \\ \underline{z} \end{bmatrix} + \begin{bmatrix} B_1 \\ B_2 \end{bmatrix} \underline{u} \quad (4.10)$$

with $\underline{x}(0) = \underline{x}^0$ and $\underline{z}(0) = \underline{z}^0$,

where \underline{x} and \underline{z} have dimensions ' m_1 ' and ' m_2 ' respectively such that $m_1 + m_2 = m$. Assume that

- (i) the perturbation parameter ' ϵ ' is small and > 0 and
- (ii) the matrix $[A_{22}]$ is nonsingular and stable.

The asymptotic solution of (4.10) is an additive function of time ' t ' and a stretched variable $\tau = t/\epsilon$. We seek the solution of (4.10) in the form [50]

$$\begin{aligned} \underline{x}(t, \epsilon) &= \underline{X}(t, \epsilon) + \epsilon \underline{p}(\tau, \epsilon) \\ \underline{z}(t, \epsilon) &= \underline{Z}(t, \epsilon) + \underline{q}(\tau, \epsilon) \end{aligned} \quad (4.11)$$

where $(\underline{X}, \underline{Z})$ is the outer expansion (i.e. the solution away from $t = 0$) and $(\epsilon \underline{p}, \underline{q})$ is the boundary layer correction, which is significant only near $t = 0$. \underline{X} , \underline{Z} , \underline{p} and \underline{q} all have asymptotic expansions as $\epsilon \rightarrow 0$ as

$$(\underline{X}, \underline{Z}, \underline{p}, \underline{q}) \sim \left(\sum_{j=0}^{\infty} \underline{X}_j \epsilon^j, \sum_{j=0}^{\infty} \underline{Z}_j \epsilon^j, \sum_{j=0}^{\infty} \underline{p}_j \epsilon^j, \sum_{j=0}^{\infty} \underline{q}_j \epsilon^j \right) \quad (4.12)$$

Under the specified hypotheses (i) and (ii), the boundary layer terms \underline{p} and \underline{q} in (4.11) will decay fast as $\epsilon \rightarrow 0$ (or $\tau \rightarrow \infty$) and $(\underline{x}, \underline{z})$ will converge to $(\underline{X}, \underline{Z})$. The equations for different terms in (4.12) can be derived by substituting the expansions for $(\underline{X}, \underline{Z})$ and $(\underline{x}, \underline{z})$ in (4.10) separately and equating the terms corresponding to equal powers of ϵ on both sides.

The first term $(\underline{X}_0, \underline{Z}_0)$ in the outer expansion is the solution of the reduced problem, which is given by setting $\epsilon = 0$ in (4.10).

$$\dot{\underline{X}}_0 = [A_R] \underline{X}_0 + [B_R] \underline{u} \quad \text{with} \quad \underline{X}_0(0) = \underline{x}^0 \quad (4.13a)$$

$$\underline{Z}_0 = -[A_{22}^{-1} \quad A_{21}] \underline{X}_0 - [A_{22}^{-1} \quad B_2] \underline{u} \quad (4.13b)$$

where

$$[A_R] = [A_{11} \quad -A_{12} \quad A_{22}^{-1} \quad A_{21}]$$

$$[B_R] = [B_1 \quad -A_{12} \quad A_{22}^{-1} \quad B_2]$$

\underline{q}_0 is obtained by solving a set of differential equations

$$\frac{d\underline{q}_0}{d\tau} = [A_{22}] \underline{q}_0 \quad ; \quad \text{with} \quad \underline{q}_0(0) = \underline{z}^0 - \underline{Z}_0(0) \quad (4.14)$$

and $\tau = t/\epsilon$

Then the zeroth order solution of $(\underline{x}, \underline{z})$ is given by

$$\underline{x}(t) = \underline{X}_0(t) + O(\epsilon) \quad (4.15)$$

$$\underline{z}(t) = \underline{Z}_0(t) + \underline{q}_0(\tau) + O(\epsilon)$$

Further improvement in the approximation to $(\underline{x}, \underline{z})$ can be obtained by deriving the first order solution of (4.10) as given below.

$$\underline{x}(t) = \underline{x}_0(t) + \epsilon [\underline{x}_1(t) + \underline{p}_0(\tau)] + O(\epsilon^2) \quad (4.16)$$

$$\underline{z}(t) = \underline{z}_0(t) + \underline{q}_0(\tau) + \epsilon [\underline{z}_1(t) + \underline{q}_1(\tau)] + O(\epsilon^2)$$

This, however, involves the solution of following additional sets of equations for $(\underline{x}_1, \underline{z}_1)$ and $(\underline{p}_0, \underline{q}_1)$ with appropriate initial conditions.

$$\frac{d\underline{p}_0}{d\tau} = [A_{12}] \underline{q}_0(\tau) \quad (4.17)$$

with $\underline{p}_0(\infty) = \underline{0}$ and $\underline{q}_0(\tau)$ is given by (4.14).

$$\dot{\underline{x}}_1 = [A_R] \underline{x}_1 + [A_{12} \ A_{22}^{-1}] \dot{\underline{z}}_0 \quad (4.18a)$$

$$\underline{z}_1 = [A_{22}^{-1}] \dot{\underline{z}}_0 - [A_{22}^{-1} A_{21}] \underline{x}_1 \quad (4.18b)$$

with initial conditions $\underline{x}_1(0) = -\underline{p}_0(0)$, and

$$\frac{d\underline{q}_1}{d\tau} = [A_{21}] \underline{p}_0 + [A_{22}] \underline{q}_1 \quad (4.19)$$

with $\underline{q}_0(0) = -\underline{z}_1(0)$

4.4 MODEL SIMPLIFICATION USING SINGULAR PERTURBATION THEORY

In this section, a systematic procedure for simplifying the dynamic model (4.9) of a power system using the theory in the preceding section is given. Since the model (4.9) of any physical power system is hardly given in the

required form (4.10), the first and important step is to rewrite the given system equations in the singular perturbation form. This needs proper identification of the perturbation parameter ' ϵ '. In physical systems (it as well applies to power systems also), the use of ϵ is symbolic and represents the presence of a fast as well as a slow phenomena in the given system equations. This is primarily ascertained if the ratio

$$\frac{\max_i |\lambda_i|}{\min_i |\lambda_i|} \gg 1$$

where λ is the eigenvalue of $[A]$. The next step is the partitioning of \underline{y}^T as $[\underline{x}^T, \underline{z}^T]$ i.e. the slow and the fast varying state variables. To start with, the state variables associated with small time constants, small rotating masses and large gains are included in the group \underline{z} by expressing them as $T_i = \epsilon \hat{T}_i$, $M_j = \epsilon \hat{M}_j$ and $K_i = \hat{K}_i / \epsilon$, where \hat{T}_i , \hat{M}_j and \hat{K}_i are the known coefficients [46]. Then the validity of grouping or of the resulting reduced system (4.13a) is verified by the condition (4.20) given below. If the grouping is not valid, the state variables have to be regrouped and the procedure is repeated.

Vidyasagar [60], by considering the eigenvalues of $[A]$ as the perturbation of the eigenvalues of $[A_R]$ and $[A_{22}/\epsilon]$ showed that if

$$s = - \frac{\min_i [\operatorname{Re} \Omega_i]}{2} / |\sigma_j| > 1 \quad (4.20)$$

$j=1, 2, \dots, m_1$

where σ_j = eigenvalue of $[A_R]$

Ω_i = eigenvalue of $[A_{22}/\epsilon]$

then ' m_1 ' eigenvalues of $[A_R]$ and ' m_2 ' eigenvalues of $[A_{22}/\epsilon]$ are close to the corresponding eigenvalues of $[A]$. We will use (4.20) to verify the validity of grouping the state variables \underline{y}^T as $[\underline{x}^T, \underline{z}^T]$.

4.4.1 Numerical Example to Illustrate the Grouping of State Variables:

We now illustrate the above aspect of grouping the state variables with a small numerical example. Consider a single machine infinite bus example (Fig. 4.2). The synchronous machine model as given in Appendix C is considered and the control equipments are ignored for the sake of brevity. For $H = 3.5$, $D = 0.005$ and other parameters given in Section 4.5.1, the system equations are given by

$$\begin{bmatrix} \Delta \dot{E}'_q \\ \Delta \dot{\omega} \\ \Delta \dot{\delta} \\ \Delta \dot{E}'_d \\ \Delta \hat{E}''_d \\ \Delta \hat{E}''_q \end{bmatrix} = \begin{bmatrix} -1.58 & 0.0 & -0.06 & -0.01 & 0.66 & -0.01 \\ -127.86 & -0.22 & -148.84 & 93.12 & -127.86 & 97.12 \\ 0.0 & 1.0 & 0.0 & 0.0 & 0.0 & 0.0 \\ 0.23 & 0.0 & 0.46 & -14.94 & 0.23 & 2.42 \\ 22.82 & 0.0 & -2.258 & -0.17 & -24.24 & -0.17 \\ 5.35 & 0.0 & 10.68 & 55.52 & 5.35 & -26.43 \end{bmatrix} \begin{bmatrix} \Delta E'_q \\ \Delta \omega \\ \Delta \delta \\ \Delta E'_d \\ \Delta \hat{E}''_d \\ \Delta \hat{E}''_q \end{bmatrix} + \begin{bmatrix} 0.0735 & 0.0 \\ 0.0 & 44.8786 \\ 0.0 & 0.0 \\ 0.0 & 0.0 \\ 0.0 & 0.0 \\ 0.0 & 0.0 \end{bmatrix} \begin{bmatrix} \Delta E_{fd} \\ \Delta T_m \end{bmatrix} \quad (4.21)$$

In (4.21), the state variables $\Delta \hat{E}_q''$ and $\Delta \hat{E}_d''$ are associated with the time constants T_{do}'' and T_{qo}'' respectively. Similarly $\Delta E_q'$ and $\Delta E_d'$ are associated with the time constants T_{do}' and T_{qo}' respectively. Typical values of T_{do}'' and T_{qo}'' for synchronous machines are very small and are in the range 0.01 - 0.1 sec. whereas the values of T_{qo}' and T_{do}' are in the range 1 - 6 secs. and above. Therefore we group \underline{y} as

$$\underline{x}^T = [\Delta E_q', \Delta \omega, \Delta \delta, \Delta E_d'] \text{ and } \underline{z}^T = [\Delta \hat{E}_q'', \Delta \hat{E}_d'']$$

Such a separation of state variables gives the following matrices $[A_R]$ and $[A_{22}/\epsilon]$ corresponding to the slow and fast subsystems (4.13) and (4.14) respectively as given below.

$$[A_R] = \begin{bmatrix} -0.9638 & 0.0 & -0.1319 & -0.0310 \\ -209.3901 & -0.2244 & -99.2697 & 303.5656 \\ 0.0 & 1.0 & 0.0 & 0.0 \\ 1.4048 & 0.0 & 1.3793 & -9.8583 \end{bmatrix}$$

$$[A_{22}/\epsilon] = \begin{bmatrix} -24.34 & -0.1765 \\ 5.3524 & -26.4377 \end{bmatrix}$$

The eigenvalues of $[A]$, $[A_R]$ and $[A_{22}/\epsilon]$ are as follows:

$$\begin{aligned} &-2.5189 \pm j10.4483, -0.519, -24.6926, -33.1087, -4.1741 \\ &-1.7228 \pm j8.8404, -7.0425, -0.557 \\ &-25.7830, -24.9947 \end{aligned}$$

For the above grouping, $s = 1.4$ hence the grouping is satisfactory and the resulting reduced system is correct.

Another partitioning of \underline{y} as $\underline{x}^T = [\Delta E'_q, \Delta\omega, \Delta\delta]$ and $\underline{z}^T = [\Delta E'_d, \Delta \hat{E}''_q, \Delta \hat{E}''_d]$ for (4.21) results in $[A_R]$ and $[A_{22}/\epsilon]$ matrices which have the following eigenvalues.

$$\begin{aligned} &-0.5684, \quad -0.3109 \pm j7.5029 \\ &-7.3674, \quad -24.3674, \quad -33.5953 \end{aligned}$$

For this grouping $s = 0.486$ and the condition (4.20) is not satisfied. Therefore, such a grouping will not give the correct reduced model.

After grouping the state variables, the parameter ϵ is assigned a small value $\ll 1$, usually equal to the smallest time constant and all other time constants associated with the decay of variables \underline{z} are expressed as $\epsilon \hat{T}_i$. Equation (4.9) is now in the form (4.10) by taking ϵ to the left hand side along with $\dot{\underline{z}}$.

4.4.2 Solution Procedure:

(a) Reduced Model: The reduced model of (4.9) is given by

$$\dot{\underline{X}}_0 = [A_R] \underline{X}_0 + [B_R] \underline{u} \quad \text{with} \quad \underline{X}_0(0) = \underline{x}^0 \quad (4.22)$$

where $[A_R]$ and $[B_R]$ are defined in equation (4.13a) and the dimension of \underline{X}_0 is $m_1 < m$. \underline{X}_0 is termed as the zeroth order solution of \underline{x} . \underline{Z}_0 is given from the algebraic equation (4.13b).

(b) Zeroth Order Solution of \underline{z} : The zeroth order solution to \underline{z} is obtained by solving equations (4.13b) and (4.14) and adding the responses as indicated in (4.15).

(c) First Order Solution of \underline{x} : The first order solution of \underline{x} is obtained by adding the term $\epsilon[\underline{X}_1(t) + \underline{p}_0(\tau)]$ to \underline{X}_0 where \underline{p}_0 and \underline{x}_1 are obtained by solving (4.17) and (4.18a).

(d) First Order Solution of \underline{z} : The first order solution of \underline{z} is obtained by adding the term $\epsilon[\underline{Z}_1(t) + \underline{q}_1(\tau)]$ to the zeroth order solution of \underline{z} in the step (b). $\underline{Z}_1(t)$ and $\underline{q}_1(\tau)$ are obtained by solving (4.18b) and (4.19) respectively. Higher order responses can be obtained in a similar manner, if necessary.

In the above solution procedure the equations (4.22) and (4.18a) which correspond to the \underline{X}_0 and \underline{X}_1 (slow subsystem) and the equations (4.14), (4.17) and (4.19) corresponding to \underline{q}_0 , \underline{p}_0 and \underline{q}_1 (fast subsystem) are solved separately and in different time scales. This important feature of singular perturbation theory allows larger time step size in the numerical integration because the matrices $[A_R]$ (slow subsystem) and $[A_{22}]$ (fast subsystem) are not as stiff as the original system matrix $[A]$. This leads to computational advantages as shown in the numerical examples given in the next section.

Thus, if an approximate response to \underline{x} is to be obtained, we use the reduced system (4.22) in step (a) only. This is same as the simplified model for final period in the state variable grouping technique [39] or the classical method of reduction [44]. However, if the effect of the

fast phenomena on the response of \underline{x} is to be considered, the additional steps (b) and (c) are carried out. Generally, the first order solution of \underline{x} to effect the improvement in response is adequate.

4.5 NUMERICAL EXAMPLES

4.5.1 Single Machine Infinite Bus System:

The single line diagram of the system is shown in Fig. 4.2. The system data is given below.

Synchronous Machine: MVA = 500, $H = 10$ secs, $D = 0.03$, $r_a = 0.0$, $x_d = 1.99$, $x_q = 1.87$, $x'_d = 0.3$, $x'_q = 0.45$, $x''_d = x''_q = x'' = 0.21$, $x_{al} = 0.15$, $T'_{do} = 5.4$, $T'_{qo} = 1.33$, $T''_{do} = 0.053$, $T''_{qo} = 0.061$.

Exciter-Voltage Regulator System: $K_A = 50$, $T_{A1} = 0.1$, $T_{A2} = 0.061$, $K_E = 0.0$, $T_E = 1.2$, $K_f = 0.04$, $T_f = 0.5$, $T_R = 0.05$.

Turbine-Governor System: $K_g = 20$, $T_c = 0.06$, $T_g = 0.3$, $T_h = 1.3$, $T_d = 0.0$, $K_h = 0.5$, $K_2 = 1$, $K_t = 1$, $\omega_o = 314$ rad/sec

Transmission line $r_l = 0.01$, $x_l = 0.1$

Power transmitted = $0.4 - j0.3$ p.u.

The order of the full scale model is 14. The perturbation parameter ϵ is identified in small time constants T''_{do} , T''_{qo} , T_{A2} , T_R and T_c . Therefore \underline{y} is partitioned as

$$\underline{x}^T = [\Delta E'_q, \Delta \omega, \Delta \delta, \Delta E'_d, \Delta E'_{fd}, y_{e2}, y_{e3}, y_{t1}, y_{t2}]$$

$$\underline{z}^T = [\Delta \hat{E}''_q, \Delta \hat{E}''_d, y_{e4}, y_{e5}, y_{e3}]$$

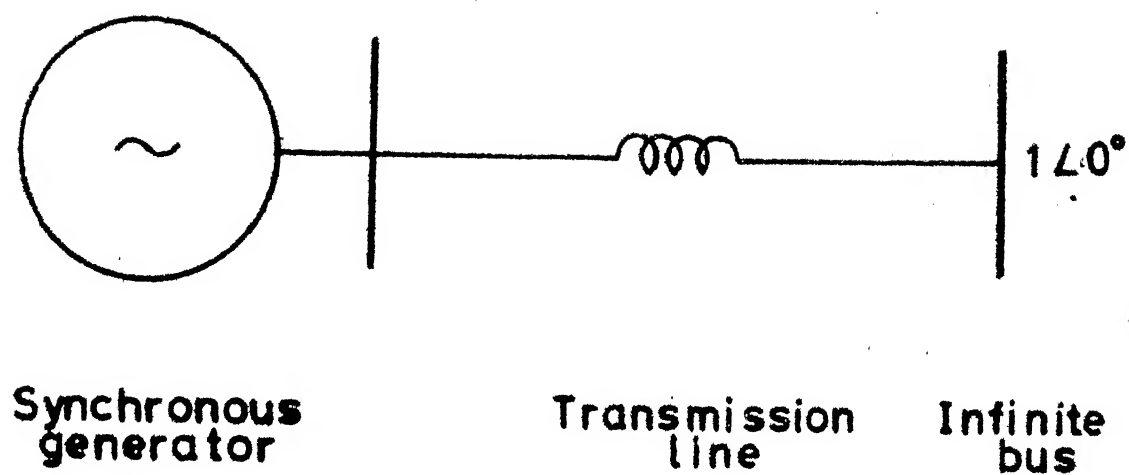


Fig.4.2 Single machine infinite bus system

The ratio in equation (4.20) for the above system is

$$s = 1.1933 > 1$$

Hence the partitioning is satisfactory. The initial conditions of the state variables are $\underline{x}(0) = \underline{0}$ and $\underline{z}(0) = \underline{0}$.

A step input equal to $\Delta V_{\text{ref}} = 0.1$ is applied and the responses are obtained for (i) the full scale system, (ii) the reduced system (zeroth order solution) and (iii) improved responses (first order solution) for both \underline{x} and \underline{z} . These responses of $\Delta\delta$ and $\Delta E'_q$ belonging to the group \underline{x} are shown in Figs. 4.3 and 4.4 respectively. The comments on the responses are given at the end of this section.

4.5.2 Three Machine System:

A single line diagram of a three machine system is given in Fig. 4.5. The line parameters and the loading conditions of the system are shown in the single line diagram. The machine parameters are:

Machines 1 and 3: 500 MVA, $H = 10$ secs., $D = 0.03$, $r_a = 0.0$, $x_d = 1.99$, $x_q = 1.87$, $x'_d = 0.3$, $x'_q = 0.45$, $x''_d = x''_q = x'' = 0.21$, $x_{al} = 0.15$, $T'_{do} = 5.4$, $T'_{qo} = 1.3$, $T''_{do} = 0.053$, $T''_{qo} = 0.061$.

Machine 2: MVA = 500, $H = 10$ secs, $D = 0.035$, $x_d = 2$, $x_q = 1.3$, $x'_d = 0.27$, $x'_q = 0.45$, $x''_d = x''_q = x'' = 0.175$, $x_{al} = 0.15$, $T'_{do} = 4.3$, $T'_{qo} = 1.4$, $T''_{do} = 0.03$, $T''_{qo} = 0.04$, $r_a = 0.0$.

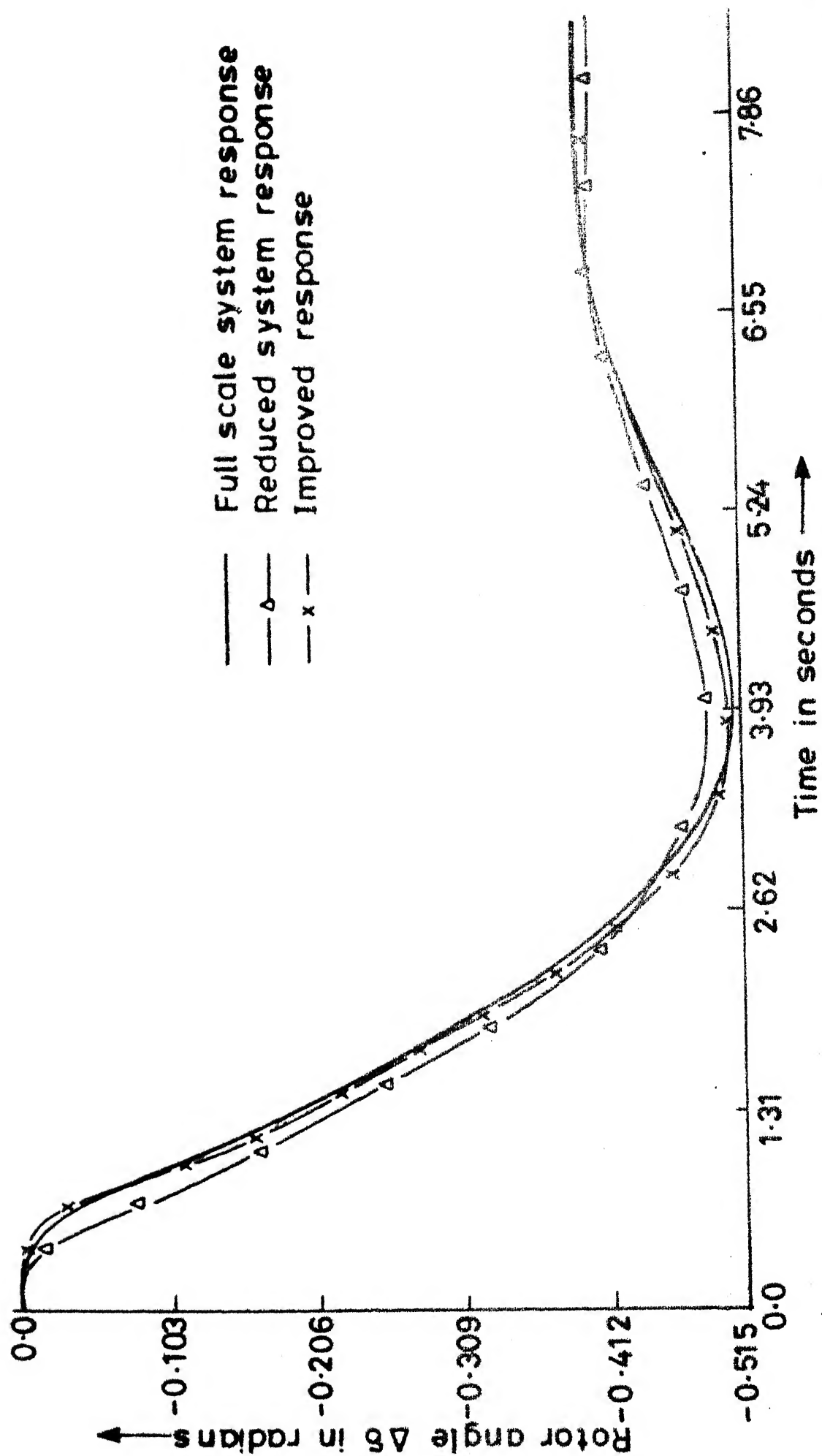


Fig. 4.3 Responses of state variable $\Delta\delta$ (Single machine infinite bus system)

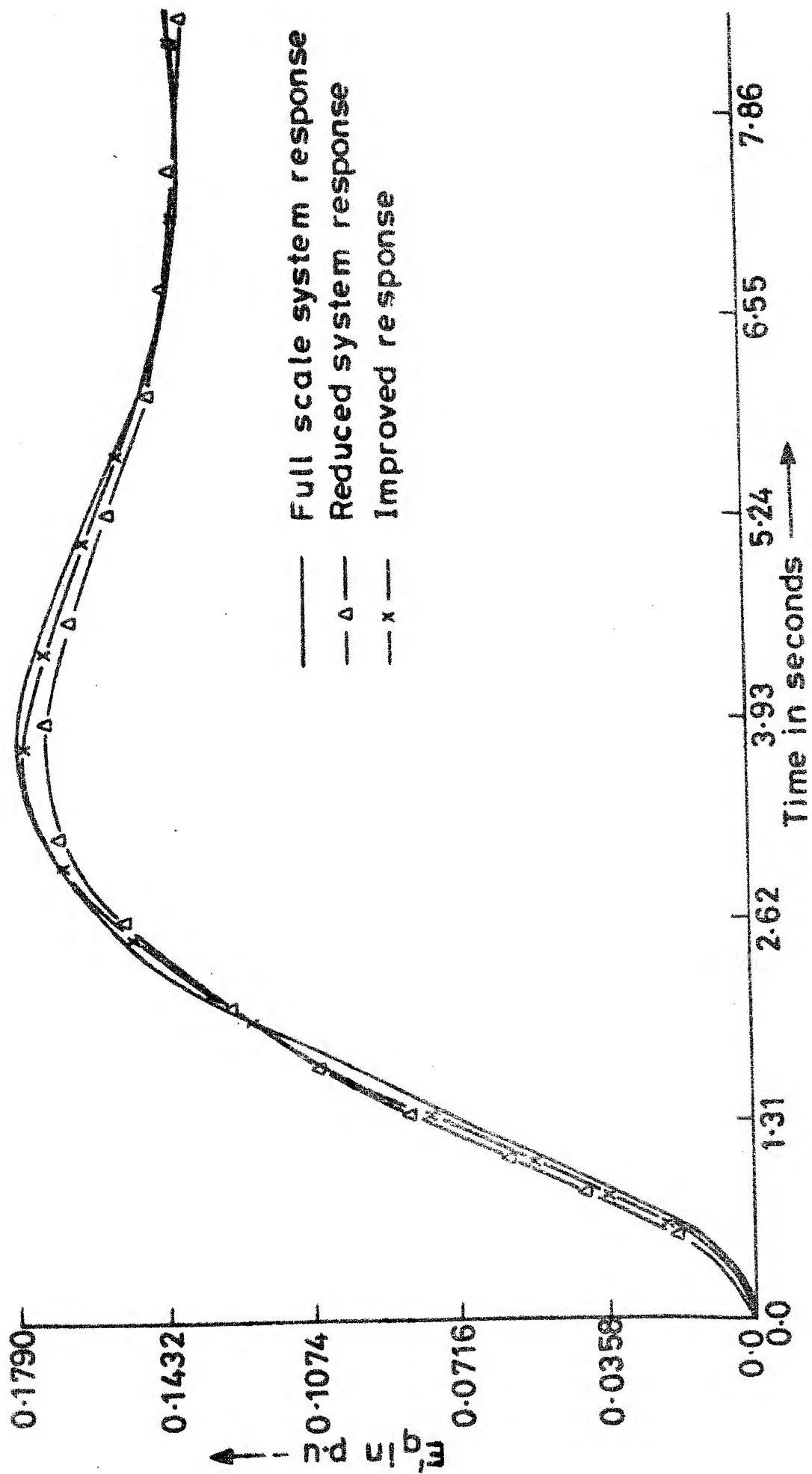


Fig.4.4 Responses of state variable $\Delta E'_q$ (Single machine infinite bus system)

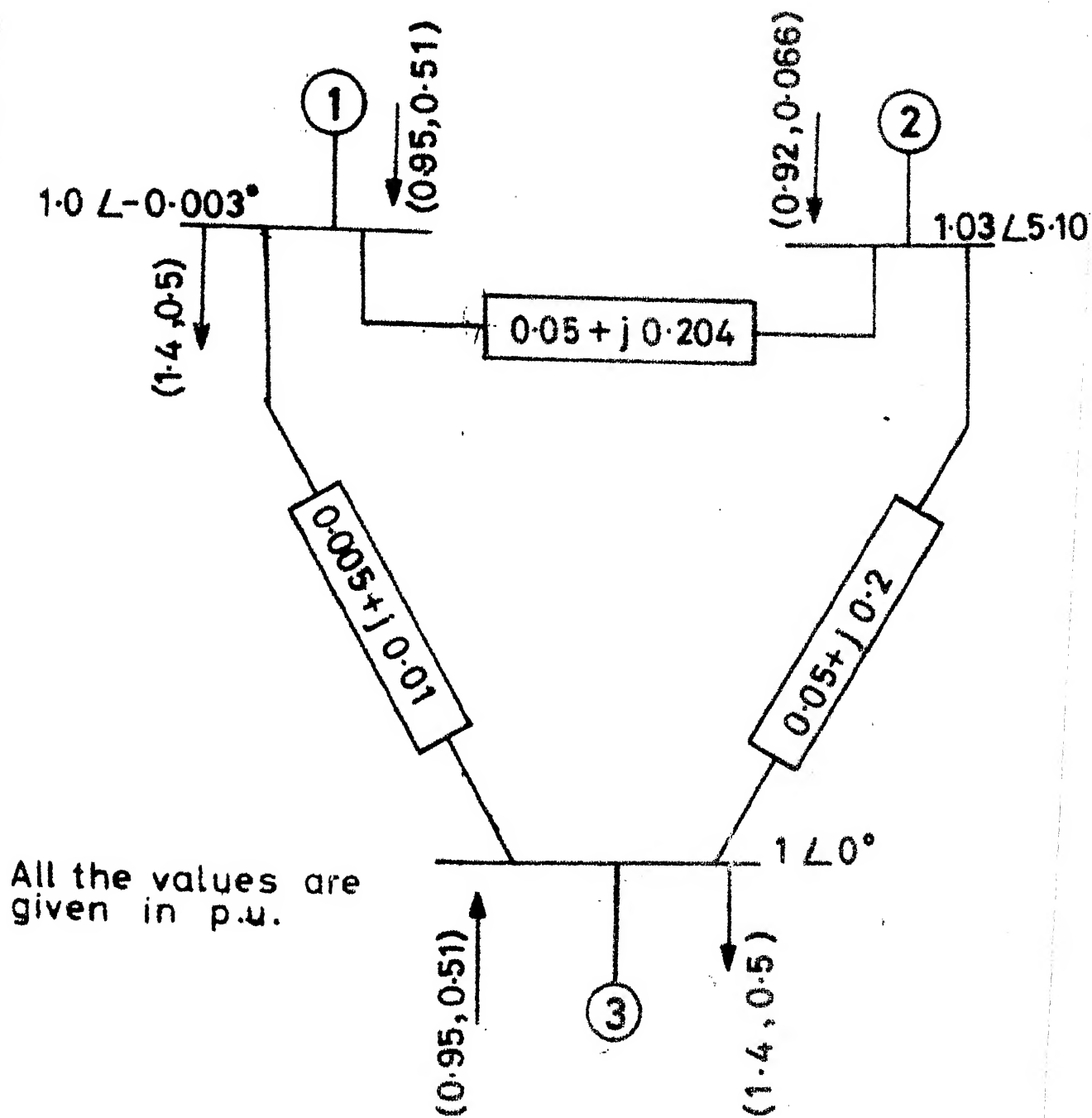


Fig. 4.5 Three machine system

Each machine is assumed to have an ~~exciter~~-regulator and a governor system and the parameters are same as in the single machine infinite bus example.

The order of the system matrix is 42. Five state variables of each machine associated with small time constants as given in the single machine infinite bus example are grouped in \underline{z} . Therefore, the dimensions of \underline{x} and \underline{z} are 27 and 15 respectively. This grouping for the given system gives

$$s = 1.0762 > 1$$

Hence the partitioning is satisfactory.

The response of the system for a step input $\Delta V_{ref1} = 0.1$ is computed for (i) the full scale system, (ii) the reduced system (zeroth order solution) and (iii) improved response (first order solution). As an illustration, the responses for the state variables, $\Delta\omega_1$ and $\Delta\delta_2$ belonging to \underline{x} are shown in Figs. 4.6 and 4.7 respectively. The response y_{e4} of machine 1 belonging to \underline{z} is shown in Fig. 4.8. All these responses are plotted for a period of 8 seconds.

4.6 DISCUSSION

4.6.1 Responses for Single and Three Machine Systems:

(i) The response of the reduced system is very approximate in both the cases. It matches for large t ,

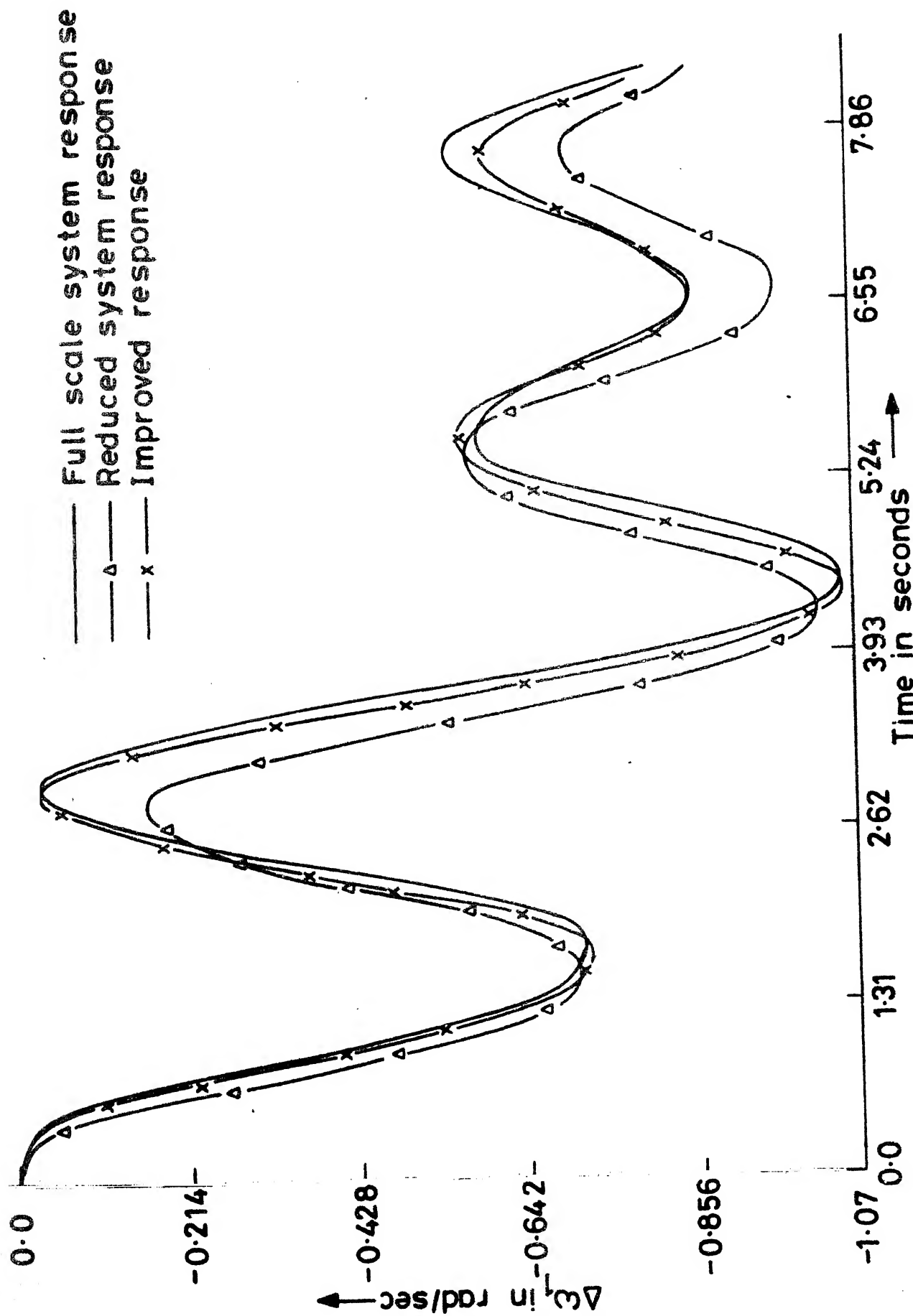


Fig.4.6 Responses of state variable $\Delta\omega_1$ (Three machine system)

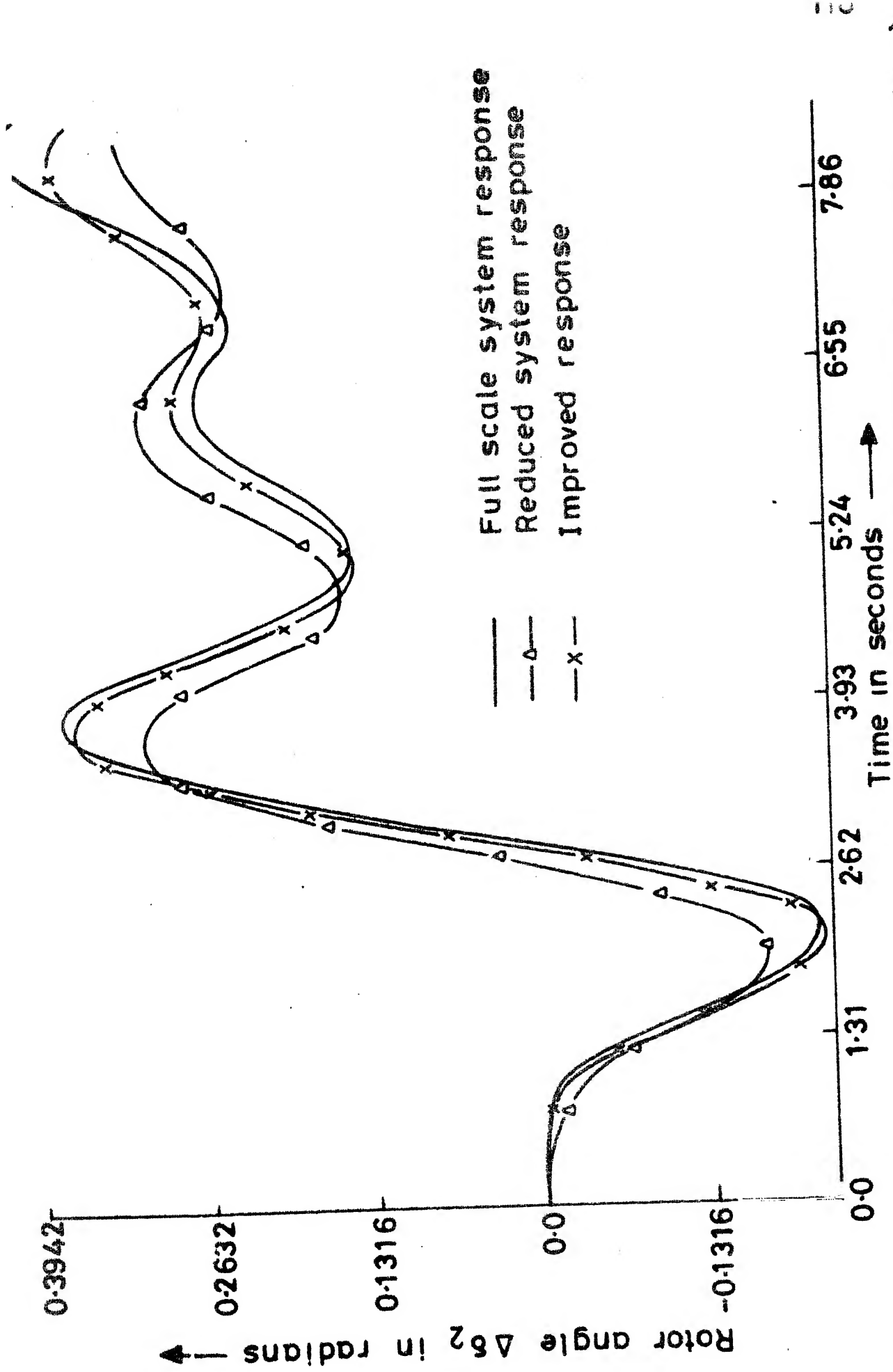


Fig. 4:7 Responses of state variable $\Delta\delta_2$ (Three machine system)

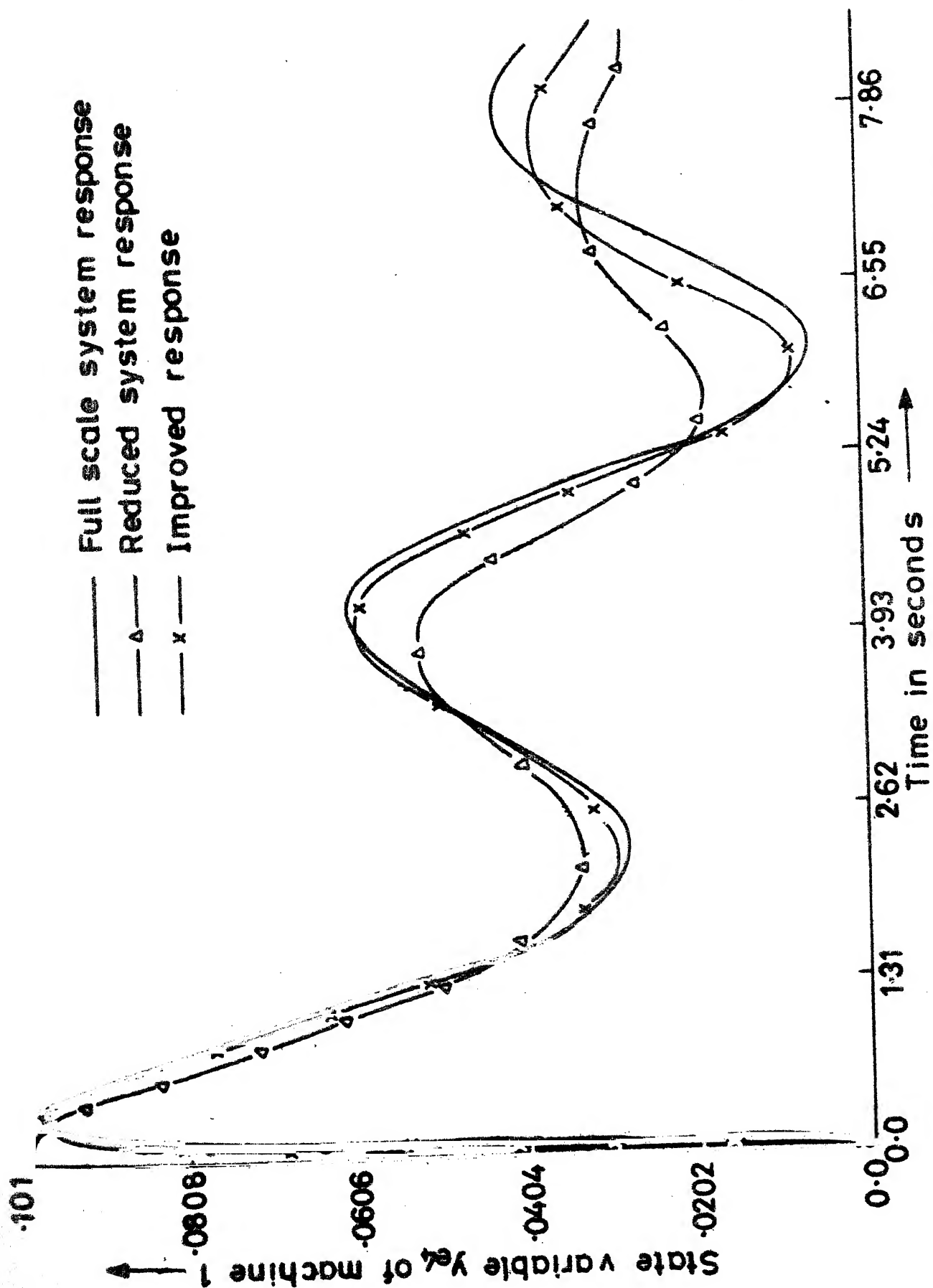


Fig. 4.8 Responses of state variable y_{e4} of machine 1 (Three machine system)

whereas for the transient period of interest, there is significant error.

(ii) As predicted by the theory, the first order solution represents significant improvement over the reduced system response.

(iii) In Fig.4.8, it may be noticed there is a difference in response near $t = 0$ of the variable y_{e4} of machine 1 (belonging to \underline{z}). This is due to the difference in initial conditions of \underline{z} and \underline{z}_0 (i.e. $\underline{q}_0(0) \neq \underline{0}$). This difference in response is known as the boundary layer jump [50].

4.6.2 Computational Times:

In the numerical integration of the original system as well as in the singular perturbation approach, we have used RKG method of integration and the integration is done with the maximum allowable step size in each case. In order to compare the permissible time step sizes in the above two approaches, the eigenvalues of the matrices $[A]$ (original system), $[A_R]$ (slow subsystem) and $[A_{22}]$ (fast subsystem) are given in Table 4.1.

As a rule of thumb, the permissible step size in an explicit method is given by

$$\Delta t < \frac{1}{\max_i |S_i|}$$

where S_i is the eigenvalue of the matrix of the system to be integrated. Thus, the eigenvalues in Table 4.1 indicate

that in the integration of the slow subsystems involving equations (4.13) and (4.18), we can use as high as five times and in the integration of the fast subsystems involving equations (4.14) and (4.17), we can use ten times larger time step size than for the original system equations. The computational saving in the singular perturbation approach is mainly derived from this fact. The permissible time step sizes in the integration and the computation times for the two numerical examples given in the preceding sections are summarised in Table 4.2.

Table 4.1 : Eigenvalues.

System	Matrix	Eigenvalue with max. magnitude	Eigenvalue with min. magnitude
Single machine infinite bus	[A]	-33.408	-0.410±j0.8241
	[A _R]	-8.1	-0.458±j0.82
	[A ₂₂]	-2.57	-1.667
	ε = 0.1		

Three machine system	[A]	-46.5972	-0.0237±j0.1165
	[A _R]	-5.9926±j4.14	-0.02586±j0.122
	[A ₂₂]	-4.6192	-1.666
	ε = 0.1		

Table 4.2 : Computation Times.

System	Integration of the original equations		Singular perturbation approach		
	Allowable step size	Time	Allowable step size	Time for zeroth order solution	Time for first order solution
Single machine infinite bus	0.01 sec.	13.30 secs.	0.05 sec.	1.9 secs.	6.01 secs. (inclusive of 1.9 secs.)

Three machine system	0.01 sec.	83 secs.	0.05 sec.	18 secs. (inclusive of computing $[A_R]$)	46 secs. (inclusive of 18 secs. for zeroth order solution)

Note: The times given in the table are CPU times on Dec System 10.

The computation times in the table indicate that the zeroth order solution can be obtained in far less time as compared to the time required for the original system response. The first order solution, which is a very good approximation to the response of the original system is obtained within 50% of the time required for the original system response. We expect similar results with other explicit methods of integration, where numerical instability is the dominant factor in determining the time step size. Since the basic motivation involved in the chapter is that of the

dynamic simplification. We have not compared the times using the different methods of integration.

In comparison with the conventional modal methods, the singular perturbation technique is simple and does not need the computation of the eigenvectors and reciprocal basis vectors of the system matrix. Although the grouping of the state variable is intuitive to start with, the validity of the reduced model is verified by the criterion (4.20). This needs the computation of eigenvalues of $[A_{22}]$ and the eigenvalue with the largest magnitude of $[A_R]$. Once the equations are put in the singular perturbation form correctly, the subsequent analysis is straightforward.

4.7 CONCLUSION

In this chapter we have presented a new technique based on singular perturbation theory for the dynamic simplification of the linear models of power systems. The technique is validated on two power system examples and its merits are brought out. The technique is simple and has potential for application in the dynamic studies of large scale power systems.

CHAPTER 5

DYNAMIC SIMPLIFICATION USING SINGULAR PERTURBATION THEORY (TRANSIENT STABILITY STUDIES)

5.1 INTRODUCTION

In this chapter, we shall extend the results of the previous chapter for transient stability studies, i.e. the application of singular perturbation theory to the nonlinear model of a power system. The chapter is organised in a similar manner as Chapter 4 except that the system equations are nonlinear and the singular perturbation theory as applied to nonlinear initial value problem [50] is used. The problems associated with the simplification of nonlinear models using the method of asymptotic expansion are discussed. The computation of first order solution involves solution of differential equations whose coefficients are functions of the reduced system response. The technique is illustrated with a single machine infinite bus example. Extension to multimachine power system in principle is possible. However, computational complexities grow enormously as compared to the dynamic stability problem of Chapter 4.

5.2 SYSTEM MODEL

The overall system model for transient stability studies is obtained by assembling the differential equations represent

the dynamics of the generating units and the algebraic equations representing their interconnections.

In general, the system model is in the following form.

$$\dot{\underline{y}} = \underline{F}(\underline{y}, \underline{s}), \text{ with } \underline{y}(0) = \underline{y}^0 \quad (5.1)$$

$$\underline{0} = \underline{G}(\underline{y}, \underline{s}) \quad (5.2)$$

where \underline{y} is the state vector of dimension 'm' and \underline{s} is the vector consisting of non-state variables. In simulating the system for a given fault, equation (5.1) is numerically integrated and the network equations (5.2) are solved at the end of each integration step. The changes in the configuration of the transmission network due to initiation or clearance of a fault are appropriately reflected in equation (5.2).

In Section 5.4, where a numerical example is given, we shall give in detail the equations for a single machine infinite bus power system and the equations involved in the subsequent dynamic simplification process, i.e. computation of the first order solution.

5.3 DYNAMIC SIMPLIFICATION OF THE SYSTEM MODEL

The nonlinear initial value problem in the singular perturbation theory, which forms the basis of the dynamic simplification of power system model given in (5.1) and (5.2), is discussed in Appendix D. The basic steps in the simplification procedure are as follows.

- (i) Formulation of the given system equations in the singular perturbation form (equation (5.3)).
- (ii) Computation of the reduced system and the zeroth order solution.
- (iii) Computation of the first order solution.

In step (i), equation (5.1) is transformed in the singular perturbation form as

$$\begin{aligned}\dot{\underline{x}} &= \underline{f}(\underline{x}, \underline{z}, \epsilon, \underline{s}) \\ \epsilon \dot{\underline{z}} &= \underline{g}(\underline{x}, \underline{z}, \epsilon, \underline{s})\end{aligned}\tag{5.3}$$

with initial conditions $\underline{x}(0) = \underline{x}^0$ and $\underline{z}(0) = \underline{z}^0$ and the network equation (5.2) is written in the form

$$\underline{G}(\underline{x}, \underline{z}, \underline{s}) = \underline{0}\tag{5.4}$$

The dimensions of \underline{x} and \underline{z} are m_1 and m_2 respectively such that $m_1 + m_2 = m$. ϵ is the perturbation parameter, small and > 0 .

The above process of writing the equations in the singular perturbation form requires the partitioning of \underline{y}^T as $[\underline{x}^T, \underline{z}^T]$ i.e. the slow and fast state variables respectively. The physical significance of ϵ , partitioning of the state variables and the validity of the resulting reduced system have been discussed for linear time invariant systems in Section 4.3. As far as the grouping of the state variable is concerned, the same procedure as discussed in Chapter 4

may be used by linearizing the given equations around the pre-fault operating point. Alternatively the physical basis for separating the fast and the slow variables may be used based on prior experience. In addition to this we have to verify the hypothesis (D.5) given in Appendix D, i.e. in equation (5.3) by setting $\varepsilon = 0$, \underline{z} should be expressible as a function of \underline{x} .

Then the resulting reduced system is given by

$$\begin{aligned}\dot{\underline{x}}_0 &= \underline{f}_0(\underline{x}_0, \underline{\phi}(\underline{x}_0), \underline{s}) \\ &= \hat{\underline{f}}_0(\underline{x}_0, \underline{s})\end{aligned}\tag{5.5}$$

$$\underline{z}_0 = \underline{\phi}(\underline{x}_0, \underline{s})\tag{5.6}$$

with initial conditions $\underline{x}_0(0) = \underline{x}^0$ along with the network equation

$$\begin{aligned}\underline{g}(\underline{x}_0, \underline{\phi}(\underline{x}_0), \underline{s}) &= \underline{0} \\ \hat{\underline{g}}(\underline{x}_0, \underline{s}) &= \underline{0}\end{aligned}\tag{5.7}$$

Solution of equations (5.5)-(5.7) gives $(\underline{x}_0(t), \underline{z}_0(t))$. The response $\underline{x}_0(t)$ is termed as the zeroth order approximation to \underline{x} . In physical terms, setting $\varepsilon = 0$ to obtain the reduced system amounts to deletion of fast phenomena in the original model. Therefore, the response of the reduced system will, in general, be approximate.

First Order Solution : In order to account for the effect of the fast phenomena on the system response, the first order solution of the system equations (5.3) and (5.4) is derived. The first order solution is defined as

$$\begin{aligned}\underline{x}(t) &= \underline{x}_0(t) + \varepsilon [\underline{x}_1(t) + \underline{p}_0(\tau)] + O(\varepsilon^2) \\ \underline{z}(t) &= \underline{z}_0(t) + \underline{q}_0(\tau) + \varepsilon [\underline{z}_1(t) + \underline{q}_1(\tau)] + O(\varepsilon^2)\end{aligned}\tag{5.8}$$

This needs the solution of the sets of differential equations for \underline{q}_0 , \underline{p}_0 , \underline{x}_1 , \underline{z}_1 and \underline{q}_1 as given in (D.8) to (D.12) of Appendix D respectively. It is important to note that the equations (D.10) and (D.11) have coefficients dependent on $(\underline{x}_0(t), \underline{z}_0(t))$, i.e. the reduced system response. In power system problems, the analytical expression for the reduced system response i.e. $(\underline{x}_0(t), \underline{z}_0(t))$ is rarely available and it has to be stored to evaluate the elements of matrices in (D.10) and (D.11). This fact makes the first order solution computationally unattractive for large scale power systems.

5.4 SINGLE MACHINE INFINITE BUS EXAMPLE

In this section, the procedure for dynamic simplification described in the previous section is illustrated with the help of a single machine infinite bus power system example (Fig. 5.1). In the example we consider a three winding model for the synchronous machine as shown in Fig. 5.

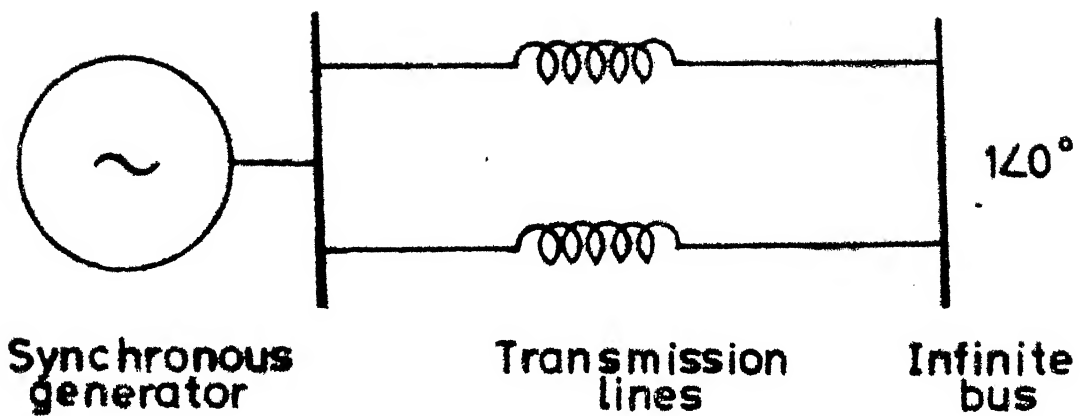
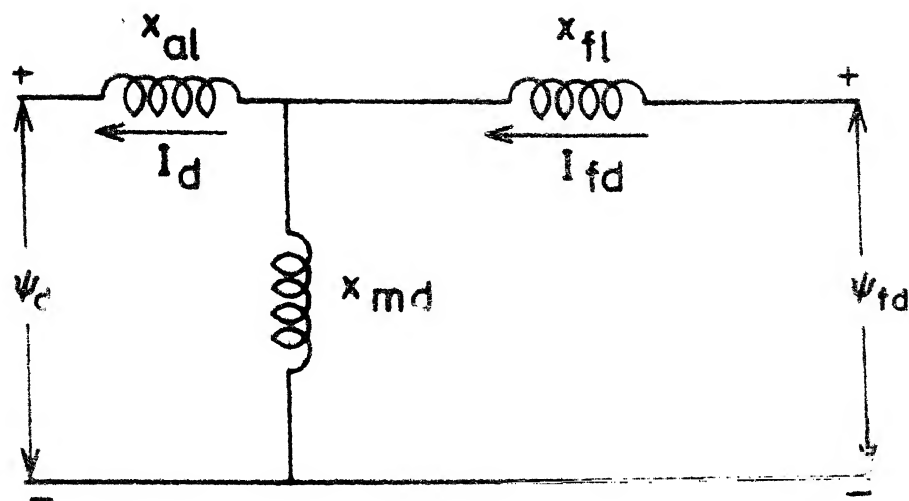
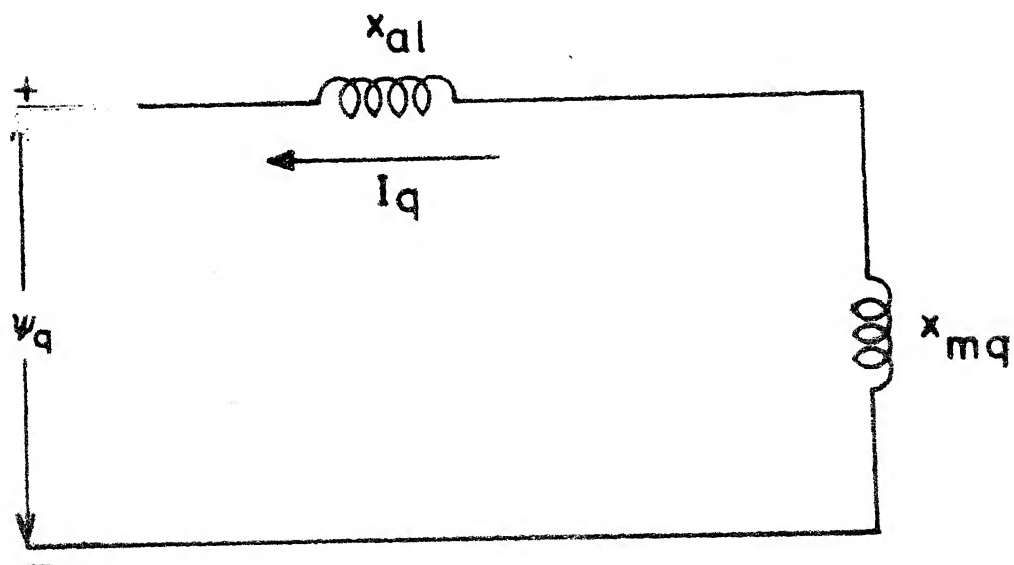


Fig. 5-1 Single machine infinite bus system with a double circuit transmission line



$$\frac{1}{x'_{md}} = \frac{1}{x_{md}} + \frac{1}{x_{fl}} \quad , \quad x'_d = x_{al} + x'_{md}$$

(a) Direct axis



$$x_q = x_{al} + x_{mq}$$

(b) Quadrature axis

Fig. 5.2 Three winding model of a synchronous machine

and the simplified exciter-voltage regulator and turbine-governor models as shown in Figs. 5.3 and 5.4 respectively.

The time constants T_A , T_E , T_C and T_h in the above control circuits are identified as shown in Figs. 5.3 and 5.4.

Generally the time constants T_A and T_C are very small as compared to T_E and T_h . Therefore, by expressing them as $\epsilon \hat{T}_A$ and $\epsilon \hat{T}_C$ the system equations are written in the required singular perturbation form (5.3). In the system equations the different variables used are as follows

$$x_1 = E'_q, \quad x_2 = \omega, \quad x_3 = \delta, \quad x_4 = E_{fd}$$

The variables x_5 , z_1 and z_2 are identified as shown in Figs. 5.3 and 5.4 respectively. Initial conditions of the state variables are $\underline{x}(0) = \underline{x}^0$ and $\underline{z}(0) = \underline{z}^0$.

(a) Full scale system : The original system equations in the singular perturbation form are given below.

$$\dot{x}_1 = [-x_1 + x_4 - (x_d - x'_d) I_d] / T'_{do} \quad (5.9)$$

$$\dot{x}_2 = [P_m - P_e - D(x_2 - \omega_0)] / M \quad (5.10)$$

where

$$P_m = x_5 + k_1 (T_{mo} + z_2)$$

$$P_e = x_1 I_q + I_d I_q (x_q - x'_d)$$

$$\dot{x}_3 = x_2 - \omega_0 \quad (5.11)$$

$$\dot{x}_4 = [-K_E x_4 + z_1] / T_E \quad (5.12)$$

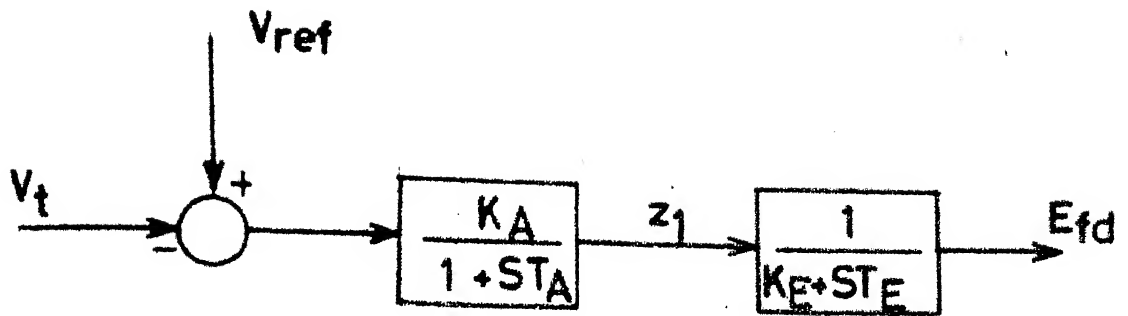


Fig. 5.3 Simplified model of an exciter-voltage regulator system

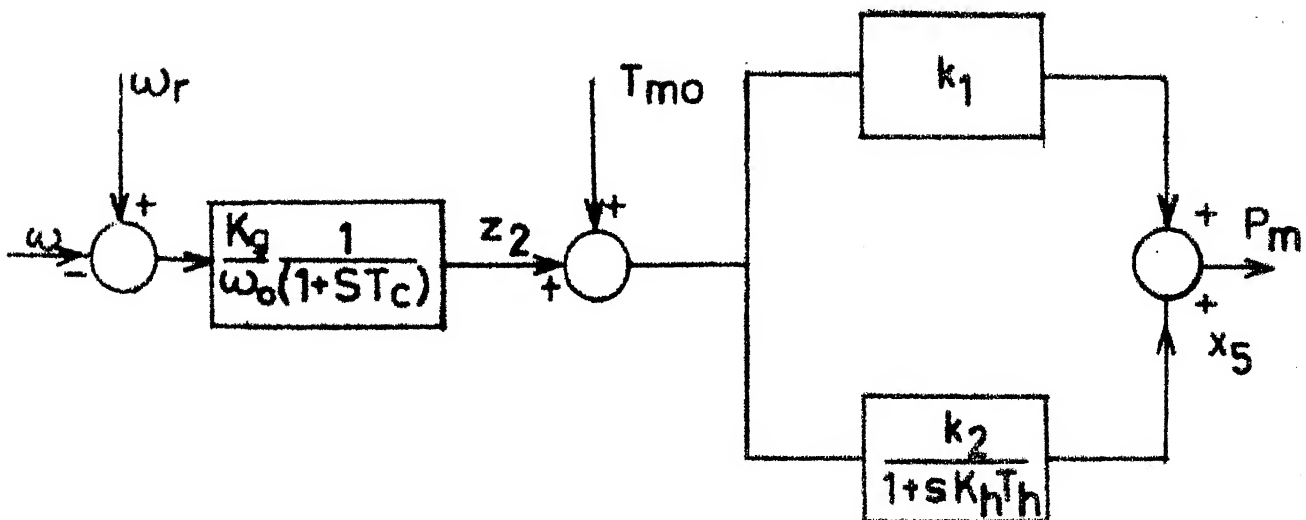


Fig. 5.4 Simlified model of a turbine-governor system

$$\dot{x}_5 = [k_2 (\dot{\theta}_{mo} + z_2) - x_5] / (K_h T_h) \quad (5.13)$$

$$\varepsilon \dot{z}_1 = [-z_1 + K_A (V_{ref} - V_t)] / \hat{T}_A \quad (5.14)$$

$$\varepsilon \dot{z}_2 = [-z_2 + K'_g (\omega_r - x_2)] / \hat{T}_c, \text{ where } K'_g = \left(\frac{K_g}{\omega_0} \right) \quad (5.15)$$

The network reference frame is assumed to coincide with that of the infinite bus. Using the transformation given in equation (4.4), the network equations are written as

$$\begin{bmatrix} I_d \\ I_q \end{bmatrix} = \begin{bmatrix} y_{11} & y_{12} \\ y_{21} & y_{22} \end{bmatrix} \begin{bmatrix} -\sin(x_3) \\ x_1 - \cos(x_3) \end{bmatrix} \quad (5.16)$$

where

$$\begin{bmatrix} y_{11} & y_{12} \\ y_{21} & y_{22} \end{bmatrix} = \begin{bmatrix} r_a + r_\ell & -x_q - x_\ell \\ x'_d + x_\ell & r_a + r_\ell \end{bmatrix}^{-1}$$

The terminal voltage V_t of the machine is given by

$$\begin{bmatrix} V_d \\ V_q \end{bmatrix} = \begin{bmatrix} -r_a & x_q \\ -x'_d & -r_a \end{bmatrix} \begin{bmatrix} I_d \\ I_q \end{bmatrix} + \begin{bmatrix} 0 \\ x_1 \end{bmatrix} \quad (5.17a)$$

$$V_t = \sqrt{V_d^2 + V_q^2} \quad (5.17b)$$

Simulation of the original system involves the numerical integration of equations (5.9) to (5.15) and the solution (5.16) and (5.17) at the end of each integration step. The fault condition is appropriately reflected in equations

(5.16) and (5.17).

(b) Reduced System : Setting $\epsilon = 0$ and substituting for z_1 and z_2 from (5.14) - (5.15) in equations (5.10), (5.12) and (5.13), we get the reduced system as follows. The reduced system variables are denoted as $[X_{01}, X_{02}, \dots, X_{05}]$ and $[Z_{01}, Z_{02}]$.

$$\dot{X}_{01} = [-X_{01} + X_{04} - (x_d - x'_d) I_d] / T'_{do} \quad (5.18)$$

$$\dot{X}_{02} = [P_m - P_e - D (X_{02} - \omega_o)] / M \quad (5.19)$$

where

$$P_m = X_{05} + k_1 [T_{mo} + K'_g (\omega_r - X_{02})]$$

$$P_e = X_{01} I_q + I_d I_q (x_q - x'_d)$$

$$\dot{X}_{03} = (X_{02} - \omega_o) \quad (5.20)$$

$$\dot{X}_{04} = [-K_E X_{04} + K_A (V_{ref} - V_t)] / T_E \quad (5.21)$$

$$\dot{X}_{05} = [-X_{05} + k_2 (T_{mo} + K'_g (\omega_r - X_{02}))] / (K_h T_h) \quad (5.22)$$

The network equations for the reduced system are same as given in (5.16) and (5.17) except that the variables x_i 's are replaced by X_{0i} 's.

Z_{01} and Z_{02} are obtained from equations (5.14) and (5.15) as

$$Z_{01} = K_A (V_{ref} - V_t) \quad (5.23)$$

$$Z_{02} = K'_g (\omega_r - X_{02})$$

Initial conditions for X_{0i} 's are $X_{0i} = x_i^o$, $i = 1, \dots, 5$.

Structurally, the equations (5.18)-(5.22) correspond to the set of equations (5.5) and (5.23) correspond to (5.6).

(c) First Order Solution : The equations for deriving the first order solution of $q_0 = [q_{01}, q_{02}]^T$ is obtained by solving the differential equations corresponding to (D.8) of Appendix D as given below.

$$\begin{bmatrix} \frac{dq_{01}}{d\tau} \\ \frac{dq_{02}}{d\tau} \end{bmatrix} = \begin{bmatrix} -\frac{1}{T_A} & 0 \\ 0 & -\frac{1}{T_C} \end{bmatrix} \begin{bmatrix} q_{01} \\ q_{02} \end{bmatrix} \quad (5.24)$$

with initial conditions $q_{01}(0) = -K_A (V_{ref} - V_t(0^+)) + z_1^0$

$$q_{02}(0) = -K_g' (\omega_r - x_2(0^+)) + z_2^0$$

and $\tau = t/\epsilon$. With the initiation of an electrical fault, the terminal voltage of the generator changes instantaneously and this provides the initial condition for (5.24). The differential equations for $p_0 = [p_{01}, \dots, p_{05}]^T$ corresponding to (D.8) of Appendix D are as follows

$$\begin{bmatrix} dp_{01}/d\tau \\ dp_{02}/d\tau \\ dp_{03}/d\tau \\ dp_{04}/d\tau \\ dp_{05}/d\tau \end{bmatrix} = \begin{bmatrix} 0 & 0 \\ 0 & k_1/M \\ 0 & 0 \\ 1/T_E & 0 \\ 0 & k_2/(K_h T_h) \end{bmatrix} \begin{bmatrix} q_{01}(\tau) \\ q_{02}(\tau) \end{bmatrix} \quad (5.25)$$

with initial conditions $p_0(\infty) = 0$.

The variables $\underline{X}_1 = [X_{11}, \dots, X_{15}]^T$ and $\underline{Z}_1 = [Z_{11}, Z_{12}]^T$ are obtained from solving the equations (5.26) and (5.27) given below (refer to equations (D.10) and (D.11) of Appendix D).

$$\begin{aligned}
 \begin{bmatrix} \dot{X}_{11} \\ \dot{X}_{12} \\ \dot{X}_{13} \\ \dot{X}_{14} \\ \dot{X}_{15} \end{bmatrix} &= \begin{bmatrix} a_{11} & 0 & a_{13} & 1/T_{do} & 0 \\ a_{21} & -D/M & a_{23} & 0 & 1/M \\ 0 & 1 & 0 & 0 & 0 \\ 0 & 0 & 0 & -K_E/T_E & 0 \\ 0 & 0 & 0 & 0 & -1/(K_h T_h) \end{bmatrix} \begin{bmatrix} X_{11} \\ X_{12} \\ X_{13} \\ X_{14} \\ X_{15} \end{bmatrix} \\
 &+ \begin{bmatrix} 0 & 0 \\ 0 & k_1/M \\ 0 & 0 \\ 1/\tau_{11} & 0 \\ 0 & k_2/M \end{bmatrix} \begin{bmatrix} Z_{11} \\ Z_{12} \end{bmatrix} \quad (5.26)
 \end{aligned}$$

with initial conditions $X_{1i} = -p_{oi}(0)$, $i = 1, \dots, 5$, where $p_i(0)$ is obtained from equation (5.25).

$$\begin{bmatrix} \dot{z}_{01} \\ \dot{z}_{02} \end{bmatrix} = \begin{bmatrix} b_{11} & 0 & b_{13} & 0 & 0 \\ 0 & -K'_g/\hat{T}_c & 0 & 0 & 0 \end{bmatrix} \begin{bmatrix} x_{11} \\ x_{12} \\ x_{13} \\ x_{14} \\ x_{15} \end{bmatrix} + \begin{bmatrix} -1/\hat{T}_A & 0 \\ 0 & -1/\hat{T}_c \end{bmatrix} \begin{bmatrix} z_{11} \\ z_{12} \end{bmatrix} \quad (5.27)$$

In the above equations, a_{ij} 's are the corresponding elements of the Jacobian $\left[\frac{\partial \underline{f}_0}{\partial \underline{x}} (\underline{X}_0, \underline{Z}_0) \right]$ and b_{ij} 's are the elements of $\left[\frac{\partial \underline{g}_0}{\partial \underline{x}} (\underline{X}_0, \underline{Z}_0) \right]$, where $\underline{f}_0 = [f_{01}, f_{02}, \dots, f_{0m}]^T$ and $\underline{g}_0 = [g_{01}, g_{02}, \dots, g_{0m2}]^T$ are obtained from R.H.S. in (5.3) by setting $\varepsilon = 0$. Then the functional expressions for a_{ij} and b_{ij} are as given below

$$a_{11} = \frac{\partial f_{01}}{\partial x_1} = [-1 - (x_d - x'_d) \frac{\partial I_d}{\partial x_1}] / T'_{do} \quad (5.28)$$

$$a_{13} = \frac{\partial f_{01}}{\partial x_3} = [-(x_d - x'_d) \frac{\partial I_d}{\partial x_3}] / T'_{do} \quad (5.29)$$

$$\begin{aligned} a_{21} = \frac{\partial f_{02}}{\partial x_1} = & [-I_q - x_1 \frac{\partial I_q}{\partial x_1} - I_d \frac{\partial I_q}{\partial x_1} (x_q - x'_d) \\ & - I_q \frac{\partial I_d}{\partial x_1} (x_q - x'_d)] / M \end{aligned} \quad (5.30)$$

$$a_{23} = \frac{\partial f_{02}}{\partial x_3} = [-x_1 \frac{\partial I_q}{\partial x_3} - I_d \frac{\partial I_q}{\partial x_3} (x_q - x_d') - I_q \frac{\partial I_d}{\partial x_3} (x_q - x_d')] / M \quad (5.31)$$

$$b_{11} = \frac{\partial g_{01}}{\partial x_1} = - \frac{K_A}{\hat{T}_A} \frac{\partial V_t}{\partial x_1} \quad (5.32)$$

$$b_{13} = \frac{\partial g_{01}}{\partial x_3} = - \frac{K_A}{\hat{T}_A} \frac{\partial V_t}{\partial x_3} \quad (5.33)$$

In the above expressions, the partial derivatives of I_d , I_q and V_t w.r.t. x_1 and x_3 are computed from the network equations (5.16) and (5.17) and are dependent on $\underline{x}_0(t)$. Hence a_{ij} 's and b_{ij} 's are, in general, functions of $(\underline{x}_0(t), Z_0(t))$.

Equation (5.26) is solved by eliminating $[Z_{11}, Z_{12}]^T$ by using (5.27). $[\dot{Z}_{01}, \dot{Z}_{02}]$ is a known response derived from equation (5.23) as given below.

$$\dot{Z}_{01} = -K_A \frac{dV_t}{dt} \quad (5.34)$$

$$\begin{aligned} \dot{Z}_{02} &= -K'_g \dot{X}_{02} \\ &= -K'_g [P_m - P_e - D (X_{02} - \omega_0)] / M \text{ from (5.19)} \end{aligned}$$

In (5.34) we have

$$\frac{dV_t}{dt} = \frac{\partial V_t}{\partial x_1} \frac{dx_1}{dt} + \frac{\partial V_t}{\partial x_3} \frac{dx_3}{dt} \quad (5.35)$$

which is evaluated along $\underline{x}_0(t)$. With this step we can integrate (5.26) to obtain $\underline{x}_1(t)$ and hence $\underline{z}_1(t)$ from (5.27).

To complete the first order solution, it now remains to solve for $\underline{q}_1 = [q_{11}, q_{12}]^T$ whose differential equations corresponding to (D.12) of Appendix D are given by

$$\begin{bmatrix} \frac{dq_{11}}{d\tau} \\ \frac{dq_{12}}{d\tau} \end{bmatrix} = \begin{bmatrix} -\frac{1}{\hat{T}_A} & 0 \\ 0 & -\frac{1}{\hat{T}_C} \end{bmatrix} \begin{bmatrix} q_{11} \\ q_{12} \end{bmatrix} \quad (5.36)$$

with initial conditions

$$q_{11}(0) = -z_{11}(0)$$

$$q_{12}(0) = -z_{12}(0)$$

In the present example, the equations for the boundary layer terms \underline{q}_0 , \underline{p}_0 and \underline{q}_1 given in (5.24), (5.25) and (5.36) respectively are linear and time invariant. In general, these equations have the form as given in (D.8), (D.9) and (D.12) of Appendix D. It is important to note that in the boundary layer equations the variables $(\underline{x}_0, \underline{z}_0)$ are assumed to be constant at their initial values $(\underline{x}_0(0), \underline{z}_0(0))$. This assumption is justified on the basis that \underline{q}_0 , \underline{p}_0 and \underline{q}_1 represent the **fast** variables and decay rapidly. $(\underline{x}_0(t), \underline{z}_0(t))$, being slow variables, can be assumed to be constant at their initial values $(\underline{x}_0(0), \underline{z}_0(0))$ in the region near $t = 0$ (boundary layer region).

The first order solution of $(\underline{x}, \underline{z})$ is obtained by adding the responses as given below.

To complete the first order solution, it now remains to solve for $q_1 = [q_{11}, q_{12}]^T$ whose differential equations corresponding to (D.12) of Appendix D are given by

$$\begin{bmatrix} \frac{dq_{11}}{d\tau} \\ \frac{dq_{12}}{d\tau} \end{bmatrix} = \begin{bmatrix} -\frac{1}{\hat{T}_A} & 0 \\ 0 & -\frac{1}{\hat{T}_C} \end{bmatrix} \begin{bmatrix} q_{11} \\ q_{12} \end{bmatrix} \quad (5.36)$$

with initial conditions

$$q_{11}(0) = -z_{11}(0)$$

$$q_{12}(0) = -z_{12}(0)$$

In the present example, the equations for the boundary layer terms q_0 , p_0 and q_1 given in (5.24), (5.25) and (5.36) respectively are linear and time invariant. In general, these equations have the form as given in (D.8), (D.9) and (D.12) of Appendix D. It is important to note that in the boundary layer equations the variables $(\underline{x}_0, \underline{z}_0)$ are assumed to be constant at their initial values $(\underline{x}_0(0), \underline{z}_0(0))$. This assumption is justified on the basis that q_0 , p_0 and q_1 represent the fast variables and decay rapidly. $(\underline{x}_0(t), \underline{z}_0(t))$, being slow variables, can be assumed to be constant at their initial values $(\underline{x}_0(0), \underline{z}_0(0))$ in the region near $t = 0$ (boundary layer region).

The first order solution of $(\underline{x}, \underline{z})$ is obtained by adding the responses as given below.

responses for the above disturbance are plotted for (i) the full scale system, (ii) the reduced system and (iii) the improved response (first order solution). As an illustration, the responses for the state variables δ , ω and E_{fd} are shown in Figs. 5.5, 5.6 and 5.7 respectively.

5.5. DISCUSSION AND CONCLUSION

The responses in Figs. 5.5-5.7 clearly indicate that the deletion of two small time constants T_A and T_C results in the reduced system response differing from that of the original system response. The effect of these time constants on the system response is retrieved to a sufficient accuracy by deriving the first order solution. It is seen that first order approximation improves the response of the reduced system considerably. However, this improvement in response is at the cost of increased computation time. In a large scale power system model, deletion of small time constants as in the classical method [44] may lead to erroneous response. The singular perturbation technique proposed in this chapter can be used to obtain more accurate system response. However, as is evident from the numerical example, the major problems in obtaining improved responses are: (i) separation of the slow and fast variables, i.e. writing the given system equations in the required form (5.3) and (ii) solution of the differential equations with variable coefficients. The computational burden associated with the technique increases rapidly with the size of the system. Hence before it can become a practical tool for industry, improved algorithms for quick solution of the differential equations involved (with variable coefficients) are needed.

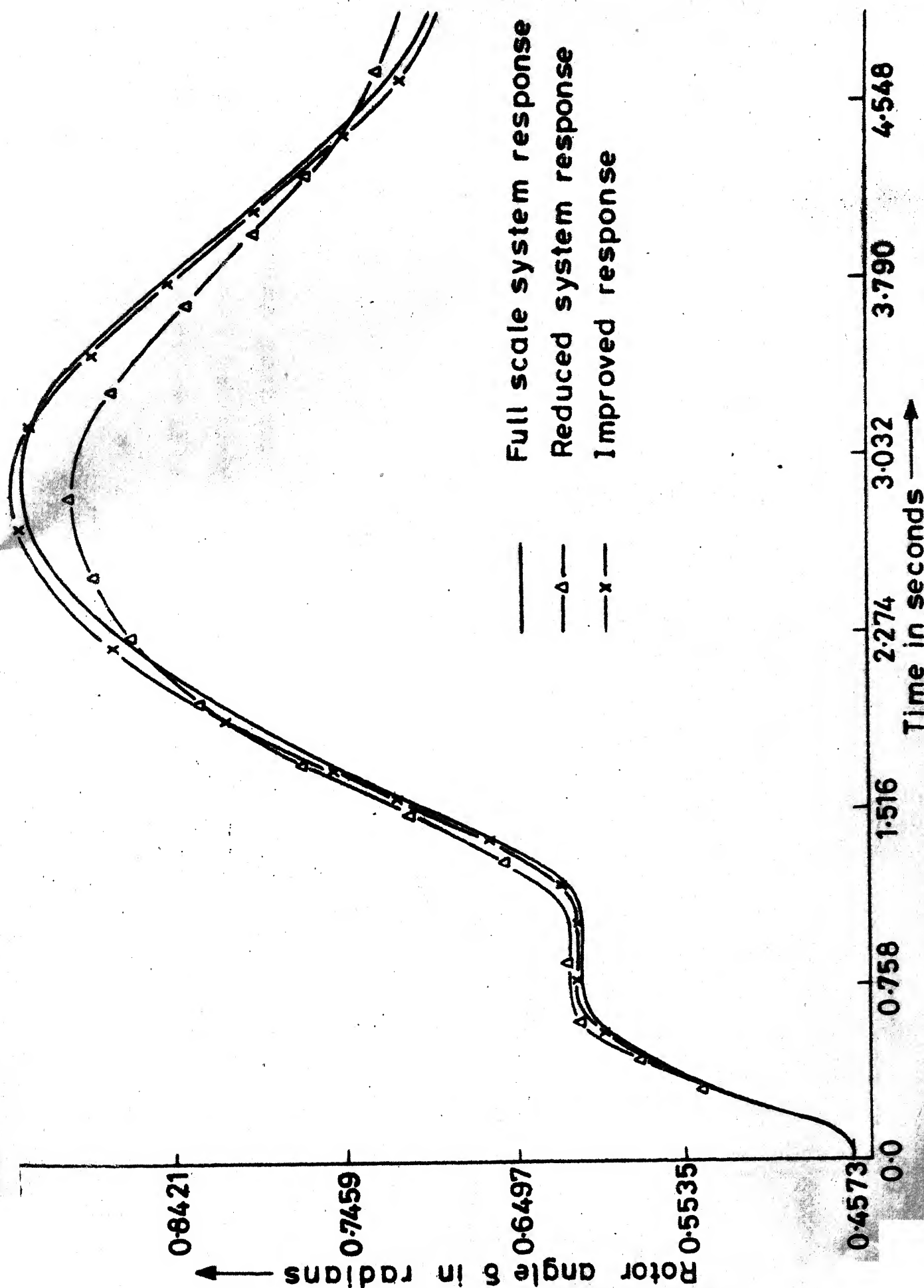


Fig. 5.5 Responses of δ (Single machine infinite bus system)

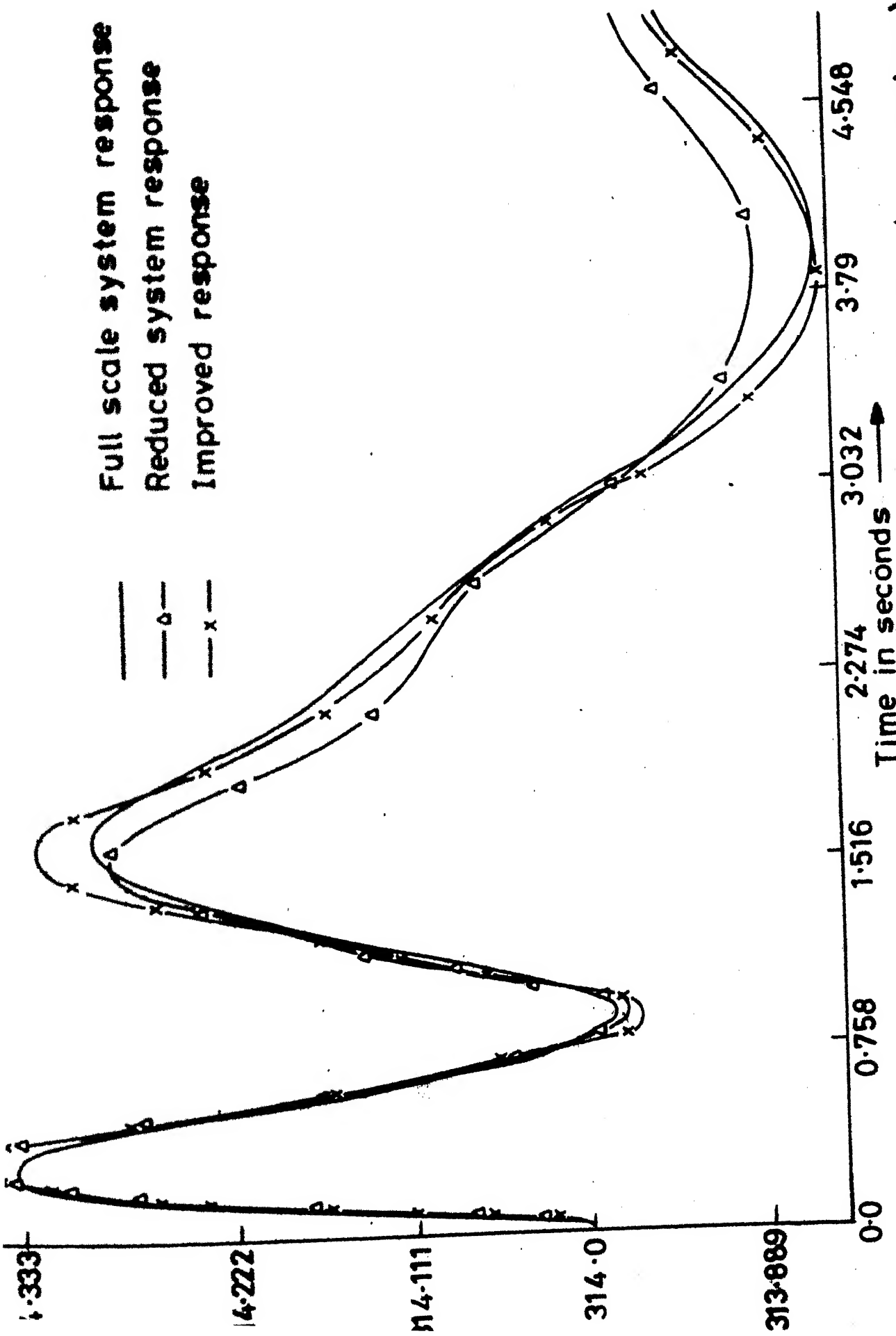


Fig. 5.6 Responses of ω (Single machine infinite bus system)

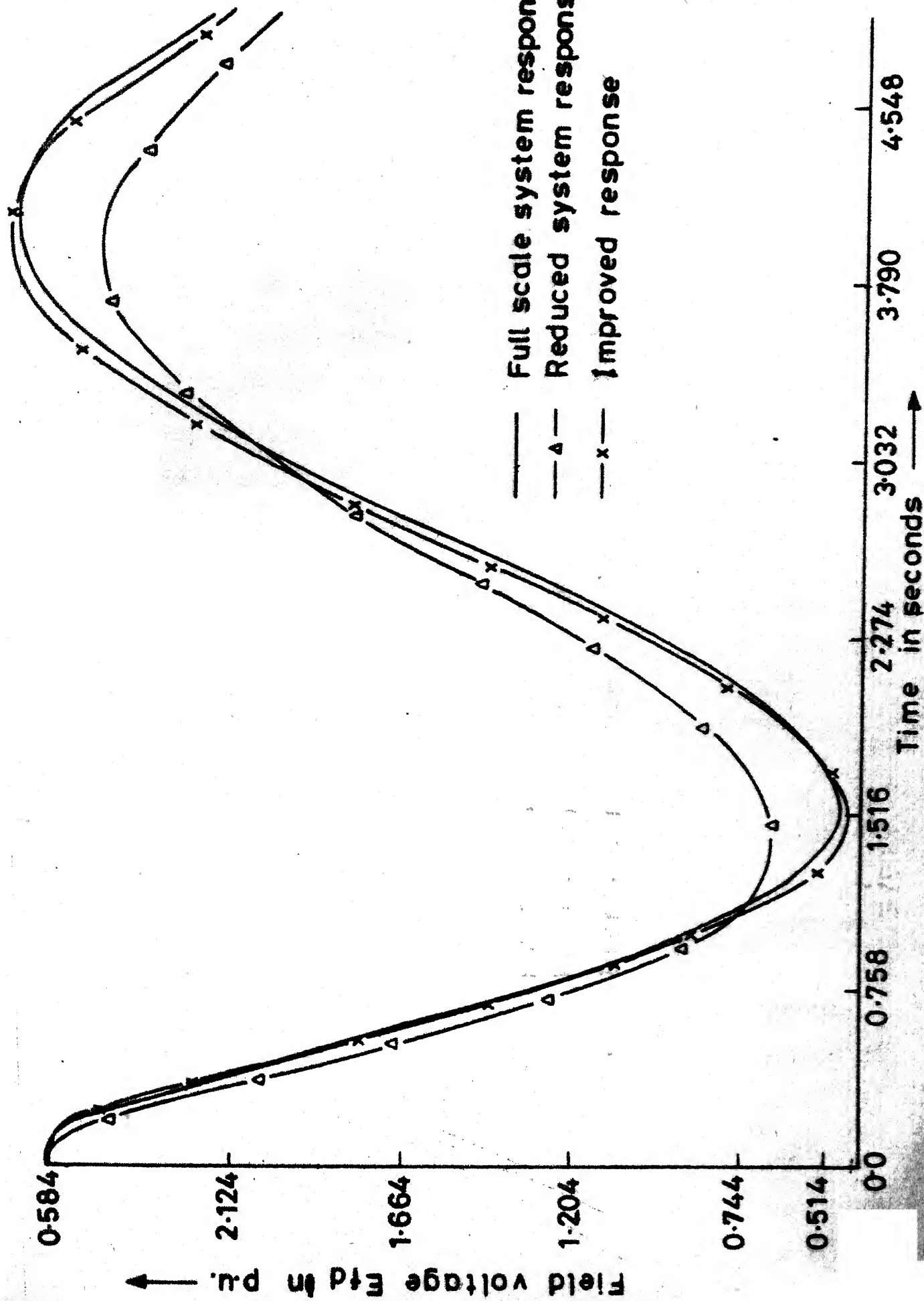


Fig. 5.7 Responses of E_{fd} (Single machine infinite bus system)

CHAPTER 6

CONCLUSION

6.1 SUMMARY AND CONCLUSION

In this chapter, we summarise the important results of this thesis and indicate suggestions for future work.

(a) Identification of Coherency : Among the existing methods for identifying coherency, the linear simulation method proposed by Podmore [24] is the most promising one. But it involves numerical integration and its repetition for each fault location in the system. On the other hand, it is convenient for a power engineer to deal with an index representing the coherent behaviour between two machines rather than computing and processing the swing curves.

With this background, we have proposed in this thesis two methods for identifying coherency.

- (i) A method involving the comparison of swing curves obtained from the closed form solution.
- (ii) The direct method using the concept of coherency index reflecting the coherent behaviour between two machines.

The analytical approach used in the above methods, eliminates the numerical integration of the system equations and provides a better understanding of the system dynamics from the coherency viewpoint. Repetitive computations for multiple fault locations are also eliminated by the appropriate use of linear transformation. Therefore, the technique is suitable for identifying (i) the coherent groups for a set of fault locations in the given study system, or (ii) the coherent groups for different study systems. The proposed methods have been validated on realistic power systems. For large scale power systems, computation of all eigenvectors and reciprocal basis vectors may involve increased computer time. However, the use of the concept of dominant modes may alleviate this difficulty.

(b) Decomposition of Power Systems and Construction of Coherency Based Equivalents : It is logical to represent the dynamics of those generators in detail, which are sensitive to the given fault than those which are insensitive to it. The prevalent basis for modelling of generators does not consider this aspect of electromechanical interaction between the machines. The decomposition technique proposed in this thesis incorporates this feature and divides the power system into different regions for the purpose of modelling the generators. Since decomposition and coherency analysis are interrelated, a procedure has

been proposed to ensure that a coherent group is not spread over two regions. Such a decomposition facilitates the grouping of coherent generators in each region separately and hence simplifies the grouping procedure by reducing the comparisons. For the sake of completeness of the topic, we have also presented the case study for a realistic power system involving decomposition, coherency analysis and the subsequent aggregation of coherent generators.

(c) Dynamic Simplification Using the Singular Perturbation Theory (Dynamic Stability Studies) : The conventional modal methods for simplifying linear models of power systems require computation of the eigenvectors and reciprocal basis vectors of the system matrix, which may be very large in size. The state variable grouping technique [39] and the classical method [44] are simple but need a physical insight into the dynamics of the system to neglect certain variables or small time constants etc. Moreover, these methods give a less accurate reduced order model of the system.

In this thesis, we have proposed a new technique based on singular perturbation theory for dynamic simplification of linear power system models. It involves separation of the linear dynamics of the given system into slow and fast subsystems, which are integrated separately in two different time scales. These responses are added to obtain

the response of the original system. Separation of the state vector into slow and fast variables is achieved through a systematic procedure, which ensures the validity of the resulting reduced system. The existing methods in the literature neglect the fast phenomena in the system altogether. In the proposed technique, this is taken into consideration to obtain an improved response through first order solution. The technique gives computational advantages over the integration of the original system equations. The method has been validated on two power system examples. Computation of the first order solution requires higher computer storage and therefore, it has to be supported by efficient programming methods.

(a) Dynamic Simplification Using Singular Perturbation Technique (Transient Stability Problem) : Singular perturbation theory has been extended to simplify the dynamic models for transient stability studies. As compared to the classical method of reduction, where small time constants, rotating masses etc. are totally neglected, the proposed method takes their effect into consideration in the first order solution. However, as compared to the linear problem of Chapter 4, it entails the solution of the differential equations with variable coefficients. The technique has been demonstrated using a single machine infinite bus example.

Extension of the technique to multi-machine system, in principle, is possible but needs further refinement to make it computationally attractive.

6.2 SCOPE FOR FURTHER RESEARCH

(i) In the coherency analysis, computations involving eigenvectors and reciprocal basis vectors could be reduced if we consider only the dominant modes in the closed form solution. Our experience with different systems indicate that it is sufficient to consider the modes in the lower natural frequency range for identifying coherency. This may be due to the fact that the modes of lower frequency are dominant [76]. This assumption need to be investigated in detail. Then the corresponding eigenvectors and reciprocal basis vectors could be easily derived by using the modified power method given in Ref. [77]. This will make the direct method of coherency analysis more efficient.

(ii) With the assumption of linearity in coherency analysis, the generators near a fault location are sometimes wrongly grouped as coherent. Therefore, instead of assuming a linear model for the complete system, it is logical to represent the study system by a nonlinear model and the external system by a linear model. The coherency analysis with such mathematical development may lead to useful results.

(iii) The existing techniques for dynamic aggregation of coherent generating units use frequency response approach. The time domain approaches could also be considered or the problem be analysed as the parameter identification problem of modern control theory.

(iv) Dynamic simplification of multi-machine system for transient stability studies using singular perturbation theory results in enormous computational complexities and need further refinement.

(v) In Ref. [57], singular perturbation approach has been used to retrieve the high frequency oscillations occurring between the coherent machines. For large scale systems this needs to be examined further using criteria for coherency as well singular perturbation approach.

REFERENCES

1. J.B. Ward, 'Equivalent circuits for power flow studies', AIEE Trans. on PAS, vol.68, 1949, pp. 373-382.
2. W.T. Brown and W.J. Clouse, 'Combination of load flow and stability equivalent for power system representation on A.C. network analyser', AIEE Trans. on PAS, vol.74, 1955, pp. 782-787.
3. H.E. Brown et al., 'A study of stability equivalents', IEEE Trans. on PAS, vol.88, 1969, pp. 200-207.
4. J.M. Undrill, J.A. Casazza and E.M. Gulachenski, 'Electromechanical equivalents for the use in power system stability', IEEE Trans. on PAS, vol.90, 1971, pp. 2060-2071.
5. J.M. Undrill and A.E. Turner, 'Construction of power system electromechanical equivalents by modal analysis', IEEE Trans. on PAS, vol.90, 1971, pp. 2049-2059.
6. W.W. Price, et al., 'Testing of the modal dynamic equivalents', IEEE Trans. on PAS, vol.97, 1978, pp. 1366-1372.
7. A. Chang and M.M. Adibi, 'Power system dynamic equivalents', IEEE Trans. on PAS, vol.89, 1970, pp. 1737-1744.
8. S.T.Y. Lee, 'Transient Stability Equivalents for Power System Planning', Ph.D. Thesis, Massachusetts Institute of Technology, 1972.
9. W.A. Mittestat, 'Proposed algorithm for approximate reduced equivalents', BPA Internal Memorandum.
10. R.W. de Mello, R. Podmore and K.N. Stanton, 'Coherency based dynamic equivalents: Applications in transient stability studies', PICA Conference Proceedings, 1975, pp. 23-31.
11. System Control Inc., 'Coherency based dynamic equivalents for transient stability studies', Final Report on EPRI Project RP-90-4, Phase II, 1975.

12. System Control Inc., 'Development of dynamic equivalents for transient stability studies', EPRI EL 456, Project 763, Final Report, 1977.
13. A.J. Germond and R. Podmore, "Dynamic aggregation of the generating unit models", IEEE Trans. on PAS, vol. 97, 1978, pp. 1060-1069.
14. M.L. Pai and C.L. Narayana, 'Dynamic equivalents using energy functions', Paper no. A 78 246-1, IEEE PES Winter Power Meeting, New York, 1978.
15. B.D. Spadling, D.B.Goudie, H.Yee and F.J. Evans, 'Use of dynamic equivalents and reduction techniques in transient stability computations', Proc. Fifth PSCG, Cambridge, 1975, paper no. 3.2/10.
16. D.G. Rumey, R.T.Byerly and D.E. Sherman, 'Application of transfer impedances to the analysis of power system transient stability studies', IEEE Trans. on PAS, vol. 90, 1971, pp. 993-999.
17. A. Rahimi, K.N.Stanton and D.M. Salmon, 'Dynamic aggregation and calculation of transient stability indices', IEEE Trans. on PAS, vol. 91, 1972, pp.118-122.
18. A.De Sarkar and N. Dharmarao, 'Dynamic system simplification and an application to power system solution', Proc. IEE, vol.119, 1972, pp. 904-910.
19. M.L. Chau, R.D. Dunlop and F.C. Schweppe, 'Dynamic equivalents for average frequency behaviour following major disturbances', IEEE Trans. PAS, vol.91, 1972, pp. 1637-1642.
20. M. Darwish, J. Fantin, 'Decomposition - aggregation of large scale power systems and stability studies', To appear in International Journal on Control.
21. Hirasa and Nakamura, 'Justification of equivalent power sources during powerswings in a multimachine system', Electrical Engineering in Japan, vol.84, 1964, pp.11-19.
22. S.T.Y. Lee and F.C. Schweppe, 'Distance measures and coherency recognition for transient stability equivalents', IEEE Trans. on PAS, vol.92, 1973, pp.1550-1557.
23. B.D. Spadling, H. Yee and D.B.Goudie, 'Coherency recognition for transient stability studies', IEEE Trans. on PAS, vol.96, 1977, p. 1368-1375.

24. R. Podmore, 'Identification of coherent generators for dynamic equivalents', IEEE Trans. on PAS, vol.97, 1978, pp.1344-1354.
25. A. Stott, 'Fast decoupled load flow', IEEE Trans. on PAS, vol.93, 1974, pp. 859-870.
26. H.W. Dommel and N. Sato, 'Fast transient stability solutions', IEEE Trans. on PAS, vol.91, 1972, pp. 1643-1650.
27. R.A. Schluter et al., 'An R.M.S. coherency measure: A basis for unification of coherency and modal analysis', Paper no. A 78 733-2 presented at IEEE PES Summer Meeting, 1978, Los Angeles, U.S.A.
28. V.I. Voropai, 'Power system equivalents at the time of big disturbances', Elektrichestvo, No.9, 6-13, 1975, pp. 74-90.
29. S.D. Varwandkar, 'Stability Investigations in Multi-machine Power Systems', Ph.D. Thesis, I.I.T. Kanpur, 1977.
30. D. Crevier and F.C. Schweppe, 'Use of Laplace transform in the simulation of power frequency transients', IEEE Trans. on PAS, vol.94, 1975, pp.236-241.
31. E.J. Davison, 'A method for simplifying linear dynamic systems', IEEE Trans. on AC, vol.11, 1966, pp.93-101.
32. E.J. Davison, 'A new method for simplifying linear dynamic systems', IEEE Trans. on AC, vol.13, 1968, pp. 214-215.
33. M.R. Chidambara, 'Two simple techniques for simplification of large dynamic systems', Joint Automatic Control Conference, 1969.
34. M. Aoki, 'Control of large scale dynamic systems by aggregation', IEEE Trans. on AC, vol. 13, 1968, pp. 246-253.
35. M.R. Chidambara and E.J. Davison, 'On a method for simplifying linear dynamic systems', IEEE Trans. on AC, vol.12, 1967, pp. 119-121.
36. M.R. Chidambara and E.J. Davison, 'Further remark on simplifying linear dynamic systems', IEEE Trans. on AC, vol. 12, 1967, pp. 213-214.

37. M.R. Chidambara and E.J. Davison, 'Further comments on a method for simplifying linear dynamic systems', IEEE Trans. on AC, vol.12, 1967, pp. 799-800.
38. A. Kuppurajulu and S. Elangovan, 'System analysis by simplified models', IEEE Trans. on AC, vol. 15, 1970, pp. 234-237.
39. A. Kuppurajulu and S. Elangovan, 'Simplified power systems models for dynamic stability studies', IEEE Trans. on PAS, vol.90, 1971, pp.11-23.
40. H.Y. Altalib and P.C. Krause, 'Dynamic equivalents by combination of reduced order models of system components', IEEE Trans. on PAS, vol. 95, 1976, pp. 1535-1544.
41. Hisham Y. Altalib, 'A Reduced Order Model for Power System Dynamic Stability Studies', Ph.D. Thesis, Purdue University, 1974.
42. C. Rudhakrishna, C. Lakshminarayana and M. Yadav Reddy, 'Simplified model control for dynamic stability studies', Paper no.A 78 609-0 IEEE PES Summer Meeting, Los Angeles, 1978.
43. R.D. Milne, 'Analysis of weakly coupled dynamical systems', International Journal of Control, vol.2, 1965, pp.177-199.
44. J.E. Van Ness, H. Zimmer and M. Cault, 'Reduction of dynamic models of power systems', Proc. PICA Conference, 1973, pp. 105-111.
45. J.E. Van Ness, 'Improved reduced dynamic models of power systems', PICA Conference, 1975, pp. 155-157.
46. P.V. Kokotovic, R.E. O'Malley and P. Sannuti, 'Singular perturbation and order reduction in control theory', An Overview', Automatica, vol.12, 1976, pp.123-132.
47. P.V. Kokotovic, 'A control system engineer's introduction to the singular perturbation', ASME, New York, 1972, pp. 1-12.
48. W. Wasow, Asymptotic Expansions for Ordinary Differential Equations, Interscience, New York, 1965.
49. A.M. Nayfeh, Perturbation Methods, Wiley, New York, 1973.
50. R.E. O'Malley Jr., Introduction to Singular Perturbations, Academic Press, New York, 1974.

51. P.V. Kokotovic and P. Sannuti, 'Singular perturbation method for reducing the order in optimal control design', IEEE Trans. on AC, vol.13, 1968, pp. 377-384.
52. P. Sannuti, 'Asymptotic series solution of singularly perturbed optimal control problems', Automatica, vol.10, 1974, pp.183-194.
53. P.V. Kokotovic and R.A. Yackel, 'Singular perturbations of linear regulators - basic theorems', IEEE Trans. on AC, vol.17, 1972, pp. 29-37.
54. R.R. Wilde and P.V. Kokotovic, 'Stability of singularity perturbed systems and networks with parasitics', IEEE Trans. on AC, vol.AC-17, 1972, pp. 245-246.
55. C.A. Desoer and M.J. Shensa, 'Network with very small and very large parasitics : Natural frequencies and stability', Proc. IEEE, vol.58, 1970, pp. 1933-1938.
56. F. Hoppensteadt, 'Asymptotic stability in singular perturbation problems', J. of Differential Equations, vol.15, 1974, pp. 510-521.
57. J.H. Chow, J.J. Allemon and P.V. Kokotovic, 'Singular perturbation analysis of systems with sustained high frequency oscillations', Automatica, vol.44, 1978, pp. 271-279.
58. J.H. Chow and P.V. Kokotovic, 'Asymptotic stability of a class of nonlinear singularly perturbed systems', J. Franklin Inst., vol.306, 1978, pp. 275-281.
59. J.H. Chow and P.V. Kokotovic, 'Eigenvalue Placement in Two Time Scale Systems in Large Scale System Theory and Applications', G. Guardabassi and A. Locatelli, Ed., IFAC Symposium, Udine, Italy, June 1976.
60. M. Vidyasagar, Nonlinear System Analysis, Prentice-Hall, Inc., Englewood Cliffs, New Jersey, 1978.
61. J.M. Undrill, 'Dynamic stability calculations of arbitrary number of interconnected synchronous machines', IEEE Trans. on PAS, vol.87, 1966, pp. 325-336.
62. M. Riaz, 'Hybrid parameter models of synchronous machines', IEEE Trans. on PAS, vol. 93, 1974, pp. 849-858.
63. K.R. Padiyar and R.S. Ramshaw, 'Dynamic analysis of multimachine power systems', IEEE Trans. on PAS, vol.91, 1972, pp.526-535.

64. M.A. Pai and P.S. Shetty, 'An algorithm for formation of system matrix of a multimachine power system', Paper no. A 77 162-1, IEEE PES Winter Meeting, New York, 1977.
65. IEEE Committee Report, 'Dynamic models for steam and hydro turbines for power system studies', IEEE Trans. on PAS, vol.92, 1973, pp. 1904-1915.
66. IEEE Committee Report, 'Excitation system dynamic characteristics', IEEE Trans. on PAS, vol.92, 1973, pp. 64-75.
67. IEEE Committee Report, 'Computer representation of excitation systems', IEEE Trans. on PAS, vol. 87, 1968, pp. 1460-1464.
68. R.T. Byerly and E.W. Kimbark, Stability of Large Scale Power Systems, IEEE Press (Selected Reprints), 1974.
69. H. Yee and B.D. Spadling, 'Transient stability analysis of multimachine power systems by the method of hyperplanes', IEEE Trans. on PAS, vol.96, 1977, pp.276-284.
70. C.A. Desoer, 'Modes in linear circuits', IRE Trans. on Circuit Theory, Vol. 7, 1960, pp. 211-213.
71. M.A. Pai and P.G. Murthy, 'New Lyapunov functions for power systems based on minimal realizations', International Journal of Control, vol.19, 1974, pp.401-415.
72. P.S. Satsangi et al., 'Graph theory in dynamic equivalencing for large scale power system studies', Paper to be presented at IFAC Symposium, New Delhi, 1979.
73. D.L. Bauer, et al., 'Simulation of low frequency undamped oscillations in large power systems', IEEE Trans. on PAS, vol.94, 1975, pp. 207-213.
74. M.A. Pai and R.P. Adgaonkar, 'Identification of coherent generators using weighted eigenvectors', Paper no. A 79 022-5, presented at IEEE PES Winter Meeting, New York, 1979.
75. Anderson and Fouad, Power System Control and Stability, The Iowa State University Press, 1977.

76. G. Quazza, "Large scale control problems in electric power systems", Automatica, Vol.13, 1977, pp. 579-593.
77. R.T. Byerly et al., "Normal modes and mode shapes applied to dynamic stability analysis", IEEE Trans. on PAS, Vol. 94, 1975, pp. 224-229.
78. P.M. De Russo and G.M. Close, State Variables for Engineers, N.Y., Wiley, 1965.

APPENDIX A

1. CLOSED FORM SOLUTION OF EQUATION (2.5)

The solution of (2.5) is given by [78]

$$\underline{X}_{pf} = e^{[A]t} \underline{X}_e \quad (A.1)$$

This is expressed as the linear combination of decoupled modes as

$$\underline{X}_{pf} = \sum_{i=1}^{2m} \underline{X}_i \langle \underline{Y}_i, \underline{X}_e \rangle e^{\lambda_i t} + \sum_{i=2m+1}^{2n-2} \underline{X}_i \langle \underline{Y}_i, \underline{X}_e \rangle e^{\lambda_i t} \quad (A.2)$$

where λ_i , \underline{X}_i and \underline{Y}_i are defined in equation (2.6). The first '2m' terms corresponds to 'm' complex pairs of eigenvalues and the rest are corresponding to real eigenvalues.

The terms corresponding to a complex pair λ_1 and λ_{m+1} in (A.2) are

$$= \underline{X}_1 \langle \underline{Y}_1, \underline{X}_e \rangle e^{\lambda_1 t} + \underline{X}_{m+1} \langle \underline{Y}_{m+1}, \underline{X}_e \rangle e^{\lambda_{m+1} t} \quad (A.3)$$

Since λ_{m+1} , \underline{X}_{m+1} and \underline{Y}_{m+1} are the complex conjugates of λ_1 , \underline{X}_1 and \underline{Y}_1 respectively, equation (A.3) reduces to

$$= 2 \operatorname{Re} [\underline{X}_1 \langle \underline{Y}_1, \underline{X}_e \rangle e^{\lambda_1 t}] \quad (A.4)$$

By rearranging the terms, equation (A.4) is simplified to

$$= e^{\alpha_1 t} [(\ell_1' \cos \beta_1 t + \ell_1'' \sin \beta_1 t) \underline{X}_1' - (\ell_1' \sin \beta_1 t - \ell_1'' \cos \beta_1 t) \underline{X}_1''] \quad (A.5)$$

The response contributed by '2m' oscillatory modes is then generalised from (A.5) and equation (A.2) is written as

$$\begin{aligned} \underline{X}_{pf} = & \sum_{i=1}^m e^{\alpha_i t} \left[(\ell_i' \cos \beta_i t + \ell_i'' \sin \beta_i t) \underline{X}_i' \right. \\ & \left. - (\ell_i' \sin \beta_i t - \ell_i'' \cos \beta_i t) \underline{X}_i'' \right] + \sum_{i=2m+1}^{2n-2} \underline{X}_i' \ell_i' e^{\alpha_i t} \end{aligned} \quad (A.6)$$

where

$$\ell_i' = \langle \underline{Y}_i', \underline{X}_e \rangle, \quad \ell_i'' = \langle \underline{Y}_i'', \underline{X}_e \rangle$$

The response (A.6) is cast in the matrix form by rearranging the terms as

$$\underline{X}_{pf} = [S] \underline{z}_s(t) \quad (A.7)$$

where the columns of [S] and the elements of $\underline{z}_s(t)$ are defined in equation (2.8).

2. CLOSED FORM SOLUTION OF EQUATION (2.4)

The solution of equation (2.4) is given by [78]

$$\underline{X}_f = \int_0^t e^{[A](t-\tau)} [B] \underline{u} \, d\tau \quad (A.8)$$

This is expressed as a linear combination of modes as

$$\underline{X}_f = \sum_{i=1}^{2m} \int_0^t \underline{X}_i \langle \underline{Y}_i, \hat{\underline{u}} \rangle e^{\lambda_i(t-\tau)} \, d\tau + \sum_{i=2m+1}^{2n-2} \int_0^t \underline{X}_i \langle \underline{Y}_i, \hat{\underline{u}} \rangle e^{\lambda_i(t-\tau)} \, d\tau \quad (A.9)$$

where $\hat{\underline{u}} = [B] \underline{u}$.

Equation (A.9) is simplified to

$$\begin{aligned} \underline{x}_f = & \sum_{i=1}^m (f_i k'_i + g_i k''_i) \underline{x}'_i + (f_i k''_i - g_i k'_i) \underline{x}''_i \\ & + \sum_{i=2m+1}^{2n-2} \underline{x}'_i \frac{k'_i}{\alpha_i} (-1 + e^{\alpha_i t}) \end{aligned} \quad (A.10)$$

where

$$f_i = q_i \left[-\frac{\alpha_i}{\beta_i^2} (1 - e^{\alpha_i t} \cos \beta_i t) + \frac{1}{\beta_i} (e^{\alpha_i t} \sin \beta_i t) \right]$$

$$g_i = q_i \left[\frac{1}{\beta_i} (1 - e^{\alpha_i t} \cos \beta_i t) + \frac{\alpha_i}{\beta_i} (e^{\alpha_i t} \sin \beta_i t) \right]$$

$$k'_i = \langle \underline{y}'_i, \hat{\underline{u}} \rangle, \quad k''_i = \langle \underline{y}''_i, \hat{\underline{u}} \rangle, \quad q_i = \frac{\beta_i^2}{\alpha_i^2 + \beta_i^2}$$

Equation (A.10) is rearranged as

$$\begin{aligned} \underline{x}_f = & \sum_{i=1}^m \underline{p}'_i (1 - e^{\alpha_i t} \cos \beta_i t) + \underline{p}''_i (e^{\alpha_i t} \sin \beta_i t) \\ & + \sum_{i=2m+1}^{2n-1} \underline{p}_i (-1 + e^{\alpha_i t}) \end{aligned} \quad (A.11)$$

where \underline{p}'_i , \underline{p}''_i and \underline{p}_i are defined in equation (2.6). Then equation (A.11) is cast in the matrix form as

$$\underline{x}_f = [P] \underline{z}_p(t) \quad (A.12)$$

where the elements of $\underline{z}_p(t)$ and the columns of $[P]$ are defined in (2.6).

APPENDIX B

DATA FOR UPSEB SYSTEM

Number of buses = 71 Number of machines = 13
 Number of lines = 94 Number of shunt loads = 23
 Base MVA = 200

BUS DATA

Bus No.	Name	Generation		Load Power		Bus voltage	
						Mag.	Ang.
1	OBRAEXT11	630.667	169.722	0.0	0.0	1.030	0.0
2	OBRAEXT400	0.0	0.0	0.0	0.0	1.057	-5.931
3	OBRA(T)11	506.0	149.492	0.0	0.0	1.025	-1.406
4	OBRA(T)220	0.0	0.0	0.0	0.0	1.054	-6.061
5	OBRA(T)132	0.0	0.0	0.0	0.0	1.047	-5.064
6	OBRA(H)11	98.0	31.986	0.0	0.0	1.025	0.397
7	OBRA(H)132	0.0	0.0	12.8	8.3	1.045	-5.723
8	RIH11	297.0	124.227	0.0	0.0	1.025	-0.204
9	RIH132	0.0	0.0	185.0	130.0	1.0433	-4.976
10	ROB132	0.0	0.0	80.0	50.0	1.026	-7.413
11	MUG132	0.0	0.0	155.0	96.0	1.023	-11.762
12	MUG220	0.0	0.0	0.0	0.0	1.003	-10.057
13	MAU132	0.0	0.0	100.0	62.0	1.007	-13.839
14	MAU220	0.0	0.0	0.0	0.0	1.004	-11.984
15	GOR11	184.08	114.0	0.0	0.0	1.005	-9.413
16	GOR132	0.0	0.0	73.0	45.5	1.024	-16.682
17	GOR220	0.0	0.0	36.0	22.4	1.005	-14.460
18	KHAL132	0.0	0.0	16.0	9.9	1.009	-17.881
19	BAST132	0.0	0.0	32.0	19.8	0.981	-19.786

continued..

Bus No.	Name	Generation		Load Power		Bus Voltage	
						Mag.	Ang.
20	GON132	0.0	0.0	27.0	16.8	1.003	-21.838
21	FAI132	0.0	0.0	32.0	19.8	1.016	-21.376
22	SUL220	0.0	0.0	0.0	0.0	1.008	-17.625
23	SUL132	0.0	0.0	75.0	46.6	1.036	-19.815
24	SUL400	0.0	0.0	0.0	0.0	0.985	-16.193
25	ALL132	0.0	0.0	133.0	82.5	1.039	-17.441
26	ALL220	0.0	0.0	0.0	0.0	1.016	-14.382
27	MAT11	304.0	76.287	0.0	0.0	1.025	-5.453
28	MAT400	0.0	0.0	30.0	20.0	1.055	-12.342
29	PANK11	261.0	70.506	0.0	0.0	1.025	-15.519
30	PANK132	0.0	0.0	120.0	74.5	1.057	-19.947
31	PANK220	0.0	0.0	160.0	99.4	1.014	-22.817
32	PANK400	0.0	0.0	0.0	0.0	1.025	-15.936
33	LUCK220	0.0	0.0	0.0	0.0	0.998	-25.515
34	LUCK132	0.0	0.0	112.0	69.5	1.306	-29.639
35	LUCK400	0.0	0.0	0.0	0.0	0.966	-21.803
36	SIT132	0.0	0.0	50.0	32.0	0.994	-34.030
37	SHL132	0.0	0.0	147.0	92.0	0.967	-37.982
38	BAR132	0.0	0.0	93.5	88.0	0.972	-37.638
39	KHAT11	25.0	30.383	0.0	0.0	1.025	-34.166
40	KHAT132	0.0	0.0	0.0	0.0	1.018	-36.913
41	MOR132	0.0	0.0	255.0	123.0	1.007	-34.778
42	MOR220	0.0	0.0	0.0	0.0	0.979	-31.484
43	MOR400	0.0	0.0	0.0	0.0	0.946	-27.835
44	RAM11	180.0	55.037	0.0	0.0	1.025	-24.448
45	RAM132	0.0	0.0	0.0	0.0	1.048	-30.514
46	NEH132	0.0	0.0	78.0	38.6	1.020	-32.678
47	MLI220	0.0	0.0	234.0	145.0	0.989	-29.053
48	HLRJ11	341.0	256.0	0.0	0.0	1.005	-25.781
49	HLRJ220	0.0	0.0	295.0	183.0	0.997	-30.500

continued...

Bus No.	Name	Generation		Load Power		Bus Voltage	
						Mag.	Ang.
50	MUR220	0.0	0.0	40.0	24.6	0.977	-32.056
51	MUR132	0.0	0.0	227.0	142.0	1.005	-35.309
52	MUR400	0.0	0.0	0.0	0.0	0.957	-26.552
53	MEER220	0.0	0.0	0.0	0.0	0.972	-32.845
54	MEER132	0.0	0.0	108.0	68.0	1.004	-35.318
55	SILM220	0.0	0.0	25.5	48.0	0.985	-31.313
56	SILM220	0.0	0.0	0.0	0.0	1.013	-29.253
57	SALM132	0.0	0.0	55.6	35.6	1.016	-29.967
58	HARD132	0.0	0.0	42.0	27.0	1.018	-30.261
59	ROO132	0.0	0.0	57.0	27.4	1.013	-30.715
60	ROO220	0.0	0.0	0.0	0.0	1.008	-29.974
61	RIS220	0.0	0.0	0.0	0.0	1.019	-27.874
62	RIS132	0.0	0.0	40.0	27.0	1.044	-28.940
63	DEH132	0.0	0.0	33.2	20.6	1.042	-27.695
64	YAMI111	300.0	72.882	0.0	0.0	1.025	-19.401
65	YAMI220	0.0	0.0	0.0	0.0	1.057	-24.662
66	YAMI,IV11	96.0	25.636	0.0	0.0	1.025	-20.610
67	YAMI,IV32	0.0	0.0	14.0	6.5	1.055	-25.641
68	MAN11	89.0	26.689	0.0	0.0	1.025	-19.829
69	MAN220	0.0	0.0	0.0	0.0	1.050	-25.363
70	WALD132	0.0	0.0	11.4	7.0	0.998	-34.790
71	SILM220	0.0	0.0	0.0	0.0	0.927	-35.329

continued...

GENERATOR DATA

Gen.No.	Bus From	Name	Inertia Const.(sec)	Trans. React.	Damp const.
1	1	OBRAEXT11	12.900	0.0488	0.0
2	3	OBRA(T)11	9.000	0.0690	0.0
3	6	OBRA(H)11	1.923	0.5278	0.0
4	8	RIH11	6.648	0.2010	0.0
5	15	GOR11	2.590	0.2440	0.0
6	27	MLT11	2.550	0.1455	0.0
7	29	PLANK11	2.700	0.1355	0.0
8	30	KHAT11	1.035	1.0820	0.0
9	44	RAM11	5.430	0.2270	0.0
10	48	HARJ11	7.808	0.0595	0.0
11	64	YAMI11	7.140	0.1300	0.0
12	66	YAMI,IV11	2.176	0.4860	0.0
13	68	MAN11	1.473	0.5990	0.0

LINE DATA

Line No.	From Bus	To Bus	Line Impedance		$\frac{1}{2}Y$ charge	Turns Ratio
1	9	8	0.0	0.0570	0.0	1.05
2	9	7	0.0320	0.0780	0.0090	1.00
3	9	5	0.0660	0.1600	0.0047	1.00
4	9	10	0.0520	0.1270	0.0140	1.00
5	10	11	0.0660	0.1610	0.0180	1.00
6	7	10	0.0270	0.0700	0.0070	1.00
7	12	11	0.0	0.0530	0.0	0.95
8	11	13	0.0600	0.1480	0.0360	1.00
9	14	13	0.0	0.0800	0.0	1.00
10	13	16	0.0970	0.2380	0.270	1.00
11	17	15	0.0	0.0920	0.0	1.05

continued...

Line No.	From Bus	To Bus	Line Impedance		$\frac{1}{2}Y_{\text{charge}}$	Turns Ratio
12	7	6	0.0	0.2220	0.0	1.05
13	7	4	0.0	0.0800	0.0	1.00
14	4	3	0.0	0.0330	0.0	1.05
15		5	0.0	0.1600	0.0	1.00
16	4	12	0.0160	0.0790	0.0710	1.00
17	12	14	0.0160	0.0790	0.0710	1.00
18	17	16	0.0	0.0800	0.0	0.95
19	2	4	0.0	0.0620	0.0	1.00
20	4	26	0.0190	0.0950	0.1930	1.00
21	2	1	0.0	0.0340	0.0	1.05
22	31	26	0.0340	0.1670	0.1500	1.00
23	26	25	0.0	0.0800	0.0	0.95
24	25	23	0.2040	0.5200	0.0130	1.00
25	22	23	0.0	0.0800	0.0	0.95
26	24	22	0.0	0.0840	0.0	0.95
27	22	17	0.0480	0.2500	0.0505	1.00
28	2	24	0.0100	0.0200	0.3353	1.00
29	23	21	0.0366	0.1412	0.0140	1.00
30	21	20	0.0720	0.1860	0.0050	1.00
31	20	19	0.1460	0.3740	0.0100	1.00
32	19	18	0.0590	0.1500	0.0040	1.00
33	18	16	0.0300	0.0755	0.0080	1.00
34	28	27	0.0	0.0810	0.0	1.05
35	30	29	0.0	0.0610	0.0	1.05
36	32	31	0.0	0.0930	0.0	0.95
37	31	30	0.0	0.0800	0.0	0.95
38	28	32	0.005	0.0510	0.6706	1.00
39	31	33	0.0130	0.0640	0.0580	1.00
40	31	47	0.0100	0.0790	0.1770	1.00
41	2	32	0.0158	0.1570	0.5100	1.00
42	33	34	0.0	0.0800	0.0	0.95
43	35	33	0.0	0.0840	0.0	0.95

continued..

Line No.	From Bus	To Bus	Line Impedance		$\frac{1}{2}Y_{\text{charge}}$	Turns Ratio
44	35	24	0.0062	0.0612	0.2012	1.00
45	34	36	0.0790	0.2010	0.0220	1.00
46	36	37	0.1690	0.4310	0.0110	1.00
47	37	38	0.0840	0.1880	0.0210	1.00
48	40	39	0.0	0.3800	0.0	1.05
49	40	38	0.0890	0.2170	0.0250	1.00
50	38	41	0.1090	0.1960	0.0220	1.00
51	41	51	0.2350	0.6000	0.0160	1.00
52	42	41	0.0	0.0530	0.0	0.95
53	43	42	0.0	0.0840	0.0	0.95
54	47	49	0.0210	0.1030	0.0920	1.00
55	49	48	0.0	0.0460	0.0	1.05
56	49	50	0.0170	0.0840	0.0760	1.00
57	49	42	0.0370	0.1950	0.0390	1.00
58	50	51	0.0	0.0530	0.0	0.95
59	52	50	0.0	0.0840	0.0	0.95
60	50	55	0.0290	0.1520	0.0300	1.00
61	50	53	0.0100	0.0520	0.0390	1.00
62	53	54	0.0	0.0800	0.0	0.95
63	51	54	0.0220	0.0540	0.0060	1.00
64	55	56	0.0160	0.0850	0.0170	1.00
65	56	57	0.0	0.0800	0.0	1.00
66	57	59	0.0280	0.0720	0.0070	1.00
67	59	58	0.0480	0.1240	0.0120	1.00
68	60	59	0.0	0.0800	0.0	1.00
69	53	60	0.0360	0.1840	0.0370	1.00
70	45	44	0.0	0.1200	0.0	1.05
71	45	46	0.0370	0.0900	0.0100	1.00
72	46	41	0.0830	0.1540	0.0170	1.00
73	46	59	0.1070	0.1970	0.0210	1.00
74	60	61	0.0160	0.0830	0.0160	1.00

continued..

Line No.	From Bus	To Bus	Line Impedance		$\frac{1}{2}Y_{\text{charge}}$	Turns Ratio
75	61	62	0.0	0.0800	0.0	0.95
76	54	62	0.0420	0.1080	0.0020	1.00
77	62	63	0.0350	0.0890	0.0090	1.00
78	69	68	0.0	0.2220	0.0	1.05
79	69	61	0.0230	0.1160	0.1040	1.00
80	67	66	0.0	0.1880	0.0	1.05
81	65	64	0.0	0.0630	0.0	1.05
82	65	56	0.0280	0.1440	0.0290	1.00
83	65	61	0.0230	0.1140	0.0240	1.00
84	65	67	0.0240	0.0600	0.0950	1.00
85	67	63	0.0390	0.0990	0.0100	1.00
86	61	42	0.0230	0.2293	0.0695	1.00
87	57	67	0.0550	0.2910	0.0070	1.00
88	45	70	0.1840	0.4680	0.0120	1.00
89	70	38	0.1650	0.4220	0.0110	1.00
90	33	71	0.0570	0.2960	0.0590	1.00
91	71	37	0.0	0.0800	0.0	0.95
92	45	41	0.1530	0.3880	0.0100	1.00
93	35	43	0.0131	0.1306	0.4293	1.00
94	32	52	0.0164	0.1632	0.5360	1.00

SHUNT LOAD DATA

S.No.	Bus No.	Shunt Load	Admittance
1	2	0.0	-0.4275
2	13	0.0	0.1500
3	20	0.0	0.0800
4	24	0.0	-0.2700
5	28	0.0	-0.3375
6	31	0.0	0.2000
7	32	0.0	-0.8700
8	34	0.0	0.2250
9	35	0.0	-0.3220
10	36	0.0	0.100
11	37	0.0	0.3500
12	38	0.0	0.2000
13	41	0.0	0.200
14	43	0.0	-0.2170
15	46	0.0	0.1000
16	47	0.0	0.3000
17	50	0.0	0.1000
18	51	0.0	0.1750
19	52	0.0	-0.2700
20	54	0.0	0.1500
21	57	0.0	0.1000
22	59	0.0	0.0750
23	21	0.0	0.0500

APPENDIX C

3.1 SYNCHRONOUS MACHINE

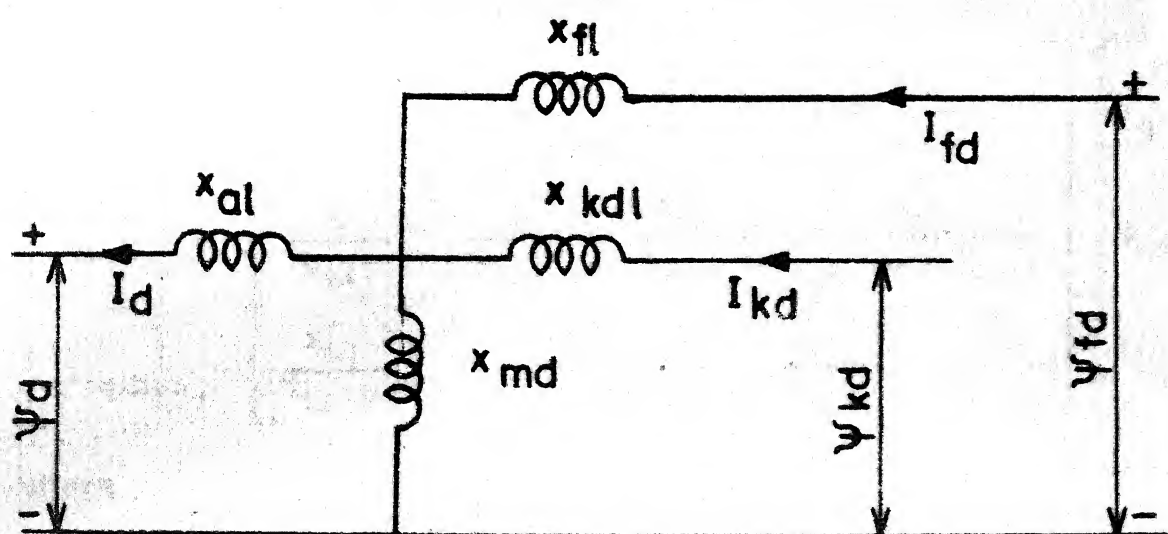
Consider a six winding model of a synchronous machines as shown in Fig. C.1. The flux current relationship in the hybrid characterisation with the assumption of common flux linking all the windings in each axis is given as [64]

Direct Axis Characterisation:

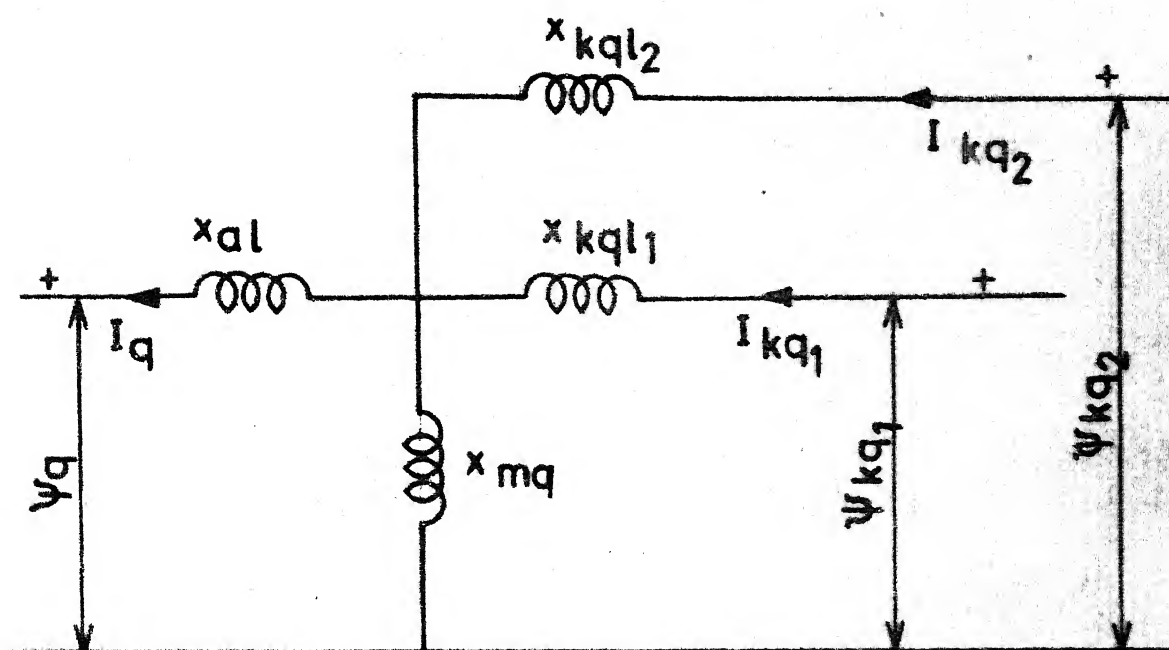
$$\begin{bmatrix} \psi_d \\ I_{fd} \\ I_{kd} \end{bmatrix} = \begin{bmatrix} -x_d'' & \frac{x_{md}''}{x_{f\ell}} & \frac{x_{md}''}{x_{kd\ell}} \\ \frac{x_{md}''}{x_{f\ell}} & \frac{1}{x_{f\ell}} \left(1 - \frac{x_{md}''}{x_{f\ell}}\right) & -\frac{x_{md}''}{x_{f\ell} x_{kd\ell}} \\ \frac{x_{md}''}{x_{kd\ell}} & -\frac{x_{md}''}{x_{kd\ell} x_{f\ell}} & \frac{1}{x_{kd\ell}} \left(1 - \frac{x_{md}''}{x_{kd\ell}}\right) \end{bmatrix} \begin{bmatrix} I_d \\ \psi_{fd} \\ \psi_{kd} \end{bmatrix} \quad (C.1)$$

$$\text{where} \quad \frac{1}{x_{md}''} = \frac{1}{x_{md}} + \frac{1}{x_{f\ell}} + \frac{1}{x_{kd\ell}} \quad (C.2)$$

$$\text{and} \quad x_d'' = x_{md}'' + x_{a\ell}$$



(a) Direct axis



(b) Quadrature axis

Fig. C.1 Multiport representation of a synchronous machine

Quadrature Axis Characterisation

$$\begin{bmatrix} \psi_q \\ I_{kq1} \\ I_{kq2} \end{bmatrix} = \begin{bmatrix} -x_q'' & \frac{x_{mq}''}{x_{kq\ell 1}} & \frac{x_{mq}''}{x_{kq\ell 2}} \\ \frac{x_{mq}''}{x_{kq\ell 1}} & \frac{1}{x_{kq\ell}} \left(1 - \frac{x_{mq}''}{x_{kq\ell 1}}\right) & -\frac{x_{mq}''}{x_{kq\ell 1} x_{kq\ell 2}} \\ \frac{x_{mq}''}{x_{kq\ell 2}} & -\frac{x_{mq}''}{x_{kq\ell 2} x_{kq\ell 1}} & \frac{1}{x_{kq\ell 2}} \left(1 - \frac{x_{mq}''}{x_{kq\ell 2}}\right) \end{bmatrix} \begin{bmatrix} I_q \\ \psi_{kq1} \\ \psi_{kq2} \end{bmatrix} \quad (C.3)$$

where

$$\frac{1}{x_{mq}''} = \frac{1}{x_{mq}} + \frac{1}{x_{kq\ell 1}} + \frac{1}{x_{kq\ell 2}} \quad (C.4)$$

and

$$x_q'' = x_{mq}'' + x_{a\ell}$$

Rotor Equivalent Voltages

The different rotor equivalent voltages are defined as

$$\begin{aligned} E_q' &= \frac{x_{md}''}{x_{fd\ell}} \psi_{fd} \\ E_d' &= -\frac{x_{mq}''}{x_{kq\ell 1}} \psi_{kq1} \\ \hat{E}_q'' &= \frac{x_{md}''}{x_{kd\ell}} \psi_{kd} \\ \hat{E}_d'' &= -\frac{x_{mq}''}{x_{kq\ell 2}} \psi_{kq2} \end{aligned} \quad \begin{aligned} E_q'' &= E_q' + \hat{E}_q'' \\ E_d'' &= E_d' + \hat{E}_d'' \end{aligned} \quad (C.5)$$

Stator Equations

Neglecting the transformer voltages, the stator equations are given by

$$\begin{bmatrix} \Delta V_d \\ \Delta V_q \end{bmatrix} = \begin{bmatrix} -r_a & x_q'' \\ -x_d'' & -r_a \end{bmatrix} \begin{bmatrix} \Delta I_d \\ \Delta I_q \end{bmatrix} + \begin{bmatrix} \Delta E_d'' \\ \Delta E_q'' \end{bmatrix} \quad (C.6)$$

Machine Model

Assuming that $x_d'' = x_q''$, the synchronous machine model with respect to its own d-q axes frame and inclusive of rotor dynamics is given by

$$\dot{\underline{Y}}_m = [A_m] \underline{Y}_m + [C_m] \Delta \underline{I}_m + [B_m] \underline{u}_m \quad (C.7)$$

where

$$\underline{Y}_m = [\Delta E_q', \Delta \omega, \Delta \delta, E_d', \Delta \hat{E}_q'', \Delta \hat{E}_d'']^T$$

$$\underline{u}_m = [\Delta E_{fd}, \Delta T_m]^T, \quad \Delta \underline{I}_m = [\Delta I_d, \Delta I_q]^T$$

$$[A_m] = \begin{bmatrix} c_1 & 0 & 0 & 0 & c_2 & 0 \\ -\frac{I_q^0}{M} & -\frac{D}{M} & 0 & -\frac{I_d^0}{M} & -\frac{I_q^0}{M} & -\frac{I_d^0}{M} \\ 0 & 1 & 0 & 0 & 0 & 0 \\ 0 & 0 & 0 & c_3 & 0 & c_4 \\ c_5 & 0 & 0 & 0 & c_6 & 0 \\ 0 & 0 & 0 & c_7 & 0 & c_8 \end{bmatrix}$$

$$[C_m] = \begin{bmatrix} c_9 & 0 \\ -E_d^0/M & -E_q^0/M \\ 0 & 0 \\ 0 & c_{10} \\ c_{11} & 0 \\ 0 & c_{12} \end{bmatrix}$$

$$[B_m] = \begin{bmatrix} c_{13} & 0 \\ 0 & 1/M \\ 0 & 0 \\ 0 & 0 \\ 0 & 0 \\ 0 & 0 \end{bmatrix}$$

The different elements of the matrices are defined as follows:

$$c_1 = - \frac{(x_d - x_{al})(x'_d - x_{al}) - (x''_d - x_{al})(x_d - x'_d)}{T'_{do}(x'_d - x_{al})^2}$$

$$c_2 = \frac{(x''_d - x_{al})(x_d - x'_d)}{T'_{do}(x'_d - x_{al})^2}$$

$$c_3 = - \frac{(x_q - x_{al})(x'_q - x_{al}) - (x''_q - x_{al})(x_q - x'_q)}{T'_{qo}(x'_q - x_{al})^2}$$

$$c_4 = \frac{(x''_q - x_{al})(x_q - x'_q)}{T'_{qo}(x'_q - x_{al})^2}$$

$$c_5 = \frac{1}{T'_{do}} \frac{x'_d - x''_d}{x''_d - x_{al}}$$

$$c_6 = - \frac{1}{T''_{do}}$$

$$c_7 = \frac{1}{T''_{qo}} \frac{x'_q - x''_q}{x''_q - x_{al}}$$

$$c_8 = - \frac{1}{T''_{qo}}$$

$$c_9 = - \frac{(x''_d - x_{al})^2 (x'_d - x'_d)}{(x'_d - x_{al})^2 T'_{do}}$$

$$c_{10} = \frac{(x''_q - x_{al})^2 (x_q - x'_q)}{(x'_q - x_{al})^2 T'_{qo}}$$

$$c_{11} = - \frac{(x'_d - x''_d)}{T''_{do}}$$

$$c_{12} = - \frac{(x'_q - x''_q)}{T''_{qo}}$$

$$c_{13} = \frac{1}{T'_{do}} \frac{(x''_d - x_{al})}{(x'_d - x_{al})}$$

The time constants T'_{do} and T'_{qo} , T''_{do} and T''_{qo} are defined in the usual manner as given in Ref. [62].

C.2 EXCITER-VOLTAGE REGULATOR SYSTEM

The state space representation of the exciter-voltage regulator system shown in Fig. C.2 is given by

$$\dot{\underline{y}}_e = [\underline{A}_e] \underline{y}_e + [\underline{C}_e] \Delta \underline{I}_m + [\underline{C}_{me}] \underline{y}_m + \underline{b}_e u_e \quad (C.8)$$

where

$$\underline{y}_e = [\Delta E_{fd}, y_{e2}, y_{e3}, y_{e4}, y_{e5}]^T$$

$$u_e = \Delta V_{ref}$$

C.3 TURBINE-GOVERNOR SYSTEM

The state space representation of the turbine governor system shown in Fig. C.3, which can represent both the systems for hydro and steam turbine by properly selecting the parameters, is given by

$$\dot{\underline{y}}_t = [\underline{A}_t] \underline{y}_t + [\underline{C}_t] \Delta \underline{I}_m + [\underline{C}_{tm}] \underline{y}_m + \underline{b}_t u_t \quad (C.9)$$

where

$$\underline{y}_t = [y_{t1}, y_{t2}, y_{t3}]$$

$$u_t = \Delta \omega_{mo}$$

The details of models (C.8) and (C.9) can be easily derived from the Figs. C.2 and C.3 respectively along with the machine equations and are not given here for the sake of brevity.

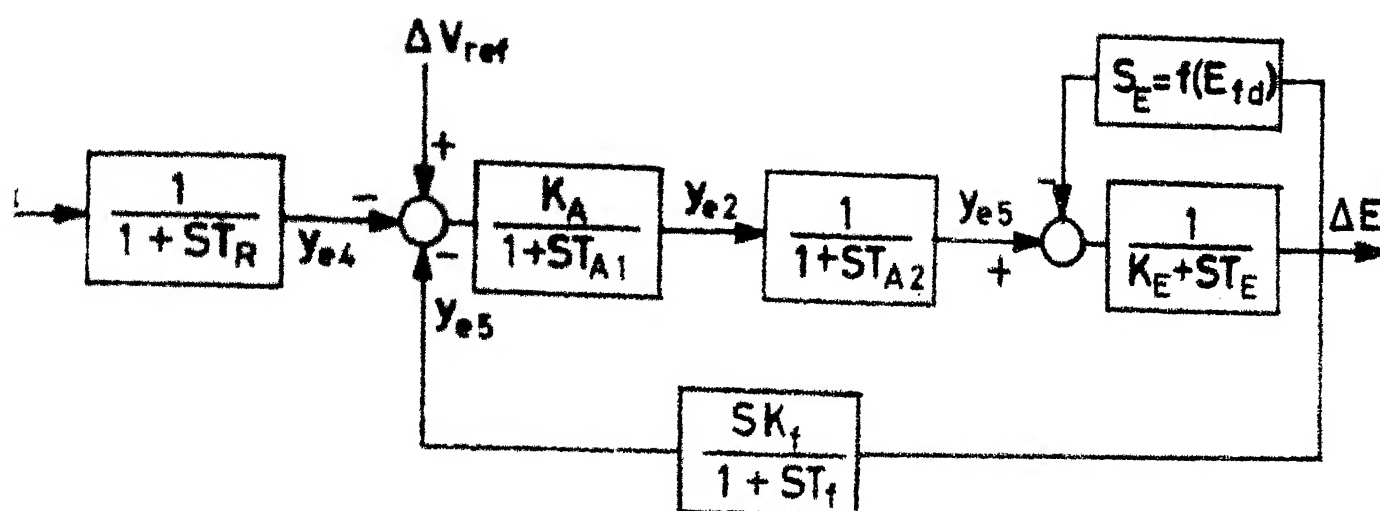


Fig. C·2 Linear model of an exciter-voltage regulator system

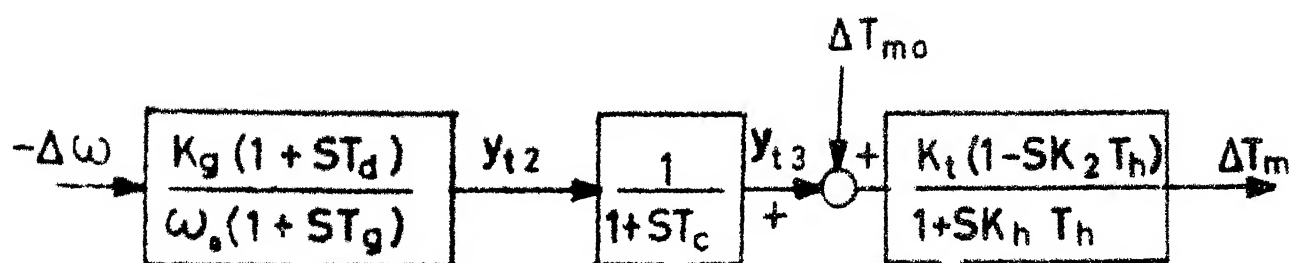


Fig. C·3 Simplified linear model of a turbine-governor system

APPENDIX D

NON-LINEAR INITIAL VALUE PROBLEM

The non-linear initial value problem given below is adapted from Ref. [50].

Consider a nonlinear system

$$\begin{aligned}\dot{\underline{x}} &= \underline{f}(\underline{x}, \underline{z}, \epsilon) \\ \epsilon \dot{\underline{z}} &= \underline{g}(\underline{x}, \underline{z}, \epsilon)\end{aligned}\tag{D.1}$$

with $\underline{x}(0) = \underline{x}^0$ and $\underline{z}(0) = \underline{z}^0$. The dimensions of \underline{x} and \underline{z} are m_1 and m_2 respectively. ' ϵ ' is the perturbation parameter small and >0 . \underline{f} and \underline{g} are continuously differentiable functions and have asymptotic expansions

$$\begin{aligned}\underline{f}(\underline{x}, \underline{z}, \epsilon) &\sim \sum_{j=0}^{\infty} \underline{f}_j(\underline{x}, \underline{z}) \epsilon^j \\ \underline{g}(\underline{x}, \underline{z}, \epsilon) &\sim \sum_{j=0}^{\infty} \underline{g}_j(\underline{x}, \underline{z}) \epsilon^j\end{aligned}\tag{D.2}$$

as $\epsilon > 0$. The reduced problem is

$$\dot{\underline{x}} = \underline{f}_0(\underline{x}, \underline{z}) \quad \text{with} \quad \underline{x}(0) = \underline{x}^0\tag{D.3a}$$

$$\underline{0} = \underline{g}_0(\underline{x}, \underline{z})\tag{D.3b}$$

Assume that

(i) There is a continuously differentiable function $\phi(\underline{x})$ such that

$$E_0(\underline{x}, \phi(\underline{x})) = 0 \quad (D.5)$$

and the resulting reduced system has a (unique) solution $(\underline{X}_0(t), \underline{Z}_0(t))$. For the sake of brevity we will not use the argument (t) with \underline{X}_0 and \underline{Z}_0 in the subsequent analysis.

(ii) The matrix $[\frac{\partial E_0}{\partial \underline{Z}}]$ is nonsingular and stable along $(\underline{X}_0, \underline{Z}_0)$.

(iii) The matrix $[\frac{\partial E_0}{\partial \underline{Z}}]$ is stable at $(\underline{X}_0(0), \underline{K})$ for all values of \underline{K} between $\underline{Z}_0(0)$ and \underline{Z}^0 .

The asymptotic solution of (D.1) is an additive function of the variable 't' and a stretched variable $\tau = t/\epsilon$, which tends to ∞ as $\epsilon \rightarrow 0$. The solution of (D.1) is written in the form

$$\begin{aligned} \underline{x}(t, \epsilon) &= \underline{X}(t, \epsilon) + \epsilon \underline{p}(\tau, \epsilon) \\ \underline{z}(t, \epsilon) &= \underline{Z}(t, \epsilon) + \underline{q}(\tau, \epsilon) \end{aligned} \quad (D.6)$$

where \underline{x} , \underline{X} , \underline{z} and \underline{Z} all have asymptotic expansions given in equation (4.12). The outer expansion $(\underline{X}, \underline{Z})$ and the boundary layer expansion $(\epsilon \underline{p}, \underline{q})$ are explained in Section 4.3.

We shall obtain the zeroth and the first order solution as defined in (4.15) and (4.16) respectively. For this purpose, the different terms in (D.6) are obtained by using Taylor series expansions of \underline{f}_0 and \underline{g}_0 around $(\underline{X}_0, \underline{Z}_0, 0)$ and substituting the expansions for $(\underline{X}, \underline{Z})$ and $(\underline{x}, \underline{z})$ in (D.1). On equating the coefficients of ε^j , we have the following equations.

Reduced system

$$\begin{aligned}\dot{\underline{X}}_0 &= \underline{f}_0(\underline{X}_0, \underline{Z}_0) \\ \dot{\underline{Z}}_0 &= \underline{\phi}(\underline{X}_0)\end{aligned}\tag{D.7}$$

\underline{q}_0 and \underline{p}_0 are given by

$$\frac{d\underline{q}_0}{d\tau} = \left[\frac{\partial \underline{f}_0}{\partial \underline{Z}}(\underline{X}_0(0), \underline{Z}_0(0) + \underline{q}_0(\tau)) \right] \underline{q}_0(\tau) \tag{D.8}$$

with initial condition $\underline{q}_0(0) = \underline{z}^0 - \underline{Z}_0(0)$

$$\frac{d\underline{p}_0}{d\tau} = \left[\frac{\partial \underline{f}_0}{\partial \underline{Z}}(\underline{X}_0(0), \underline{Z}_0(0) + \underline{q}_0(\tau)) \right] \underline{q}_0(\tau) \tag{D.9}$$

with initial condition

$$\underline{p}_0(\infty) = \underline{0}.$$

The terms \underline{X}_1 and \underline{Z}_1 are given by

$$\dot{\underline{X}}_1 = \left[\frac{\partial \underline{f}_0}{\partial \underline{X}}(\underline{X}_0, \underline{Z}_0) \right] \underline{X}_1 + \left[\frac{\partial \underline{f}_0}{\partial \underline{Z}}(\underline{X}_0, \underline{Z}_0) \right] \underline{Z}_1 + \underline{f}_1(\underline{X}_0, \underline{Z}_0) \tag{D.10}$$

$$0 = \left[\frac{\partial E_0}{\partial \underline{x}} (\underline{x}_0, \underline{z}_0) \right] \underline{x}_1 + \left[\frac{\partial f_0}{\partial \underline{z}} (\underline{x}_0, \underline{z}_0) \right] \underline{z}_1 + E_1 (\underline{x}_0, \underline{z}_0) - \dot{\underline{z}}_0 \quad (D.11)$$

with initial condition

$$\underline{x}_1(0) = -\underline{p}_0(0)$$

The term \underline{q}_1 is derived from

$$\begin{aligned} \frac{d\underline{q}_1}{dt} = & \left[\frac{\partial E_1}{\partial \underline{z}} (\underline{x}_0(0), \underline{z}_0(0) + \underline{q}_0(\tau)) \right] \underline{q}_1(\tau) + \\ & \left[\frac{\partial E_1}{\partial \underline{x}} (\underline{x}_0(0), \underline{z}_0(0) + \underline{q}_0(\tau)) \right] \underline{q}_0(\tau) \quad (D.12) \end{aligned}$$

with initial condition

$$\underline{q}_1(0) = -\underline{z}_1(0).$$

The first order approximation to $(\underline{x}, \underline{z})$ is obtained by adding the corresponding terms to $(\underline{x}_0, \underline{z}_0)$ as given in equation (4.16). The above equations for \underline{q}_0 , \underline{p}_0 and \underline{q}_1 are derived by using Taylor series expansions of \underline{f} and \underline{g} about $(\underline{x}_0(0), \underline{z}_0(0) + \underline{q}_0(\tau), 0)$.

CURRICULUM VITAE

1. Candidate's Name: R.P. ADGAONKAR

2. Academic Background:

Degree	Specialization	University	Year
B.E.	Electrical Engineering	Marathawada University, Aurangabad	1967
M.Tech.	Power System Analysis	I.I.T. Bombay	1969

3. Publications:

- (i) 'Power Systems Dynamic Equivalents' (with M.A. Pai), National Systems Conference, Ludhiana (India), 1978.
- (ii) 'Identification of Coherent Generators using Weighted Eigenvectors' (with M.A. Pai), IEEE Paper No. A79 022-5, PES Winter Meeting, New York, 1979.
- (iii) 'Dynamic Equivalents of Power Systems using Singular Perturbation Technique' (with M.A. Pai), IFAC Symposium on Computer Applications in Large Scale Power Systems, New Delhi, 1979.
- (iv) 'Stability, Decomposition and Aggregation of Large Scale Power Systems' (with M.A. Pai and Vijay Vittal), Proceedings of Symposium on Mathematical Modelling and its Applications, Indian Institute of Technology, Kanpur, 1978.
- (v) 'Decomposition and Dynamic Simplification in Large Scale Power Systems' (with M.A. Pai and Vijay Vittal), submitted to Large Scale Systems: Theory and Applications.